UNIVERSITY OF CALIFORNIA, SAN DIEGO

Spatial and Temporal Dynamics of Marine Natural Products Biosynthesis

A dissertation submitted in partial satisfaction of the
requirements for the degree Doctor of Philosophy

in

Biology

by

Eduardo Esquenazi

Committee in charge:

Professor Eduardo Macagno, Chair
Professor Pieter C. Dorrestein, Co-Chair
Professor William H. Gerwick, Co-Chair
Professor Mark H. Ellisman
Professor James Golden
Professor Kit Pogliano

2010

The Dissertation of Eduardo Esquenazi is approved, and it is acceptable in quality and form for publication on microfilm and electronically:

_____

_____

_____

_____
Co-Chair

_____
Co-Chair

_____
Chair

University of California, San Diego

2010

DEDICATION

This dissertation is dedicated to my mother whose sacrifices, guidance and belief in my abilities have made this dissertation possible.

This dissertation is dedicated to my father, whose hard work and character have provided me with endless opportunities. Your perseverance, kindness and humor I will always strive to achieve.

Thank you both for everything.

EPIGRAPH

Imagination is more important than knowledge.
Albert Einstein

It is in the admission of ignorance and the admission of uncertainty that there is a hope for the continuous motion of human beings in some direction that doesn't get confined, permanently blocked, as it has so many times before in various periods in the history of man.
Richard P. Feynman

TABLE OF CONTENTS

Signature Page iii
Dedication iv
Epigraph v
Table of Contents vi
List of Abbreviations ix
List of Figures xi
List of Tables xiv
Acknowledgements xv
Vita xviii
Abstract of the Dissertation xxi

1.0 Chapter 1 Introduction 1
1.1 History of Natural Products 1
1.1.1 Ancient Medicine 1
1.1.2 Natural Products and the Rise of Modern Medicine 1
1.1.3 The Rise and Ebb of Synthetic Compounds 3
1.1.4 Why Natural Products? 4
1.2 Marine Natural Products 5
1.2.1 Early Marine Natural Product Efforts 6
1.2.2 Modern Marine Natural Product Efforts 7
1.2.3 Hurdles in Marine Natural Product Research 8
1.3 The natural product discovery and isolation process 11
1.3.1 Modern Methods- the rise of Spectroscopy and Bioassay Guided Fractionation 12
1.3.2 The promise of the post-genomics era 14
1.3.3 Metagenomics 17
1.4 Modern Mass Spectrometry in Natural Products Research 19
1.4.1 A Brief History of MS 19
1.4.2 Soft ionization MS 20
1.4.4 Natural product MALDI imaging 24
1.5 Dissertation Contents 25
1.6 Chapter 1 References 30

2.0 Chapter 2 Temporal Dynamics of Natural Product Biosynthesis in Marine Cyanobacteria 39
2.0.1 Abstract 39
2.1 Introduction 39
2.2 Results 44
2.2.1 Metabolome wide turnover of nitrogen containing metabolites in three different *Lyngbya* strains 44
2.2.2 Growth, and turnover of pheophytin *a* and jamaicamide B in *Lyngbya majuscula* JHB 47

2.2.3 Comparison of ^{15}N labeling states of jamaicamide B with the brominated natural product jamaicamide A over 10 days 52
2.3 Discussion 58
2.4 Materials and Methods 64
2.4.1 Cyanobacteria strains and culture maintenance 64
2.4.2 Experimental culture conditions 64
2.4.3 Sampling 65
2.4.4 LC-MS comparison of jamaicamide B and A in 16 h light/8 h dark vs. 24 h dark 66
2.4.5 MALDI MS sample preparation 67
2.4.6 Calculations 67
2.5 Chapter 2 Acknowledgements 69
2.6 Chapter 2 Supporting Information 70
2.7 Supplemental Information: Methods 72
2.7.1 Growth rates 72
2.7.2 Media extracts 74
2.7.3 MALDI-TOF settings 75
2.8 Chapter 2 References 77
2.9 Chapter 2 Appendix 82

3.0 Chapter 3 Visualizing The Spatial Distribution of Secondary Metabolites Produced by Marine Cyanobacteria and Sponges Via MALDI-TOF Imaging 96
3.0.1 Abstract 96
3.1 Introduction 97
3.2 Results and Discussion: 100
3.2.1 MALDI-TOF-imaging of natural products from single cyanobacterial filaments 100
3.2.2 Using MALDI-TOF imaging for the dereplication of individual marine cyanobacteria from mixed assemblages 107
3.2.3 Spatial distribution of secondary metabolites within the marine sponge, *Dysidea herbacea* 108
3.3 Conclusions 112
3.4 Materials and Methods 113
3.4.1 Cyanobacteria cultures 113
3.4.2 Filament sample preparation 114
3.4.3 Dysidea herbacea preparation 116
3.5 Chapter 3 Acknowledgements 118
3.6 Chapter 3 References 119
3.7 Chapter 3 Appendix 123

4.0 Chapter 4 Biosynthesis of Major Metabolites in Single Cyanobacterial Cells 135
4.0.1 Abstract 135
4.1 Introduction 136
4.2 Results and Discussion 138

4.3 Materials and Methods 145
4.3.1 Cyanobacteria strains and culture maintenance 145
4.3.2 Media 146
4.3.3 Single Cell Isolations 146
4.3.4 DAPI staining 147
4.3.5 MALDI MS Sample preparation 147
4.3.6 MALDI-TOF acquisition and settings 148
4.3.7 Calculations 149
4.4 Chapter 4 References 150

5.0 Chapter 5 Ion Mobility Mass Spectrometry Enables the Efficient Detection and Identification of Halogenated Natural Products from Cyanobacteria with Minimal Sample Preparation 153
5.0.1 Abstract 153
5.1 Introduction 153
5.2 Methods 163
5.3 Conclusion 164
5.4 Chapter 5 Acknowledgments 166
5.5 Chapter 5 References 167
5.6 Chapter 5 Supporting Information 169

6.0 Chapter 6 Future Directions 172

LIST OF ABBREVIATIONS

Abs- absolute absorbance

ACN- acetonitrile

Cnt- count

DESI- Desorption electrospray ionization

DIOS- desorption ionization on silicon

DNA- deoxyribose nucleic acid

ESI- electrospray ionization

Exc or Ex- excitation

FAB- fast atom bombardment

HPLC- high performance liquid chromatography

Hz- hertz

LCMS- liquid chromatography mass spectrometry

MALDI- matrix assisted laser desorption ionization

MS- mass spectrometry

mV- millivolt

NIMS- nanostructure-initiator mass spectrometry

NMR- nuclear magnetic resonance

NRPS- non-ribosomal peptide synthetase

PKS- polyketide synthase

SIMS- secondary ion mass spectrometry

SW- saltwater

TFA- trifluoroacetic acid

TOF- time of flight

VLC vacuum liquid chromatography

LIST OF FIGURES

Figure 1.1. Number of new drugs approved by the FDA per year from 1981 to 2007. 5
Figure 1.2. The basic steps and amount of compound needed in the process from identification of a bioactive compound to lead optimization and pre-clinical studies. 9
Figure 1.3. Disconnect between the reported sources of marine derived anti-cancer agents and their biosynthetic source. 11
Figure 1.4. Bioassay guided fractionation. 13
Figure 1.5. The *Salinospora arenicola* genome. 15
Figure 1.6. Symbiotic metabolism. 17
Figure 1.7. A basic diagram of the MALDI-TOF process. 23
Figure 2.1. Structure of metabolites in study 45
Figure 2.2. Comparison of percent 15N labeling of some known nitrogen-containing metabolites from Lyngbya majuscula 3L, JHB and Lyngbya bouillonii. 46
Figure 2.3. Comparison of growth, jamaicamide B and pheophytin *a* turnover during 10 days from small cultures of *Lyngbya majuscula* JHB grown in ^{15}N media. 49
Figure 2.4. Different ^{15}N labeling states of jamaicamide B and A over 10 days in *L. majuscula* JHB. 53
Figure 2.5. Further investigation of jamaicamide A and B biosynthesis. 55
Figure 2.6. Effect of nitrate concentration and UV light on percent ^{15}N labeling of jamaicamide A and pheophytin *a*. 71
Figure 2.7. Y-axis is percent labeling. 73
Figure 2.8. Effect of light intensity on jamaicamide B ^{15}N labeling. 82
Figure 2.9. Effect of different visible wavelengths on jamaicamide and pheophytin labeling. 83
Figure 2.10. Further experiments into the effect of green wavelength on *L.majuscula* JHB. 84
Figure 2.11. The previous (figure 2.10) experiment was repeated, this time using foil to block out all other light. 85
Figure 2.12. Effect of UV light on the ^{15}N labeling rate of jamaicamide B. 85
Figure 2.13. Effect of filament density on percent ^{15}N Labeling of jamaicamide B and pheophytin a after 5 days. 86
Figure 2.14. Summary- Impact of all the different culture conditions tested on the ^{15}N labeling of jamaicamide B (black) and pheophytin *a* (grey). 87
Figure 2.15. MALDI spectrum of *Lyngbya majuscula* JHB showing the presence the known metabolites jamaicamides A and B, hectochlorin and pheophytin *a*, as well as an unknown peak at *m/z* 400. 88
Figure 2.16. Large scale ^{15}N feeding study in *Lyngbya majuscula* JHB showing shifts of known and unknown metabolites. 89

Figure 2.17. Purification tree following the *m/z* 400 compound, cryptomaldamide performed by Robin Kinnel. 90
Figure 2.18. Structure and bioactivity comparison between cryptomaldamide and the anticancer lead compound hemiasterlin (Figure courtesy of W.H.Gewick). 91
Figure 2.19. Comparison of *L.majuscula* JHB and 3L growth rates. 92
Figure 2.20. Impact of increased temperature on the ^{15}N labeling after 5 days of various metabolites and growth in *Lyngbya majuscula* 3L..... 93
Figure 2.21. Effect of nitrate-free media on *L.majuscula* 3L growth and morphology. 94
Figure 3.1. MALDI-TOF-imaging of the intact marine cyanobacterium Lyngbya majuscula JHB filament. 101
Figure 3.2. The spatial distribution of selected ions observed to co-localize with *Lyngbya majuscula 3L* 106
Figure 3.3. npMALDI-I of a complex mixture of cyanobacteria: a single npMALDI-I run on a mixture of Lyngbya majuscula JHB (orange), and 3L(green), Lynbya bouillonii (Red) Oscillatoria nigro-viridis (Blue). 108
Figure 3.4. npMALDI-I on the sponge *Dysidea herbacea*. (A) The average mass spectrum. 110
Figure 3.5. Large scale MALDI imaging of *Dysidea herbacea* combined with epiflourescence images. 123
Figure 3.6. More MALDI imaging results from the *Dysidea herbacea* sample shown in figure 3.5..... 124
Figure 3.7. Coronal cryotome section of the nudibranch *Elysia rufescens*. 126
Figure 3.8. MALDI imaging results of section in far left panel (see figure x)..... 127
Figure 3.9. kahalalide F structure and distribution on *Elysia rufescens*. 128
Figure 3.10. Dried droplet MALDI analysis (*m/z* 1480-1550) of the various players in the kahalalide story. 129
Figure 3.11. Evidence of differential distribution of metabolites in a filament of *L.majuscula* JHB. 131
Figure 3.12. Heat map representation of MALDI imaging data of a filament of *L majuscula* JHB. 132
Figure 3.13. *Nostoc punctiforme* spatial distribution of metabolites. 133
Figure 3.14. Dried droplet MALDI analysis of different areas of a pan grown *Phormidium sp.* culture. 134
Figure 4.1. The marine filamentous cyanobacteria single cell isolation and MALDI target plate preparation. 139
Figure 4.2. Actual single cell preparation from *Lyngbya majuscula 3L*. 140
Figure 4.3. Photo micrographs of DAPI staining of live intact filaments and single cells of *L.majuscula* 3L. 142
Figure 4.4. Single cells from an *L.majuscula* 3L culture incubated with [^{15}N]NaNO3 suggest active biosynthesis of metabolites. 144
Figure 5.1. Ion mobility separation of known natural products from crude extracts of *Lyngbya majuscula*. 159

Figure 5.2. MALDI imaging of filaments of *L.majuscula* paired with ion-mobility. 161

LIST OF TABLES

Table 2.1. The Impact of UV Exposure and Two-Fold Nitrate Concentration in the Media on The Production of Pheophytin A And Jamaicamide B in L.majuscula JHB. 72

Table 2.2. Effect of 10 days in Nitrate-Free Media on Number of Cells Per Unit Length of Filament, Cell Width and Filament Width 95

ACKNOWLEDGEMENTS

It's been over 10 years since I joined the UCSD community- there are too many to acknowledge…here's the short list:

My whole, beautiful, big family- but especially my parents, my brother Moises, and sister Carolina, and stepparents Luigi and Mayra, whose support, kindness, and honesty, through both good times and bad, sustained me long enough to get this done. I share this accomplishment with you.

My girlfriend Amanda for her patience and warmth during long days and edgy nights.

All of my friends. More than a support system, you have made the everyday special and kept my soul fulfilled.

Jim Simons for his mentorship and perspective.

Silvana and Dick Christy for their good humor and home cooked meals.

The many doctors and nurses, especially Drs. Bosl and Millard, who provided outstanding care and succeeded in keeping me alive, vibrantly so.

My many collaborators- Terry Sejnowsky, Jay Coggan and Tom Bartol at Salk. All the folks at NCMIR, and the Dorrestein and Gerwick Labs. Especially my collaborators at one time or another, Cameron Coates, David Gonzales, Tara Byrum, Emily Monroe, Adam Jones, Carla Sorrels, Roland Kersten, Robin Kinnel and Masa Taniguchi- its been a pleasure to be colleagues with such diverse, sharp and kind people.

My office mates Carla Sorrels and Paul Boudreau (and Plankton). Thank you for putting up with my shenanigans, mostly with a smile.

The Natural Product group at SIO and UCSD. Especially Drs. Fenical, Moore and Jensen and their respective labs. Thank you for your support, dedication and expertise. I feel confident saying that this is the best place on the planet for this research. I feel honored to have been a part of this effort.

The Biology Graduate Department. Especially Dr. Darwin Berg, Dr. William McGinnis, Cathy Pugh and Thomas Tomp. Thank you for the many years of support, the extra paperwork and time extensions, but mainly the confidence in my abilities that enabled me to manage and complete this program. As you already know, it is the best doctoral program, and that's a reflection of you. Keep up the good work.

Dr. Mark Ellisman. Thank you for the many, many years of confidence, guidance and mentorship. I would not be here without it.

Dr. Pieter Dorrestein. You have the courage to pursue new ideas and the vision and tenacity to see them through. I'm fairly certain these qualities rubbed off on me in some degree and for that I am tremendously grateful. Thank you for giving me the opportunity to be a part of your first years at UCSD and what will be a long and radiant career.

Dr. William Gerwick. I feel honored to have been part of the lab and lucky to consider myself a member of the extended and extensive Gerwick student society. Your kindness, depth of knowledge, and enthusiasm for marine natural products (most

likely of cyanobacterial origin), have made these last years incredibly enjoyable and enlightening. Thank you for this opportunity and for your patience and guidance.

Chapter 2, in essence, includes a part that has been submitted to the Proceedings of the National Academy of Sciences in 2010. Eduardo Esquenazi, Adam Jones, Tara Byrum, Pieter C. Dorrestein and William H. Gerwick. The dissertation author is the primary investigator and author of this paper.

Chapter 3, in part, includes a reprint as it appears in Molecular Biosystems 2008, 4(6): 562-570. Eduardo Esquenazi, Cameron Coates, T. Luke Simmons, David Gonzales, Pieter C. Dorrestein and William H. Gerwick. The dissertation author was the primary investigator and author of this paper.

Chapter 4, in full, has been submitted to Chemical Communications in 2010. Eduardo Esquenazi, Michael Daly, Tasneem Barainwala, William H. Gerwick and Pieter C. Dorrestein. The dissertation author was the primary investigator and author of this paper.

Chapter 5, in full, is currently being prepared for submission in 2011. Eduardo Esquenazi, Tara Byrum, William Gerwick, and Pieter Dorrestein. The dissertation author was the primary investigator on these studies.

VITA

EDUCATION AND FIELDS OF STUDY

University of California-San Diego, La Jolla CA 2007-2010
Doctor of Philosophy in Biology
Advisors: Pieter Dorrestein and William Gerwick

University of California-San Francisco, San Francisco CA 2006-2007
Staff Research Associate, Stem Cell Division (Advisor: Arnold Kriegstein)

University of California-San Diego, La Jolla CA 2002-2004
Doctoral Program in Biology, Neurobiology Section (Advisors: Mark Ellisman and Darwin Berg)

University of California-San Diego, La Jolla CA 1999-2002
National Center for Microscopy and Imaging Research (NCMIR)
Non-Degree Graduate Student in Biology (Advisor: Mark Ellisman)

Vanderbilt University, Nashville TN 1994-1998
Bachelor of Science. Double Major: Biology and Neuroscience, Pre-med Program

Duke University, Marine Laboratory, Beaufort NC Summer 1995
Oxidative stress in Calinectes sapidus

FELLOWSHIPS

San Diego Fellowship	2010
NIH Marine Biotechnology Fellowship	2008-2009
NSF Systems Neurobiology Training Grant	2002-2005
MASEM Scholar	2001-2002
MBRS Minority research support fellowship	1999-2001

WORKSHOPS and PRESENTATIONS

American Society for Microbiology, San Diego CA May 2010
Invited Oral Presentation: *MALDI mass spectrometry insights into spatial and temporal variation in marine natural product biosynthesis*

ASP Conference in Oahu, Hawaii June 2009
Presented poster: *Spatial and Temporal Dynamics of Cyanobacterial Natural Product Biosynthesis*

University of California-San Diego, La Jolla CA January 2003
3rd Annual All-Grad Research Symposium
Presented poster: *Computer Simulations of Synaptic Ultrastructure and Microphysiology*

Society for Neuroscience Convention, San Diego, CA November 2001
Eduardo Esquenazi, Jay S. Coggan, Thomas M. Bartol, Richard D. Shoop, Terrance J. Sejnowski, Mark H. Ellisman, Darwin K. Berg. *Computer simulation of synaptic ultrastructure and microphysiology in the chick ciliary ganglion.*

Pittsburgh Supercomputer Center, Pittsburgh, PA Summer 2000
MCell Workshop

PUBLICATIONS

Eduardo Esquenazi, William H. Gerwick and Pieter C. Dorrestein. *Detecting the presence and confirming biosynthesis of major metabolites in single cyanobacterial cells using MALDI-TOF Mass Spectrometry*. Forthcoming.

Carla M. Sorrels, Eduardo Esquenazi, Pieter C. Dorrestein, and William H. Gerwick. *Probing the in vivo biosynthesis of scytonemin, a cyanobacterial sunscreen, through small-scale stable isotope incubation studies using MALDI-TOF mass spectrometry.* Forthcoming

Niclas Engene, Hyukjae Choi, Eduardo Esquenazi, Erin C. Rottacker, Mark H. Ellisman, Pieter C. Dorrestein and William H. Gerwick. *Underestimated biodiversity as major explanation for the perceived rich secondary metabolite capacity of the cyanobacterial genus Lyngbya*. Environmental Microbiology. Submitted November 2010.

Eduardo Esquenazi, William H. Gerwick and Pieter C. Dorrestein. *Ion mobility mass spectrometry enables the efficient detection of halogenated natural products from cyanobacteria with minimal sample preparation.* Submitted to Chemical Communications

Eduardo Esquenazi, Adam C. Jones, Tara Byrum, Pieter C. Dorrestein and William H. Gerwick. *Temporal dynamics of natural product biosynthesis in marine cyanobacteria.* Submitted to PNAS, under 1st revision.

Masatoshi Taniguchi, Joshawna K. Nunnery, Niclas Engene, Eduardo Esquenazi, Tara Byrum, Pieter C. Dorrestein and William H. Gerwick. Palmyramide A, a Cyclic Depsipeptide from a Palmyra Atoll Collection of the Marine Cyanobacterium Lyngbya majuscula. *J. Nat. Prod.,* 2010, 73 (3): 393–398

Eduardo Esquenazi, Yu-Liang Yang, Jeramie Watrous, William H. Gerwick, Pieter C. Dorrestein. *Imaging Mass Spectrometry of Natural Products.* Natural Product Reports, 2009, 26: 1521-1534

Eduardo Esquenazi, Pieter C. Dorrestein, William H. Gerwick. *Probing marine natural product defenses with DESI-imaging mass spectrometry*. PNAS 2009, 106: 7269-7270

Eduardo Esquenazi, Cameron Coates, Luke Simmons, David Gonzalez, William H. Gerwick, Pieter C. Dorrestein. *The spatial distribution of secondary metabolites produced by marine cyanobacteria and sponges via MALDI-TOF imaging*. Molecular Biosystems 2008, 4(6): 562-570

Luke Simmons, Cameron Coates, Ben R. Clark, Niclas Engene, David Gonzalez, Eduardo Esquenazi, Pieter C. Dorrestein, William H. Gerwick. *Biosynthetic origin of natural products isolated from marine microorganism-invertebrate assemblages*. Proceedings of the National Academy of Sciences 2008, 105(12): 4587-94

Jay S. Coggan, Thomas M. Bartol, Eduardo Esquenazi, Joel R. Stiles, Stephen Lamont, Maryann E. Martone, Darwin K. Berg, Mark H. Ellisman, Terrance J. Sejnowski. *Evidence for ectopic neurotransmission at a neuronal synapse*. Science, 2005 July 15; 309 (5733): 446-51.

Richard D. Shoop, Eduardo Esquenazi, Naoko Yamada, Mark H. Ellisman, and Darwin K. Berg. *Ultrastructure of a somatic spine mat for nicotinic signaling in neurons*, Journal of Neuroscience. (2002) 22: 748-756.

ABSTRACT OF THE DISSERTATION

Spatial and Temporal Dynamics of Marine Natural Products Biosynthesis

by

Eduardo Esquenazi

Doctor of Philosophy in Biology

University of California, San Diego, 2010

Professor Eduardo Macagno, Chair
Professor Pieter C. Dorrestein, Co-Chair
Professor William H. Gerwick, Co-Chair

The marine environment represents one of the most promising sources of novel, bioactive natural products. The process used in their discovery has been simplified and accelerated greatly in the 20th century with the advent of new technology, including spectroscopy, mass spectrometry, chromatography, in conjunction with bioassay-guided fractionation. However, more recent developments

in genomics and metabolomics suggest that the biosynthetic capacity and interrelationships between organisms has been underappreciated and could likely yield many more important discoveries, both in medical value and in basic biological understanding. Contained in this dissertation are a series of unique experiments that harness the capacity of Matrix Assisted Laser Desorption Ionization (MALDI) to detect multiple metabolites concurrently from a single, small sample. This ability is used to capture the temporal dynamics of biosynthesis and turnover of secondary metabolites from cultured marine filamentous cyanobacteria, both in relation to each other and to primary metabolites. These temporal relationships are useful for improving compound yields from cultured organisms, tracking nitrogen in nutrient cycles, as well as providing an experimental tool to explore secondary metabolism in general. Also contained are the first images of natural products captured by MALDI imaging mass spectrometry, revealing complex chemical microenvironments in marine sponges and the distribution of known bioactive metabolites in marine cyanobacteria. Initial results also suggest that there is differential distribution of metabolites in cultured cyanobacteria. A third series of experiments exploiting the sensitivity of MALDI was conducted on single cells of filamentous marine cyanobacteria that are freed from the sheath and associated heterotrophs. The results reveal that many known natural products are found in single cells, further confirming their origin of biosynthesis; however, it appears not all cells from a filament contain the same metabolites. Nitrogen labeling experiments with these same preparations suggest the biosynthesis of the metabolites that are present occurs at similar rates. The

last set of experiments employ Ion Mobility mass spectrometry on various preparations of marine filamentous cyanobacteria and show that this new technology can effectively separate out halogenated metabolites from complex mixtures, a powerful tool for the identification and discovery of bioactive metabolites.

1.0 CHAPTER 1

INTRODUCTION

1.1. History of Natural Products

1.1.1 Ancient Medicine

For thousands of years, the chemical constituents of the living world surrounding us have a played a profound role in both social and medicinal aspects of our cultures. It may be that the use of specific plants and herbs for the treatment of ailments was the dawn of medicine as the practice dates back to the earliest records of human history. These records are numerous and wide-ranging in time and culture. With herbal preparations, Traditional Chinese Medicine dates back to at least 2500 B.C. The Ebers papyrus, from 1550 B.C., details medicinal plants used by the Egyptians. In 77 A.D., Dioscorides, a Greek physician practicing in Rome, reported the possible uses of over 600 plants in the *De Materia Medica Libri Quinque*. Shamanistic cultures and other primitive cultures have been relying on the natural environment exclusively for their medicinal remedies throughout their long history[1]. From opium to coffee to aspirin, every society in history has, without doubt, been under the influence of these natural products.

1.1.2 Natural Products and the Rise of Modern Medicine

The ability to extract pure natural products, also known as secondary metabolites, led to the administration of the active constituents of plants in precise

dosages, regardless of origin. Until about 200 years ago, the compounds responsible for the observed medicinal benefits were largely unknown. In the early 1800's, a greater understanding of organic chemistry and the manipulation of plant concoctions led to relatively pure preparations with medicinal value. Two key advancements come to mind that exemplify this leap in medicine; Sertürner's isolation of morphine from the poppy plant in 1804 [2] and the purification of salicin in the 1820's (from the bark of the white willow *Salix alba*- whose use as an antipyretic dates to the Ebers papyrus) and its subsequent conversion to aspirin (Charles Frederic Gerhard and Felix Hoffman) later in the century[3]. The isolation and manipulation of natural products like these and the ability to control their administration, have since formed the cornerstone of Western medicine.

In the last century, our understanding of medicine, disease and the human body has resulted in a jump of life expectancy from 47 to 73 years[4]. Within this feat, the acceptance of the germ theory of disease and the discovery and implementation of antibiotics, specifically Alexander Fleming's discovery of penicillin in 1928, reduced the high mortality rate of infections by 99% [4].

A greater understanding of isolation and purification techniques, the advent of nuclear magnetic resonance and mass spectrometry, and an improved understanding of the molecular targets of disease, have combined to provide the 21st century human with thousands of small, well characterized molecules from plants, microorganisms, fungi, and invertebrates that are clinically used to treat a wide range of diseases [5-7]. In fact, over 60 % of our modern pharmaceutical drugs, in some form or another,

originate from these often small, naturally occurring compounds [5-7]. Some of the more famous plant compounds include the antitumor agents paclitaxel [8] (originally from *Taxus brevifolia*) and vinblastine [9] (*Catharanthus roseus*), the antimalarial quinine [10] (*Cinchona ledgeriana*), and the anticholinergic atropine [11] (*Duboisia myoporoides*). Starting with penicillin, there have been many important discoveries from microorganisms, the anti-bacterials from various *Streptomyces* species including erythromycin A [12], amphotericin B and tetracycline [13], and the cholesterol reducing agent lovastatin from the fungus *Aspergillus terreus* [14]. This small list is but a glimpse of the medical arsenal provided to us by natural products.

1.1.3 The Rise and Ebb of Synthetic Compounds

Although organic chemical synthesis started in the early to middle part of the 19th century[15], it wasn't until the 1990's that synthetic chemistry became truly favored in the pharmaceutical arena [16]. Because purely synthetic compounds are generally easier and cheaper to obtain, pharmaceutical companies began to prefer the synthetic route and reducing, or abandoning, their natural product departments. Much of this shift was due to the explosion in computational power, which when combined with a greater understanding of organic synthesis and of the molecular targets of disease, yielded combinatorial chemistry and high-throughput screening [16, 17]. This confluence of technology and knowledge led to massive screening of cheap, easy to make compounds (some inspired by natural products); an approach that quickly supplanted natural product-based drug discovery efforts. While this led to an upsurge in the

amount of purely synthetic compounds available in the clinic during 1990's, the effect was short lived and the number of FDA approved drugs has begun to fall (Figure 1.1)[18].

1.1.4 Why Natural Products?

The consensus as to why natural products have outshone synthetic compounds is intimately tied to their role in the producing organisms. Unfortunately, knowledge of their endogenous roles is somewhat limited. Some of these compounds have been shown to act as siderophores, signaling molecules, allelo-chemicals, antimicrobials or as defensive compounds, preventing herbivory or predation [19,20]. Thus, these molecules, which have been dubbed 'secondary metabolites' because they are not critical to survival, nonetheless have an energetic cost associated with their production; likely representing privileged structures as evolution has fine-tuned their ability to interact with the enzymes or proteins responsible for the native roles in their own environment[21]. Interestingly, many of these molecular targets have been conserved over time and across species, including humans, hence their benefit to human medicine. Natural products have been shown to contain a greater number of chiral centers and steric complexity and are more "drug like" than purely synthetic compounds [22-27]. A recent analysis of the hit rate of natural product compounds of polyketide origin showed that a positive result is achieved in high-throughput screening approximately 0.3% of the time, versus the 0.001% attributed to purely synthetic compounds [22]. As such, interest in natural products has once again begun to

rise, especially in conjunction with the blossoming "nutraceutical" industry and the incorporation of alternative medical approaches to Western medical approaches.

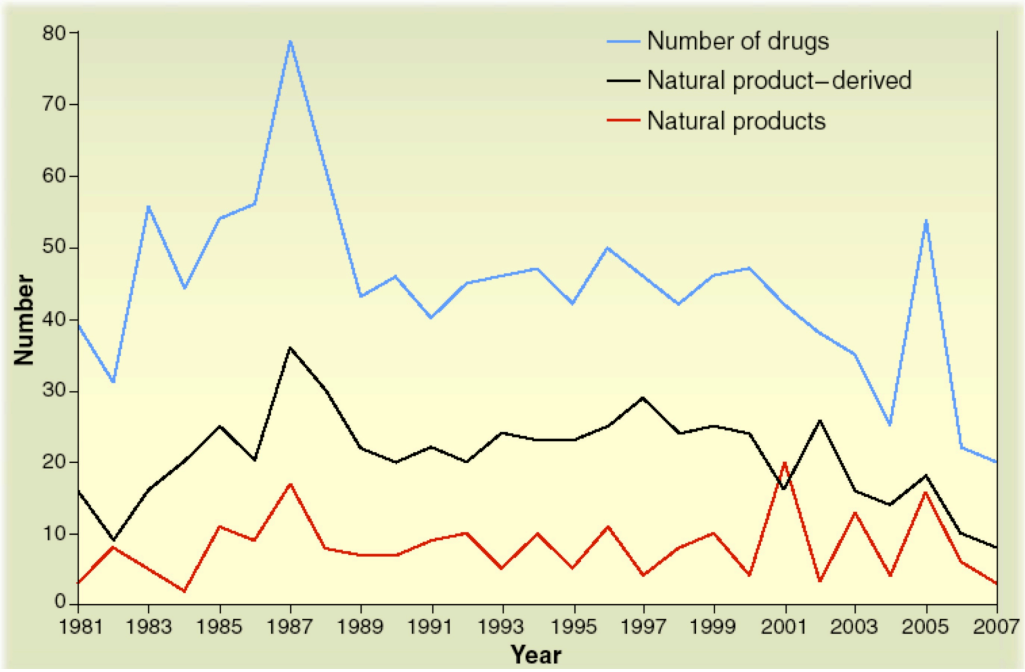

Figure 1.1. Number of new drugs approved by the FDA per year from 1981 to 2007. Apparent here is the leveling off and subsequent decline of approved drugs once pharmaceutical companies began preferring purely synthetic routes in the early 1990's.[18]

1.2 Marine Natural Products

Land-based plants have traditionally been the focus of natural product efforts, and not surprisingly, account for the majority of natural products with numerous medically active alkaloids and terpenes reported in the literature. The discovery of penicillin and many other antibiotics shifted the attention to land (soil) microorganisms, such as actinomycetes, which soon became a subject of intense

investigation, yielding many of the important polyketide type substances known today [28]. Until recently, microbial (loosely defined) and plant derived compounds from land sources accounted for all our natural products in the medical arsenal [5,6].

The chemistry of marine organisms remained a mystery until the mid 20th century. This is amazing considering that the ancient, salty, aqueous environments and ecosystems cover the majority of the planet and have undoubtedly resulted in very dissimilar selection pressures, including differences in competition for resources and space [29]. Furthermore, evolution has had its grip on the marine environment for a much longer time than on land (evidence for marine organisms dates back 3.8 billion years, versus the 600-500 million years ago for the first land organisms, resulting in a much different, if not greater, chemical diversity in the ocean [29].

1.2.1 Early Marine Natural Product Efforts

Focusing on the easily collectible benthic organisms such as sponges and soft corals, the initial efforts in the 1950's were not disappointed with their discoveries. The structures and activities of those first isolated compounds, like the pentosyl nucleosides from a Floridian sponge that would lead to the clinical anti-cancer compound cytarabine and the anti-viral vidarabine [31], reflected the uniqueness of the environment from which they originate. However, it wasn't until the 1970's that the field of marine natural products gained momentum. Intrepid scientists such as Paul Scheuer, Ken Rinehart, Richard Moore, William Fenical and John Faulkner, among a few others, began looking to the sea for novel chemistry [32-38]. These efforts resulted in

the discovery of a variety of bioactive metabolites, some with novel functionalities and halogenations, mainly from algae and sponges.

1.2.2 Modern Marine Natural Product Efforts

As the marine natural products field has matured, with growing input from genomics and metabolomics, the organisms that harbor the most intriguing chemistry have become better defined. Marine bacteria, cyanobacteria, algae and some fungi are widely considered the true, and most prolific sources[29], although invertebrates like sponges, soft corals, tunicates, nudibranchs, cone snails and even some fishes have yielded a number of bioactive compounds. Some of these natural products have directly lead to, or have been the inspiration for, compounds in clinical trials or the market place[39]. Key discoveries include the aforementioned clinical anti-viral compound ara-A (vidarabine) and anti-cancer compoud ara-C (cytarabine) isolated from a Floridian sponge, the potent peptide analgesic ω-conotoxin MVIIA from a cone snail[40], the tunicate derived compound ecteinascidin-743 approved by the European Union for the treatment of soft-tissue sarcomas[41], the protein kinase C modulator bryostatin 1 from the symbiont of the bryozan *Bugula neritina* [42]. There are many more candidates, including curacin A and salinosporamide A, which are in various stages of clinical trials in the US. [43,44]

A recent worldwide collaboration and decade long study [45] failed to approximate the number of unknown species in the ocean. It determined that approximately 90% of marine life, by weight, is microbial, with the estimate for total

number of microorganism species approaching one billion (!). With so much life remaining to be discovered, the world's oceans represent a vast, untapped source of novel chemistry.

1.2.3 Hurdles in Marine Natural Product Research

Although the potential number and novelty of compounds in the ocean is certainly tremendously attractive, as with most drug discovery efforts based on natural products, the marine field is not without its challenges. Besides the inherent difficulties and cost associated with research in the marine environment, the issue of further supply remains at the forefront. The novelty of marine chemistry raises the expense and complexity of synthesis of the compounds. [18, 43] Culturing of marine organisms (micro or macro) for the continued supply of a product has traditionally only been successful in less than 1% of cases [46], leaving the question of how to continue supplying candidate compounds for further testing and development (Figure 1.2). While this is certainly not a minor issue, some argue that if a compound confers a significant enough benefit or activity, the hurdle of supply will be tackled and overcome [18,43].

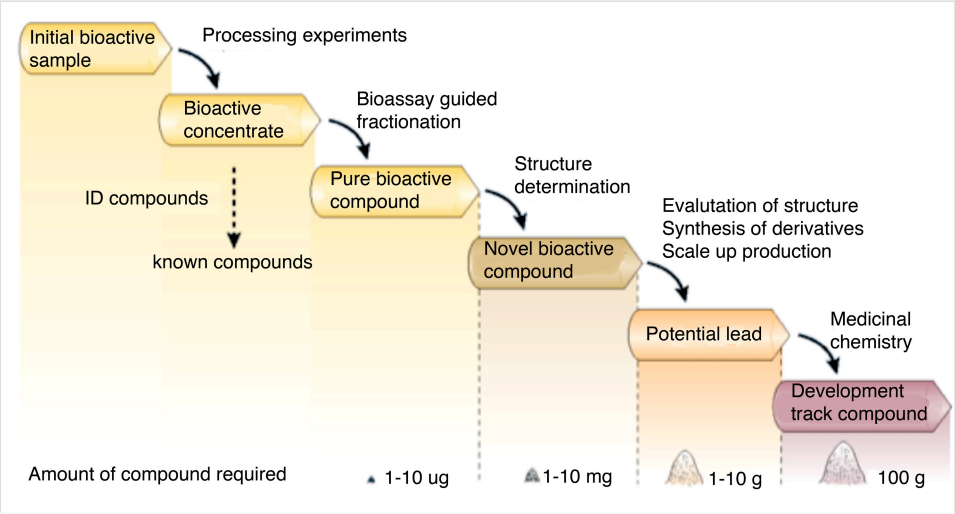

Figure 1.2. The basic steps and amount of compound needed in the process from identification of a bioactive compound to lead optimization and pre-clinical studies. As the drug discovery process progresses from the initial crude discovery to a lead candidate undergoing further development and pre-clinical studies, more and more pure compound is required. [21]

A promising solution to the supply issue is the identification and heterologous expression of the gene clusters associated with the molecules into a suitable host [47]. While this approach provides tremendous control over the production of a compound and even affords the manipulation of the cluster for the biosynthesis of new analogs, the experimental methods have not been worked out, as of yet, for certain cyanobacteria, sponges and their symbionts and other less well studied organisms that are often the most promising sources[48,49]. However, with the current pace of genome sequencing and advances in genetic manipulation, the future certainly looks bright for marine based natural products efforts.

A second hurdle for the marine natural products field is the question of true biosynthetic origin. While this issue is not exclusive to the marine realm (e.g.

although originally isolated from *Taxus brevifolia*, the biosynthetic origin of paclitaxel (Taxol) continuous to be a point of contention), the density and the interrelationships of many of marine organisms can be a dizzying issue. Thus, assigning a biosynthetic origin to a natural product, especially in the absence of genomic information, is difficult at best [29]. With an understanding of the biosynthetic mechanisms and tailoring enzymes necessary to produce a molecule, close inspection of the literature suggests many of the reported sources for marine natural products do not have the necessary synthetic machinery to produce the compounds [29,50]. As can be seen in Figure 1.3, a recent analysis of 20 marine natural products in clinical or pre-clinical trials for cancer exposed that although 60% are reported to come from macroorganisms and 25% from microorganisms, the biosynthetic origin is closer to 20% from macroorganisms and 80% from microorganisms [50]. Even a cursory glance at cyanobacterial natural product literature reveals many natural products have been isolated from mixed assemblages of two or more species [51-54]. In short, the body of work regarding the true biosynthetic origin of many marine natural products has been described as “a morass” (William Gerwick). Clearly, much work remains in both identifying the origins of bioactive natural products and solving the issue of supply. Fortunately, as discussed later, there are genomic and mass spectrometric approaches that have begun addressing these long standing hurdles in marine natural products research.

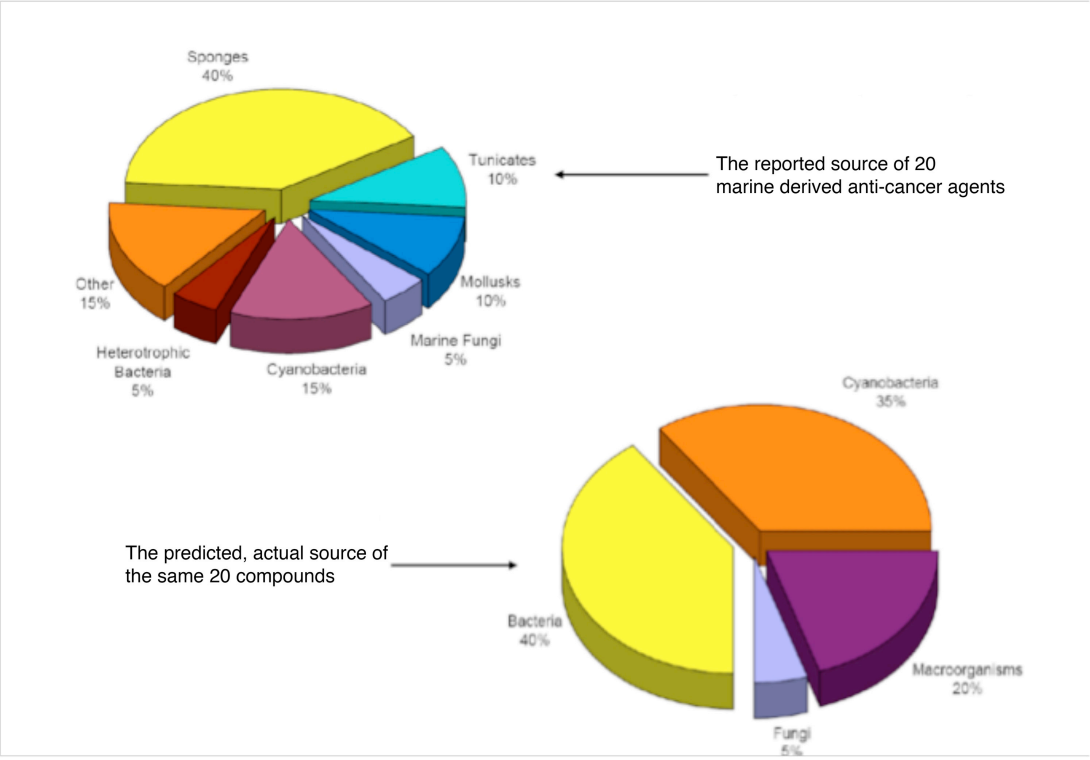

Figure 1.3. Disconnect between the reported sources of marine derived anti-cancer agents and their biosynthetic source.
Adapted from [50]

1.3 The natural product discovery and isolation process

It is thought that through a process of trial and error, the earliest cultures identified and recorded plants, organisms, and fungi (i.e *De materia medica libri quinque*) that were likely to have beneficial properties. These initial preparations included aqueous (teas and decoctions) and alcoholic extracts (tinctures) [1]. It wasn't until the 1800's that these same preparations would be the starting point for more rigorous isolation methods. The initial isolation and purification approaches relied on a better understanding of organic chemistry, including more refined solvents and purification steps [55]. However, the elucidation of the chemical structures of the

purified compounds was a different matter altogether. From the late 1800's to the first half of the 1900's, revealing the structural features of a molecule relied on degradation and derivatization approaches to explore structural possibilities, an approach that relied on huge amounts of compound by today's standards. The entire structural elucidation process could take years and stereochemical configurations were largely non-existent [56].

1.3.1 Modern Methods- the rise of Spectroscopy and Bioassay Guided Fractionation

In the middle of the 20th century, the process of identification and structure elucidation of natural products changed dramatically. The development of spectroscopy (especially Nuclear Magnetic Resonance or NMR) and X-Ray crystallography, in conjunction with mass spectrometry (MS) and chromatography, simplified the process and allowed compounds in smaller quantities to be purified and their structures elucidated, accelerating the field [39]. By the 1970's, roughly the time that marine natural products research gained momentum, a well-defined, systematic approach to the discovery of bioactive compounds began to take shape. Two main approaches have defined which sources to use: the source has been utilized by a community for a specific purpose or perhaps avoided because of its toxicity[1] (ethnobotany or ethnopharmacology, more common for land organisms), or random screening of likely organisms and plants (chemotaxic knowledge)[21,57] . Regardless of the source, once the crude extract is shown to have some activity in a biological assay, different solvents (ethanol, methanol, hexanes, etc) are used to fractionate the crude

extract into its different components based on polarity, or other molecular properties. The resulting fractions are again tested for the same biological activity[21]. These steps are repeated until the compound responsible for the activity has been identified; further purification(s) are achieved using a variety of chromatographic approaches until the compound is pure and ready for structure determination, typically using NMR and MS (Figure 1.4). This process, known as bioassay guided fractionation is, and has been, the standard for the field and is very efficient at honing in on a compound with a demonstrated bioactivity, leading to the discovery of many natural products that have advanced to clinical trials [5,58,59].

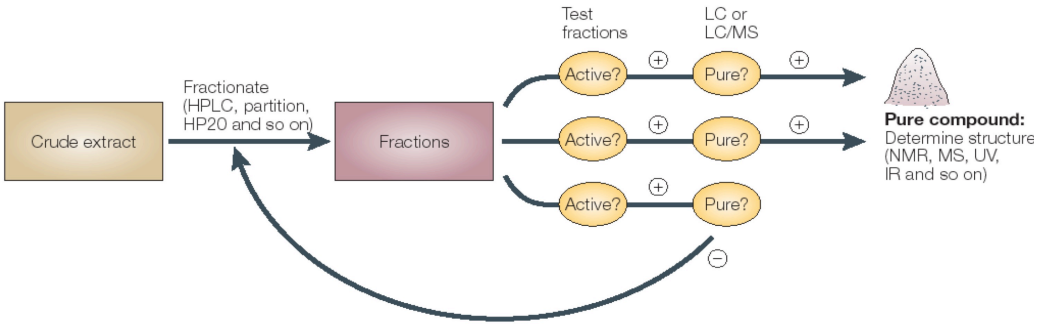

Figure 1.4. Bioassay guided fractionation.
Once a crude extract has been shown to have activity, it is fractionated or partitioned into several components (usually based on polarity). These fractions are again tested for the same bioactivity and the candidate fractions are subjected to further chromatography to assess purity. The process is repeated until the compound responsible for the activity has been isolated and deemed pure enough for structure elucidation.[21]

It was apparent from the earliest efforts in marine natural products isolation that although certainly novel, these marine metabolites were often found in very small amounts [39]. Looking back at the history of the discovery process, it appears that the

most significant progress in the field has coincided with the development and implementation of novel technology that didn't rely on vast quantities of compound. Spectroscopy, Nuclear Magnetic Resonance, Mass Spectrometry (MS), Chromatography (LC, HPLC, VLC, etc) have made the identification, purification, and structural elucidation of even less abundant secondary metabolites a relatively straightforward process [39], leading to the discovery of nearly 22,000 compounds. derived from 3,700 species, 2,255 genera and 40 phyla (MarinLit). Looking ahead, several modern advances in detection technology and in genomics will similarly have a tremendous impact on this field.

1.3.2 The promise of the post-genomics era

With the end goal of medicinal discovery, the bioassay-guided approach effectively ignores more subtle aspects of the isolated compounds, or less abundant (and perhaps more potent) molecules. By focusing on a single or small group of compounds and their bioactivity in an assay with relevance to humans, little information is gained regarding the presence of and relation to other metabolites, or aspects pertaining to their production or distribution within the organism.

The current revolution in genomics and metabolomics (the study of the suite of metabolites produced by an organism) have already impacted the field in profound ways. Microorganism derived natural products are typically encoded by polyketide synthase (PKS), non-ribosomal peptide synthetase (NRPS), or hybrids of these two modular systems of molecule assembly [60]. Fortuitously, these genes are often arranged

as a cluster within the genome, allowing relative ease of identification. Analysis of the genomes of marine microorganisms (and non-marine) known for producing natural products, such as *Salinospora arenicola* [61](Figure 1.5) and *Lyngbya majuscula* 3L (Monroe and Jones, in progress) among others, highlights the need for a more complete understanding of the metabolomes of these fascinating organisms [62]. Figure 1.5 shows the annotated genome of the marine obligate bacterium *Salinospora arenicola*. Underlined in red are the known gene clusters for the natural products cyclomarin, rifamycin and staurosporine, however there are several indications of other natural product gene clusters (labeled with PKS/NRPS). The products of these "cryptic" or silent clusters is unknown, but it is likely that they encode novel natural products that may be produced at either very low concentrations, under specific conditions, or are not active within the genome.

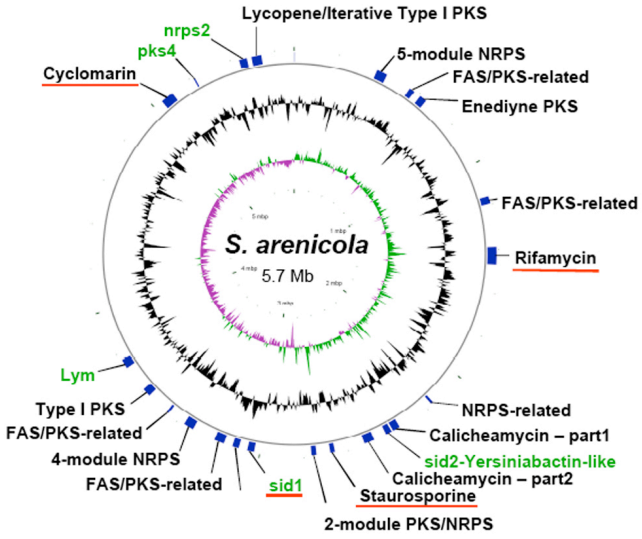

Figure 1.5. The *Salinospora arenicola* genome.
The gene clusters for known natural product are underlined in red, numerous unknown natural product gene elements (PKS/NRPS) are found in this genome, highlighting the presence of numerous orphan cluster and untapped biosynthetic potential.[61]

The discovery of Orfamide A through genomic sequencing is a prime example of how genomic information like this can lead to the identification and isolation of a novel metabolite [63]. After identifying a cryptic cluster in the genome of *Pseudomonas fluorescens* and predicting the amino acid composition of the encoded metabolite, the authors provided an isotopically labeled precursor likely to be used in its biosynthesis. By following the isotope label and a predetermined bioactivity in an assay-guided approach, Orfamide A was discovered [63].

While it is clear we have only scratched the surface regarding the number of marine organisms capable of producing biomedically useful compounds, it is now evident that even in the organisms that are well studied, we again have a limited perspective [64]. The focus on major secondary metabolites amenable to the bioassay-guided isolation process and the presence of these cryptic clusters suggests that much is left to discover regarding the secondary metabolic capacity of many of these microorganisms [65]. In this regard, genomics has already provided a leap forward in the ability to assess this capacity.

In addition to identifying new cryptic metabolites, knowing the genes associated with a natural product of interest is the first step in creating a heterologous expression system[60]. Once the genes have been identified and the biosynthetic flow understood, integrating and expressing the cluster into a host that can be easily grown and genetically manipulated can yield , in principle, copious end product as well as

permit modifications to the original structure [60,61,64].

1.3.3 Metagenomics

As mentioned previously, the density and interrelationships of the microorganisms (and macroorganisms) in the marine environment makes the biosynthetic source of a secondary metabolite very difficult to pinpoint [29]. However, it also implies a rich, small-molecule dance, where nutrients and secondary metabolites with mysterious and subtle endogenous roles are in a constant flux in spatially minute ecosystems, resulting in complex chemical displays of symbiosis[66].

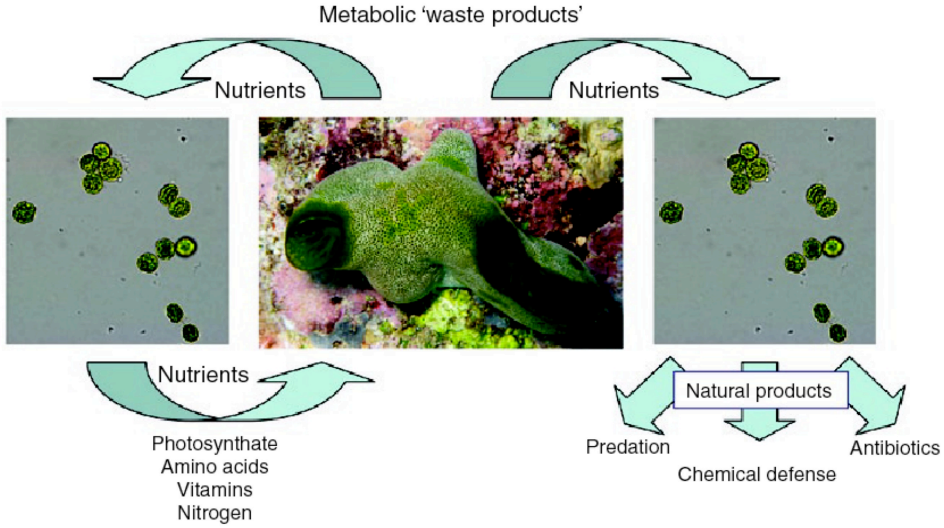

Figure 1.6. Symbiotic metabolism.
The tunicate (middle) exchanges nutrients with symbionts, such as the *Prochloron* cyanobacteria shown on the left side, or provides nutrients or metabolic precursors for the production of natural products with various roles, as shown on the right. Very little is actually known about the roles of the natural products or the extent of nutrient exchange. [66]

Assessing the biosynthetic capacity of the whole system, and not just one

individual, could provide a wealth of new molecules and a much greater understanding of marine chemical ecology [64,65]. Instead of relying on the analysis of the genomes of individual organisms, the metagenomic approach relies on a broader assessment of the genetic capacity of a complex environmental sample with multiple organisms. The total genetic information is sequenced into individual reads of varying lengths, creating a large library of genetic information with the amount of coverage for an individual species genome in proportion to its abundance in the sample [67-69]. Computationally driven processes can be used to reconstruct the pieces into larger fragments or whole genomes. Hybridization probes can be constructed for specific elements of a target cluster, like a unique enzyme, to begin to pull the genes out that are associated with the metabolites of interest [68-69].

In regards to the complex metabolic and chemical capacity of many marine organisms, the insight that genomic and genetic approaches are beginning to provide is certainly exciting. However, this information only provides part of the puzzle. A better understanding of the actual metabolite content of an organism, as well as how it is impacted by changes in the environment, including symbiotic relationships, is also needed. This will not only further refine the search for medically relevant compounds but also provide a better appreciation of the role of secondary metabolites in the marine environment [29]. Better instrumentation, sequencing and multi-disciplinary approaches are needed to really push the field forward and fulfill the potential of marine natural products [18,29]. One contributing dimension which is showing significant promise is modern mass spectrometry[29,70]; by allowing a wider range of

metabolites, in increasingly small amounts, to be detected in samples with minimal preparation, MS is a robust, analytical method that compliments genomics nicely.

1.4 Modern Mass Spectrometry in Natural Products Research

1.4.1 A Brief History of MS

Mass Spectrometry (MS) is analytical technique used to measure the mass to charge ratio of a charged molecule. The initial development of mass spectrometry occurred around the turn of the century by a combination of work from Eugen Goldstein, J.J. Thompson, W.Wien, and Francis William Aston among others [71,72]. These initial pioneers began exploring individual elements, the notion of isotopes, and developed the idea of the *m/z* ratio where *m* is the mass and *z* is the charge. Further work led to F.W. Aston receiving the Nobel Prize in 1922 for the isotopic composition of atoms and the idea that isotope masses are generally whole numbers [71].

Prior to 1960, MS was mainly confined to nuclear weapons work, the analysis of known hydrocarbons, petroleum associated products, and the efforts of chemical companies with little application to biomolecules [73]. Its lack of utilization in the life sciences stemmed from the idea that the majority of molecules of biological origin greater than 500 Da (and even smaller) were either not volatile enough, or too thermally labile to analyzed by MS [73,74]. These inherent characteristics prevented the compounds from being isolated out of an aqueous environment and then ionized and introduced into a vacuum chamber without excessive and random fragmentation [74]. In

a 1954 Nature paper, Beynon surmised that MS could be used for the analysis of unknown compounds, and devised theories regarding the nitrogen content (the nitrogen rule) and fragmentation patterns of organic molecules[75]. However, it wasn't until the 1960's, that true application of MS to structure elucidation of natural products began, mainly by analysis of fragments, with many initial examples described in Biemann's work[76].Most of these analyses were accomplished using Electron Ionization (Impact) Mass Spectrometry (EIMS), some of which was coupled to the first Time-of-Flight (TOF) analyzers. Field Desorption (FD) and Electrospray Ionization (ESI) were developed in the late 1960's by Beckey (FD) [75] and Malcolm Dole (ESI); these advancements were a leap forward in the range of molecules that could be ionized. From here on, MS instrumentation proliferated and became a mainstay in organic chemistry labs, with increasing use in the characterization of unknown natural products. The application to natural products research in the latter half of the 20th century was perhaps best explored and developed by R.Graham Cooks[73].

1.4.2 Soft ionization MS

In the 1980's three big advances in ion sources would change the range of application and the ease of use of mass spectrometry in the life and biological sciences. In the first of these, Fast Atom Bombardment (FAB), a non-volatile matrix is mixed with the sample, and then bombarded with atoms from inert gases under vacuum, causing ionization[77]. Although FAB has been used extensively and successfully in assigning precise molecular weights to natural products, it is being

supplanted by two newer developments, probably because of their ease of use and range of acceptable molecules. Matrix Assisted Laser Desorption Ionization (MALDI) first reported by Franz Hillenkamp, Michael Karas and co-workers in 1985 [78,79], uses a light-absorbing matrix to transfer laser energy into the analyte(s), and generally forms singly charged, un-fragmented ions from a wide range of molecules[74]. In 1989, John Bennett Fenn refined Electrospray Ionization (ESI) for use in larger biomolecules, this approach uses a small nozzle and a charged solvent spray to add charges to samples directly injected into the mass analyzer, a process allowing larger biomolecules to attain multiple charges, increasing the mass range of detectable molecules while avoiding fragmentation [80].

The development of soft ionization sources and their implementation to the life sciences was a huge advancement in the field of mass spectrometry. Of these, ESI and MALDI, allow a very wide range of non-volatile and thermally-labile molecules of biological origin (from very small metabolites to proteins and complexes larger than 150 kDa) to be successfully ionized into the gas phase, an impressive feat considering the "softness" which allows bonds to remain intact, effectively eliminating fragment ions that complicated earlier MS approaches (Electron Impact)[74]. The applications and impact were obvious, as suddenly almost any molecule produced by a living system could be ionized and its mass (very) accurately measured. Almost as impressive was the speed at which companies produced the equipment and its ease of use. The technology reached the hands of both industry and academia quickly, where it has since been effectively implemented by non-MS-experts in life sciences. These

ionization developments were awarded the Nobel Prize in 2002 [81,82].

Not surprisingly, the use of soft-ionization sources in the natural product discovery process became more commonplace. In recent years, ESI coupled to liquid chromatography (LC or HPLC) and UV/IR photodiode array components facilitates the detection, isolation and purification process by allowing the separation of a target metabolite from a more complex mixture in the bioassay-guided approach [83]. MALDI, FAB and ESI sources coupled to high resolution and MS/MS capable mass analyzers have also been extensively used in molecular formula assignment [83,84], structure determination by analysis of intentional fragmentation [85], and the analysis of biosynthetic machinery of natural products [86].

1.4.3 *MALDI-TOF Fingerprinting*

MALDI-Time of Flight (TOF) is a very sensitive ionization mechanism, requiring only trace amounts of a compound to achieve a clear mass to charge (*m/z*) signal, or isotopic cluster, from a single sample [87, 88]. Perhaps more importantly, many of the metabolites present in a sample can be detected concurrently in one pass. Complex mixtures and salt contamination do not pose significant hurdles in most cases, allowing minimal sample preparation and subsequent ease in data analysis [87]. A schematic diagram of the basic MALDI-TOF process is shown in Figure 1.7.

In 1997 Marcel Erhard, Hans von Doren and Peter Jungblut reported the use of MALDI-TOF MS for "Rapid typing and elucidation of new secondary metabolites of intact cyanobacteria," providing the first example of using MALDI to fingerprint the secondary metabolites of microorganism in an crude, intact sample. As mentioned

previously, up until this point the detection of these smaller secondary metabolites was performed by bioassays and/or chromatographic approaches such LCMS and HPLC

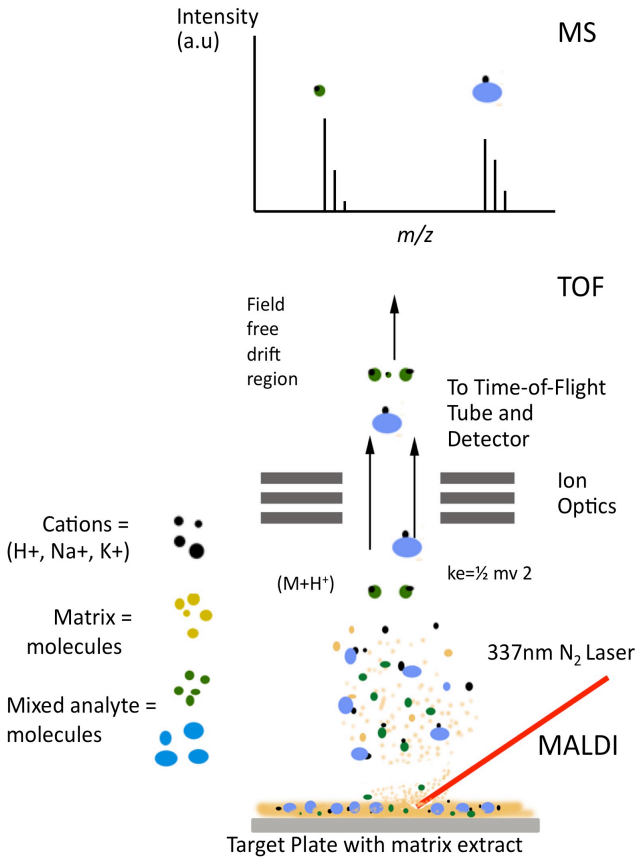

Figure 1.7. A basic diagram of the MALDI-TOF process.
A sample (which might contain mixed analyte molecules) is prepared with a light adsorbing matrix, deposited on a conductive target plate and introduced into a stage under vacuum. When the laser hits the mixed sample, the light energy is adsorbed by the matrix and a plume composed of the mixed analyte and matrix molecules is created. Ionization is thought to occur within this plume (if it hasn't up to this point). The plume is accelerated into the time-of-flight (TOF) tube by a voltage differential between the plate and the entrance to the mass spectrometer and again within the ion optics. Once in the TOF tube, the ions containing this initial kinetic energy are freed from the electric field and are allowed to drift, becoming separated by mass and charge (most commonly +1), until they contact the detector.

that require extraction steps, time and larger amounts of material. By interrogating

intact cyanobacteria using MALDI-TOF MS, Erhard et.al. were able to not only identify known secondary metabolites but also unknown constituents without the need for chromatography or large amounts of material [87], opening up MALDI-TOF as an analytical tool with strong metabolomic capacity in natural products research. Since then, several other studies "fingerprinting" secondary metabolites using MALDI-TOF have been performed in various natural product producing organisms, including bacteria, sea cucumbers, bacterial sponge isolates, and plants[89-92].

1.4.4 Natural product MALDI imaging

Another benefit of the MALDI ionization mechanism is its ability to be used as an imaging probe. Briefly, a thin section of a sample is covered with a homogenous coat of matrix, the sample is introduced into the spectrometer and the laser is targeted across the sample in a predefined raster [93, 94]. A full mass spectrum is recorded at each raster spot, the presence or absence of the various *m/z* values can then be examined at each raster spot, creating a two-dimensional map of the distribution of the ions that can be easily visualized with appropriate software [93-95]. This idea, largely credited to the lab of Richard Caprioli at Vanderbilt University, has been used extensively in imaging tissues from a variety of preparations to localize specific proteins, peptides, biomarkers as well as the location and accumulation of drug metabolites [93, 95].

The first reported experiments applying MALDI imaging to marine natural products is provided in this dissertation and has been further developed by Pieter Dorrestein's lab at UC San Diego [94,96,97]. Also recently, Desorption Ionization Mass Spectrometry (DESI), developed by the laboratory of Graham Cooks, has also been

used an imaging probe [98]. In this case, the authors explored the presence and distribution of bromophycolides, brominated diterpenes with putative antifungal activity produced by *Callophycus serratus* [98, 99], and found their distribution to be limited to the surface of the algae in concentrations sufficient to thwart fungal growth [98]. The ability to visualize the distribution of many compounds in a single preparation of an organism with a very active, small-molecule, metabolome has been likened to having "molecular eyes" and indeed provides a new tool by which to understand and explore natural products and their sources.

The initial findings utilizing soft-ionization sources that allow multiple metabolites to be analyzed concurrently further underscore the complexity, number and dynamic nature of the secondary metabolites from marine natural product-producing organisms. Multi-disciplinary approaches that can combine genomics, metabolomics and modern mass spectrometry with traditional natural products research will greatly enhance our understanding of marine natural products and their sources.

1.5 Dissertation Contents

Chapter 2 represents the major element of the dissertation and describes a novel approach to study the dynamics of biosynthesis of natural product production in cultured marine filamentous cyanobacteria, prolific producers of scores of bioactive secondary metabolites. The approach relies in replacing the available nitrogen content of the growth media with an isotopically labeled version ($^{15}N\ NaNO_3$). The

incorporation of the heavier label into many of the nitrogen containing metabolites can be followed *in-vivo* by analyzing whole cells over time by MALDI-TOF MS. Although not absolutely quantitative, the resulting data sets are incredibly rich, not only yielding the dynamics of biosynthesis and turnover of both known and unknown metabolites, but also the relationships in production between various secondary metabolites, as well as the primary metabolite chlorophyll. In this chapter I explored the differences in production rate of various important natural products from *Lyngbya* strains, drilled down into the temporal nuances between jamaicamides A and B, and explored factors that impact their biosynthesis. These findings are useful in efforts to increase natural product yields from cultures of these slow growing organisms. On a broader note, this approach provides an experimental paradigm allowing growth and the biosynthesis of a primary metabolite (chlorophyll) to be compared with the production of secondary metabolites and could be useful in assigning ecological roles to natural products as well as tracking nutrients in complex symbiotic interactions. A condensed version of this chapter has been submitted, and reviewed, at the *Proceedings of the National Academy of Sciences* and is currently undergoing minor revisions. The appendix for Chapter 2 contains the results of various experiments manipulating culture conditions to determine the effect on jamaicamide B production as measured by the ^{15}N labeling approach, a brief description of the discovery of cryptomaldamine from JHB, which originated from these data sets and initial ^{15}N labeling and growth experiments using *L. majuscula* 3L.

Chapter 3 contains the second major element in the dissertation and similarly

relies on MALDI-TOF MS. This chapter, published in the journal *Molecular Biosystems* in 2008 was in the top 50 most cited Royal Society of Chemistry (RSC) articles of the year. The reason behind this surprising level of interest is simple: it is the first published work to use imaging mass spectrometry to really explore natural products, marine or otherwise. Besides detailed methodology, the chapter includes some interesting results showing the spatial distribution of known, biomedically active, natural products on whole filaments of various *Lyngbya* strains. It also contains MALDI imaging results from the marine sponge *Dysidea herbacea,* clearly showing the presence of many unknown or unidentified metabolites specifically located within a thin-section of sponge. Perhaps more importantly, the results confirm the presence of complex and varied chemical microenvironments within sponge samples. These results provide the first insight and experimental approach that, paired with metagenomics and genomisotopic studies, might begin to address the metabolic exchange of complex marine assemblages depicted in Figure 2. The appendix that follows Chapter 3 contains more MALDI imaging results and pilot studies, including an attempt to provide greater understanding into the distribution and origin of kahalalide F, a promising anti-cancer agent in late stage clinical trials, within the nudibranch *Elysia rufescens* and its foodsource *Bryopsis pennata*. Although some appreciation for its distribution was achieved with the approach, it is likely that fresh or live samples might yield more conclusive results. Also within this appendix are encouraging results regarding the heterogenous distribution and possibly production of natural products in marine cyanobacteria.

Chapter 4 describes work that is being prepared for submission. Filamentous cyanobacteria are naturally encased by a polysaccaride sheath which has been shown to play host to a variety of heterotrophic bacteria. The possibility of natural products attributed to the cyanobacteria actually being produced by these symbionts remains unclear, especially since the genomes of most of these organisms have not been described. Using a dissecting microscope and micromanipulation, single cells from filaments of two strains of *Lyngbya* were isolated and cleaned, and run by MALDI-TOF MS. The high concentration of various secondary metabolites within the cells in combination with the sensitivity of instrument yielded positive identification of several natural products within these preparations. The single-cell MALDI approach was combined with ^{15}N incubation of the parent culture, as described in chapter 2, to show that the cells contained freshly biosynthesized compounds. More importantly however, is the initial finding that only some cells contained all metabolites at high enough concentrations to be detected, while others only contained one or two of the expected compounds. These pilot studies are in agreement with the MALDI imaging results showing that there is a heterogenous distribution of secondary metabolites in various species of cyanobacteria (appendix of chapter 3).

Chapter 5 is a brief chapter that has been submitted to *Chemical Communications*. This proof-of-concept work was performed in conjunction with Waters Corporation and describes how Ion-Mobility Mass Spectrometry, using both ESI and MALDI ion sources, can facilitate the dereplication and identification of halogenated metabolites from crude whole cell samples (MALDI) and cleaner extracts

(ESI) of marine cyanobacteria. Briefly, the presence of halogen atoms, which are generally heavier than other atoms, on a small molecule, changes its mass in disproportion to its cross-sectional area. This effect was also seen with cyclizations. This anomaly results in halogenated and possibly cyclic molecules behaving differently in the Ion-Mobility chamber, resulting in a further separation from other metabolites present in a crude mixture.

1.6 CHAPTER 1 REFERENCES

1. L. Aikman, “Nature’s healing arts. From folk medicine to modern drugs” Special Publications Division, National Geographic Society, Washington D.C., (1977).

2. A. Luch, “Molecular, clinical and environmental toxicology,” Springer. (2009): 20.

3. D.B Jack, “One hundred years of aspirin” *Lancet* 350 (1997): 437-439.

4. J.F. Fries, “The Compression of Morbidity” *Milbank Quarterly* 83 (2005): 801–823.

5. D.J. Newman, G.M. Cragg, “Natural Products as Sources of New Drugs over the Last 25 Years” *J Nat Prod.* 70, (2007): 461-477.

6. D.J. Newman, G.M. Cragg, K.M. Snader “Natural Products as Sources of New Drugs over the Period 1981−2002” David J. Newman,,, Gordon M. Cragg, and, Kenneth M. Snader, *J Nat Prod.* 66 (2003): 1022-1037.

7. D.J. Newman, P.G. Grothaus, G.M. Cragg, “Impact of Natural Products on Developing New Anti-Cancer Agents” *Chemical Reviews* 109 (2009): 3012-3043.

8. M. Wani, H. Taylor, M. Wall, P. Coggon, A. McPhail, “Plant antitumor agents. VI. The isolation and structure of taxol, a novel antileukemic and antitumor agent from *Taxus brevifolia*” *J Am Chem Soc* 93 (1971): 2325–2327.

9. D.Starling, “Two ultrastructurally distinct tubulin paracrystals induced in sea-urchin eggs by vinblastine sulphate" 20 *J Cell Sci.* (1976): 79–89.

10. R. Woodward, W. Doering, “The Total Synthesis of Quinine” *J Am Chem Soc*. 66 (1944): 849.

11. “WHO Model List of Essential Medicines” 16th edition (2009)"

12. L.P. Garrod, “Erythromycin” *British Medical Journal* (1957).

13. M.G. Watve, R. Tickoo, M.M. Jog, B.D. Bhole “How many antibiotics are produced by the genus Streptomyces?” *Archives of Microbiology* 176 (2001): 386-390.

14. A. Endo, “The origin of the statins” *Atheroscler Suppl.* 5 (2004): 125–130.

15. R.T. Morrison, R.N. Boyd, R.K. Boyd, “Organic Chemistry, 6th edition” Benjamin Cummings, (1992).

16. J.R. Archer, “ASSAY and Drug Development Technologies” 2 (2004): 675-681.

17. H.J. Federse, “Process R&D under the magnifying glass: Organization, business model, challenges, and scientific context” *Bioorganic and Medicinal Chemistry* 18 (2010): 5775-5794

18. J.W.H. Li, J.C. Vederas, “Drug Discovery and Natural Products: End of an Era or an Endless Frontier?” *Science* 325 (2009): 161-165.

19. “Ecological Roles of Marine Natural Products” Valerie Paul ed. Cornell University Press. Ithaca NY (1992)

20. J. Gershenzon, N. Dudareva, “The function of terpene natural products in the natural world” *Nat Chem Bio.* 3 (2007): 408-414.

21. F.E. Koehn, G.T. Carter, “The evolving role of natural products in drug discovery” *Nat Rev Drug Disc*. 4 (2005): 206-220.

22. K.J. Weissman, P.F. Leadlay, “Combinatorial biosynthesis of reduced polyketides” *Nat Rev Mic* 3 (2005): 925-936.

23. M. Feher, J.M. Schmidt “Property distributions: Differences between drugs, natural products, and molecules from combinatorial chemistry” *J Chem Inf Comput Sci.* 43 (2003): 218–227.

24. C.A. Lipinski, F. Lombardo, B.W. Dominy, P.J. Feeney “Experimental and computational approaches to estimate solubility and permeability in drug discovery and development settings” *Adv Drug Del Rev.* 23 (1997): 3–25.

25. M.L. Lee, G. Schneider “Scaffold architecture and pharmacophoric properties of natural products and trade drugs: Application in the design of natural product-based combinatorial libraries” *J Comb Chem.* 3 (2001): 284–289.

26. F. Stahura, J.W. Godden, X. Ling, J.Bajorath “Distinguishing between natural products and synthetic molecules by descriptor Shannon entropy analysis and binary QSAR calculations” *J. Chem. Inf. Comput. Sci.* 40 (2000): 1245–1252.

27. T. Henkel, R. Brunne, H. Muller, F. Reichel "Statistical investigation of structural complementarity of natural products and synthetic compounds" *Angew Chem Int Ed. Engl.* 38 (1999): 643–647.

28. P.R. Jensen, T.J. Mincer, P.G. Williams, W. Fenical "Marine actinomycete diversity and natural product discovery" *Antonie van Leeuwenhoek* 87 (2005): 43-48.

29. T.L. Simmons, R.C. Coates, B.R. Clark, N. Engene, D. Gonzalez, E. Esquenazi, P.C. Dorrestein, W.H. Gerwick "Biosynthetic origin of natural products isolated from marine microorganism-invertebrate assemblages" *Proc Nat Aca. Sci USA.* 105 (2008): 4587-4591

30. Wikipedia: Timeline of evolution

31. W. Bergman, R.J. Feeney "Nucleosides of sponges" *J Org Chem*. 16 (1951): 981–987.

32. D.J. Faulkner "Interesting aspects of marine natural products chemistry" *Tetrahedron* 33 (1977): 1421-1443.

33. "Special Issue in Honor of Professor Kenneth L. Rinehart." *J Nat Prod* 70 (2007): 329-331

34. R.E. Moore "Toxins from Blue-Green Algae" *BioScience* 27 (1977): 797-802.

35. Marine natural products. IV. Prepacifenol, a halogenated epoxy sesquiterpene and precursor to pacifenol from the red alga, *Laurencia filiformis*

36. J.J. Sims, W. Fenical, R.M. Wing, P. Radlick *Journal of the American Chemical Society* 95 (1973): 972-972 .

37. P.J. Scheur "Chemistry of marine natural products" (1973)

38. D. R. Hirschfeld, W. Fenical, G.H.Y. Lin, R.M. Wing, P. Radlick, J.J. Sims "Marine natural products. VIII. Pachydictyol A, an exceptional diterpene alcohol from the brown alga, *Pachydictyon coriaceum*" *Journal of the American Chemical Society* 95 (1973): 4049-4050.

39. D.J. Newman, G.M. Cragg "Marine natural products and related compounds in clinical and advanced preclinical trials" *J Nat Prod.* 67 (2004): 1216–1238.

40. G. P. Miljanich "Ziconotide: Neuronal Calcium Channel Blocker for Treating Severe Chronic Pain" *Current Medicinal Chemistry* 11 (2004): 3029-3040.

41. Y.Takebayashi, P.Pourquier, D.B. Zimonjic, K. Nakayama, S. Emmert, T. Ueda, Y. Urasaki, A. Kanzaki, S. Akiyama, N. Popescu, K. H. Kraemer, Y. Pommier "Antiproliferative activity of ecteinascidin 743 is dependent upon transcription-coupled nucleotide-excision repair" *Nature Medicine* 7 (2001): 961–966.

42. G.R. Pettit, C.L. Herald, D.L. Doubek, D.L. Herald, E.Arnold, J. Clardy "Isolation and structure of bryostatin 1" *Journal of the American Chemical Society* 104 (1982): 6846-6848.

43. T. Molinski "Drug development from marine natural products" *Nature Reviews Drug Discovery* 8 (2009): 69-85.

44. D.J. Newman, G.M. Cragg, "Marine Anticancer Compounds in the Era of Targeted therapies" 1st edn ed. Chapner, B. Permanyer Publications, Barcelona, (2008).

45. "First Census of Marine Life, 2010". J.H. Ausubel, D.T. Crist, P.E. Waggoner eds. Consortium of Ocean Leadership. NY, NY (2010).

46. A. Saklani, S. K. Kutty, *Drug Discov Today* 13 (2008).

47. S.C Wenzel, R. Müller, "Recent developments towards the heterologous expression of complex bacterial natural product biosynthetic pathways" *Current Opinion in Biotechnology* 16 (2005): 594-606

48. J.Piel, "Metabolites from symbiotic bacteria" *Nat Prod Rep.* 21 (2004): 519-538.

49. K.M. Fisch, C. Gurgui, N. Heycke, S.A. van der Sar, S.A. Anderson, V.L. Webb, S.Taudien, M. Platzer, B.K. Rubio, S.J. Robinson, P.Crews, J.Piel. "Polyketide assembly lines of uncultivated sponge symbionts from structure-based gene targeting" *Nature Chemical Biology* 5 (2009): 494-501.

50. T.L. Simmons, W.H. Gerwick, "Anticancer Drugs Of Marine Origin" in Oceans and Human Health, Risks and Remedies, P. Walsh, L. Fleming, H. Solo-Gabriele, W.H. Gerwick, eds., Elsevier Press (2008): 429-449.

51. L.M. Nogle, W.H. Gerwick, "Somocystinamide A, a novel cytotoxic disulfide dimer from a Fijian marine cyanobacterial mixed assemblage" *Organic Letters* 4 (2002): 1095-1098.

52. G.G. Harrigan, W.Y. Yoshida, R.E. Moore, D.G. Nagle, P.U. Park, J. Biggs, V.J. Paul, S.L. Mooberry, T.H. Corbett, F.A. Valeriote, "Isolation, structure determination, and biological activity of dolastatin 12 and lyngbyastatin 1 from *Lyngbya majuscula/Schizothrix calcicola* cyanobacterial assemblages" *Journal of Natural Products* 61 (1998): 1221-1225.

53. D.G. Nagle, P.U. Park, V.J. Paul, "Pitiamide A, a new chlorinated lipid from a mixed marine cyanobacterial assemblage" *Tetrahedron Letters* 38 (1997): 6969-6972.

54. D.G. Nagle, V.J. Paul, M.A. Roberts, "Ypaoamide, a new broadly acting feeding deterrent from the marine cyanobacterium *Lyngbya majuscula*" *Tetrahedron Letters* 37 (1996): 6263-6266.

55. E. Marris, "Drugs from the Deep" *Nature* 443 (2006): 904-905.

56. K.C. Nicolaou, and S.A. Snyder, "Chasing Molecules That Were Never There: Misassigned Natural Products and the Role of Chemical Synthesis in Modern Structure Elucidation" *Angewandte Chemie International Edition* 44 (2005): 1012-1044.

57. P.G. Waterman "Searching for Bioactive Compounds: Various Strategies" *J Nat Prod.* 53 (1990): 13-22.

58. F.E. Koehn, R.E. Longley, J.K. Reed, "Microcolins A and B, New Immunosuppressive Peptides from the Blue-Green Alga *Lyngbya majuscula*" *J Nat Prod* 55 (1992): 613-619.

59. W.H. Gerwick, P.J. Proteau, D.G. Nagle, E.Hamel, A.Blokhin, D.L. Slate "Structure of Curacin A, a Novel Antimitotic, Antiproliferative and Brine Shrimp Toxic Natural Product from the Marine Cyanobacterium *Lyngbya majuscula*" *J Org Chem*. 59 (1994): 1243-1245.

60. J. L. Fortman, D.H. Sherman, "Utilizing the Power of Microbial Genetics to Bridge the Gap Between the Promise and the Application of Marine Natural Products" *ChemBioChem* 6 (2005): 960-978.

61. D.W. Udwary, L. Zeigler, R.N. Asolkar, V. Singan, A. Lapidus, W. Fenical, P.R. Jensen, B.S. Moore, " Genome sequencing reveals complex secondary metabolome in the marine actinomycete Salinospora tropica" *Proc Natl Acad Sci USA* 104 (2007):10376-10381.

62. J.B. McAlpine, “Advances in the Understanding and Use of the Genomic Base of Microbial Secondary Metabolite Biosynthesis for the Discovery of New Natural Products” *J Nat Prod.* 72 (2009): 566–572.

63. H. Gross, V.O. Stockwell, M.D. Henkels, B. Nowak-Thompson, J.E. Loper, W.H. Gerwick, “The genomisotopic approach: a systematic method to isolate products of orphan biosynthetic gene clusters” *Chem Biol.* 14 (2007): 53-63.

64. G.M. Cragg, P.G. Grothaus, D.J. Newman, “Impact of Natural Products on Developing New Anti-Cancer Agents” *Chemical Reviews* 109 (2009): 3012-3043.

65. M.G. Haygood, E.W. Schmidt, S.K. Davidson and D.J. Faulkner, “Microbial Symbionts of Marine Invertebrates: Opportunities for Microbial Biotechnology” *J Molec Microbiol and Biotechnol* 1 (1999): 33-43.

66. E.W. Schmidt, “Trading molecules and tracking targets in symbiotic interactions” *Nature Chemical Biology* 4 (2008): 467-473.

67. M. Keller, K. Sengler, ”Tapping into microbial diversity” *Nature Reviews Microbiology* 2 (2004): 141-150.

68. J. Handelsman, M.R. Rondon, S.F. Brady, J. Clardy, R.M. Goodman, "Molecular biological access to the chemistry of unknown soil microbes: a new frontier for natural products" *Chemistry & Biology* 5 (1998): 245-249.

69. J. Handelsman “Metagenomics: Application of Genomics to Uncultured Microorganisms” *Microbiology and Molecular Biology Reviews* 68 (2004): 669-685.

70. R.D. Kersten, P.C. Dorrestein, “Secondary Metabolomics: Natural Products Mass Spectrometry Goes Global” *Chemical Biology* 4 (2009): 599-601.

71. K.M. Downard "William Aston - the man behind the mass spectrograph". *European Journal of Mass Spectrometry* 13 (2007): 177-190.

72. H. Budzikiewicz, R.D. Grigsby, “Mass spectrometry and isotopes: A century of research and discussion” *Mass Spectrom Rev*. 25 (2006): 146-57.

73. J.S. Grossert, “A retrospective view of mass spectrometry and natural products--sixty years of progress, with a focus on contributions by R. Graham Cooks” *International Journal of Mass Spectrometry* 212 (2001): 65-79.

74. “MALDI MS. A practical guide to instrumentation, methods and applications” F.Hillenkamp and J.Peter-Katalinic eds. WILEY-VCH Verlag GmbH & Co. Weinheim (2007).

75. H.D. Beckey, “Field ionization mass spectrometry” *Research/Development* 20 (1969): 26.

76. K. Biemann, “Mass Spectrometry: Organic Chemical Applications” McGraw-Hill, New York, (1962).

77. M. Barber, R.S. Bordoli, R.D. Sedgwick, A.N. Tyler, “Fast atom bombardment of solids as an ion source in mass spectrometry” *Nature* 293 (1981): 270-275.

78. M. Karas, D. Bachmann, F. Hillenkamp, "Influence of the Wavelength in High-Irradiance Ultraviolet Laser Desorption Mass Spectrometry of Organic Molecules". *Anal Chem.* 57 (1985): 2935-2939.

79. M. Karas, D. Bachmann, U. Bahr, F. Hillenkamp, “Matrix-Assisted Ultraviolet Laser Desorption of Non-Volatile Compounds” *Int J Mass Spectrom Ion Proc.* 78 (1987): 53-68.

80. J.B. Fenn, M. Mann, C.K. Meng, S.F. Wong, C.M. Whitehouse, "Electrospray ionization for mass spectrometry of large biomolecules". *Science* 246 (1989): 64–71.

81. J.B. Fenn, “Electrospray wings for molecular elephants (Nobel lecture),” *Angew Chem Int Ed.* 42 (2003): 3871–3894.

82. K. Tanaka, “The origin of macromolecule ionization by laser irradiation (Nobel lecture),” *Angew Chem Int Ed*. 42 (2003): 3861–3870.

83. T.L. Simmons, K.L. McPhail, E. Ortega-Barria, W.H. Gerwick, "Belamide A, a new cytotoxic tetrapeptide from a Panamanian marine cyanobacterium," *Tetrahedron Lett*. 47 (2006): 3387-3390.

84. D.J. Edwards, B.L. Marquez, L.M. Nogle, K. McPhail, D.E. Goeger, M.A. Roberts, W.H. Gerwick, “Structure and biosynthesis of the jamaicamides, new mixed polyketide-peptide neurotoxins from the marine cyanobacterium *Lyngbya majuscula*,” *Chem. Biol.* 11 (2004): 817-833.

85. W.T Liu, Y.L. Yang, Y. Xu, A. Lamsa, N.M. Haste, J.Y. Yang, J. Ng, D.Gonzalez, C.D. Ellermeier, P.D. Straight, P.A. Pevzner, J. Pogliano, V. Nizet, K.Pogliano, P.C. Dorrestein, “Imaging mass spectrometry of intraspecies metabolic

exchange revealed the cannibalistic factors of Bacillus subtilis.*" Proc. Nat. Acad. Sci. USA.*107 (2010): 16286-90.

86. P.C. Dorrestein, N.L. Kelleher, "Dissecting Non-ribosomal and Polyketide Biosynthetic Machineries Using Electrospray Ionization Fourier-Transform Mass Spectrometry," *Nat Prod Rep* 23 (2006): 893-918.

87. M. Erhard, H. von Dohren, and P. Junblut, "Rapid Typing and Elucidation of New Secondary Metabolites of Intact Cyanobacteria Using MALDI-TOF Mass Spectrometry," *Nature Biotechnology* 15 (1997): 906-9.

88. K. Hollywood, D.R. Brison, R. Goodacre, "Metabolomics: Current technologies and future trends" *Proteomics* 6 (2006): 4716-4723.

89. R. Dieckmann, I. Graeber, I. Kaesler, U. Szewzyk and H. von Döhren, "Rapid screening and dereplication of bacterial isolates from marine sponges of the Sula Ridge by Intact-Cell-MALDI-TOF mass spectrometry (ICM-MS*)*" *Applied Microbiology and Biotechnology* 67 (2005): 539-548.

90. F. Leenders, T.H. Stein, B. Kablitz, P.Franke , J.Vater, "Rapid typing of *Bacillus subtilis* strains by their secondary metabolites using matrix-assisted laser desorption/ionization mass spectrometry of intact cells" *Rapid Communications in Mass Spectrometry* 13 (1999): 943-949.

91. S.V. Dycka, P.Gerbauxb, P. Flammang, "Elucidation of molecular diversity and body distribution of saponins in the sea cucumber *Holothuria forskali* (Echinodermata) by mass spectrometry" *Comparative Biochemistry and Physiology Part B: Biochemistry and Molecular Biology* 152: 124-134.

92. P. Champy, V. Guérineau, O. Laprévote, "MALDI-TOF MS Profiling of *Annonaceous Acetogenins* in *Annona muricata* Products for Human Consumption" Molecules 14 (2009): 5235-5246.

93. L.A. McDonnell, R.M. Heeren, "Imaging mass spectrometry" *Mass spectrometry reviews* 26 (2007): 606-643.

94. E.Esquenazi, Y.L.Yang, J.Watrous, W.H. Gerwick, P.C. Dorrestein, "Imaging Mass Spectrometry of Natural Products" *Natural Product Reports* 26 (2009): 1521-1534.

95. D.S .Cornett, M.L. Reyzer, P. Chaurand, R.M. Caprioli, "MALDI imaging mass spectrometry: molecular snapshots of biochemical systems" *Nature Methods* 4 (2007): 828-833.

96. E. Esquenazi, C. Coates, T.L. Simmons, D. Gonzalez, W.H. Gerwick, P.C. Dorrestein, “The spatial distribution of secondary metabolites produced by marine cyanobacteria and sponges via MALDI-TOF imaging” *Molecular Biosystems* 4 (2008): 562-570.

97. Y.L. Yang, Y.Xu, P. Straight & Pieter C Dorrestein, “Translating metabolic exchange with imaging mass spectrometry” *Nature Chemical Biology* 5 (2009): 885-887.

98. E.Esquenazi, P.C. Dorrestein, W.H. Gerwick, “Probing marine natural product defenses with DESI-imaging mass spectrometry” *Proc Natl Acad Sci USA* 106 (2009): 7269-7270.

99. A.L. Lane, L. Nyadong, A. S. Galhena, T.L. Shearer, E.P. Stout, R.M. Parry, M. Kwasnik, M.D. Wang, M.E. Hay, F.M. Fernandez and J. Kubanek, “Desorption electrospray ionization mass spectrometry reveals surface-mediated antifungal chemical defense of a tropical seaweed” *Proc Natl Acad Sci USA* 106 (2009): 7314.

2.0 CHAPTER 2

TEMPORAL DYNAMICS OF NATURAL PRODUCT BIOSYNTHESIS IN MARINE CYANOBACTERIA

2.0.1 Abstract

Sessile marine organisms are prolific sources of biologically active natural products. However, these compounds are often found in highly variable amounts, with the abiotic and biotic factors governing their production remaining poorly understood. We present an approach that permits monitoring of *in vivo* natural product turnover and production using mass spectrometry and stable isotope (^{15}N) feeding with small cultures of various marine strains of the natural product-rich cyanobacterial genus *Lyngbya*. A temporal comparison of the amount of *in vivo* ^{15}N labeling of nitrogen-containing metabolites represents a direct way to discover and evaluate factors influencing natural product biosynthesis, as well as the timing of specific steps in metabolite assembly, and is a strong complement to more traditional *in vitro* studies. Relative quantification of ^{15}N labeling allowed the comparison of rates of turnover of multiple natural products from small amounts of biomass and provided new insights into the biosynthetic timing of jamaicamide A bromination.

2.1 Introduction

The secondary metabolites of marine organisms are a valuable and inspirational source for a host of biomedical and technological applications. Since the emergence of marine natural products research as a discipline 40 years ago,

approximately 17,000 compounds have been isolated from a variety of prokaryotic and eukaryotic organisms, and several of these have advanced from initial evaluations of bioactivity to preclinical and clinical trials that target specific diseases.[1, 2] Of prokaryotic marine natural products identified and evaluated for their biomedical potential, it is estimated that approximately 40% are of cyanobacterial origin.[3]

Important advances in exploring the biosynthesis of cyanobacterial compounds have been achieved in the past decade, coinciding with new developments in the areas of genetics and genomics. Gene clusters encoding the production of the freshwater hepatotoxins microcystin [4, 5] and nodularin[6] have been identified, as well as several from the marine cyanobacterium *Lyngbya majuscula* (Gomont), including those for the molluscicide barbamide,[7] cancer cell toxin curacin A,[8] dermatotoxin lyngbyatoxin,[9] antifungal agent hectochlorin[10] and the neurotoxins jamaicamides A-C.[11] Cyanobacterial natural product gene clusters are typically composed of mixed polyketide synthases (PKS) and non-ribosomal peptide synthetases (NRPS), and often include several enzymatic reactions rarely seen in any other bacterial system.[12-16]

One of the most significant impediments to further pursuit of cyanobacterial lead compounds for biotechnological applications is the problem of supply.[17] Filamentous cyanobacteria of the orders Nostocales and Oscillatoriales produce the majority of cyanobacterial natural products,[18] but many of these grow very slowly in laboratory culture (with doubling times of 20 days in some cases).[19] Overall compound yield from cultured material is typically low, meaning that expensive and difficult chemical synthesis or repeated field collections are required to obtain

sufficient material for downstream purposes. Although genetic manipulations have been developed for some freshwater filamentous cyanobacteria,[20, 21] no transformations of DNA into filamentous marine cyanobacteria have been accomplished to date. If natural product yields from cultured cyanobacteria are to be increased through changes in culture conditions, it is essential to have a reliable method to determine what factors directly impact the rate of metabolite biosynthesis and ultimately contribute to the generation of more isolated compound.

The marine cyanobacterial genus *Lyngbya* represents one of the most important sources of cyanobacterial natural products yet discovered. Over 700 compounds with a wide range of bioactivities have been isolated from *Lyngbya* collections from tropical locations worldwide.[22, 23] Our laboratory has been successful in growing a variety of marine *Lyngbya* strains.[24, 25] The stability of *Lyngbya* filaments in culture, coupled with reliable growth rate measurements of filaments using digital images, provides for a powerful model system with which to conduct further investigation into the dynamics of natural product biosynthesis. By replacing virtually all of the available nitrogen in the culture media with [^{15}N]$NaNO_3$, it is possible to monitor the rate of biosynthesis of various nitrogen containing molecules by mass spectrometry. There have been previous reports of using ^{15}N to track the biosynthesis of chlorophyll and its derivatives in cyanobacteria[26, 27] as well as in plants.[28] Recently, specific natural products produced by *Lyngbya* and located within the confines of its polysaccharide sheath have been visualized directly using Matrix Assisted Laser Desorption Ionization (MALDI) imaging techniques,[29, 30] confirming

that MALDI approaches can be used to study small molecules in these prokaryotic organisms. MALDI-Time of Flight (TOF) is a sensitive ionization mechanism, requiring only minimal amounts of compound to achieve a clear mass to charge (*m/z*) signal, or isotopic cluster, of a broad range of small molecules from a single sample.[31, 32] Complex mixtures and salt contamination do not pose significant hurdles in most cases, allowing minimal sample preparation and subsequent ease in data analysis.[33] The combination of these attributes enables the efficient monitoring of large numbers of samples for *m/z* shifts that accompany biosynthesis of nitrogen-containing metabolites in small, [^{15}N] $NaNO_3$-enriched cultures of *Lyngbya*. By comparing the changes in the isotopic profiles of metabolites, such as pheophytin *a*, a stable breakdown product of chlorophyll *a*[34, 35] and various other metabolites, it is possible to determine the percentage of ^{15}N labeling (representing new biosynthesis) of each compound at various time points and, in turn, gain insight into their turnover rates *in vivo*.

Although understanding the time course and factors influencing the production of cyanobacterial natural products is important for determining ecological functions of compounds, as well as how to modify yields from laboratory cultures, an experimental framework by which to reliably measure their production *in vivo* has been lacking. Presented here is an approach that permits monitoring the net production (turnover) of nitrogen-containing metabolites, as well as the relationships between growth and primary and secondary metabolism, under different experimental conditions. By growing *Lyngbya* cultures in ^{15}N-enriched growth media and probing over time using

micro-extraction and MALDI mass spectrometry, the dynamics of cyanobacterial natural product biosynthesis can be observed and conditions that may influence the turnover of these molecules can be tested.

Herein, a comparison of the variability in turnover of metabolites produced by three different *Lyngbya* strains is provided. A more detailed set of studies are also described using a Jamaican strain of *Lyngbya majuscula* (JHB), showing that the turnover rate of the neurotoxin jamaicamide B is significantly faster than the chlorophyll derivative pheophytin *a* or the related, brominated molecule jamaicamide A. It was possible to observe measurable differences in the production rate of jamaicamide B and pheophytin *a* when experimental cultures were exposed to UV light. Manipulating the nitrate concentration in the media also appreciably affected the turnover of these two metabolites, but only when the concentration was decreased. Bromine supplementation in the culture media was found to result in higher net production of the brominated metabolite jamaicamide A. Furthermore, this approach was successfully implemented to gain insight into the timing of the bromination in jamaicamide A biosynthesis, and reveals that jamaicamide B likely serves as an intermediate in this process. Collectively, these studies suggest that combining MALDI mass spectrometry and ^{15}N feeding is a powerful way to discover new means of manipulating natural product production rates, investigate the timing of compound biosynthesis and complement more traditional *in vitro* approaches by providing insights of *in vivo* relevance.

2.2 Results

2.2.1 Metabolome wide turnover of nitrogen containing metabolites in three different *Lyngbya* strains

Cultures of *Lyngbya majuscula* 3L, originally collected from Curaçao, Netherlands Antilles,[36] *Lyngbya bouillonii*, collected from Papua New Guinea, and *Lyngbya majuscula* JHB, collected from Hector Bay, Jamaica,[37] were inoculated at comparable filament densities in two six-well culture plates containing 10 mL salt-water BG-11 media per well (one [^{14}N]$NaNO_3$ control group and two 100% [^{15}N]$NaNO_3$ experimental groups for each species) and sampled over a 10-day period. On days 1-5, 7 and 10, 1-2 filaments (approximately 0.5 mg wet weight) were removed and stored at - 20 °C. After the 10 days, each sample was mixed with 1 μL per μg MALDI matrix (50:50 mixture of DHB and HCCA), and the resulting crude solution was spotted on a MALDI plate and subjected to MALDI MS with the detector set to collect the *m/z* region between 300-2000 (see methods section). A variety of known metabolites displayed evidence of ^{15}N labeling, indicating active compound production and turnover (figure 2.1). Other nitrogen containing metabolites that have not been identified also underwent mass shifts. From these spectra, we were able to accurately calculate, with weighted isotopic averages,[38] the overall ^{15}N percent labeling for pheophytin *a* (**1**) and the natural products jamaicamide B (**2**) and A (**3**) in *Lyngbya majuscula* JHB, curazole (**4**) and carmabin A (**5**) in *Lyngbya majuscula* 3L, and apratoxin A (**6**) in *Lyngbya bouillonii* (structures and figure 2.1b).

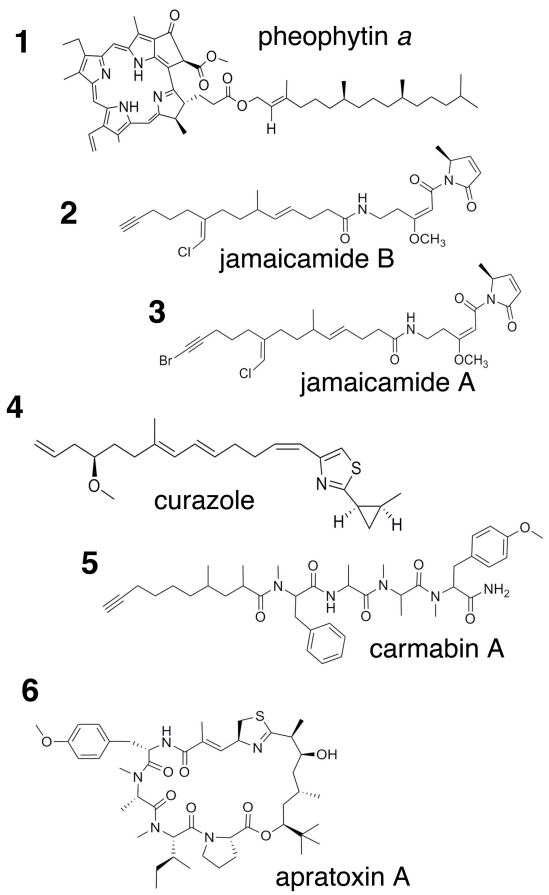

Figure 2.1. Structure of metabolites in study

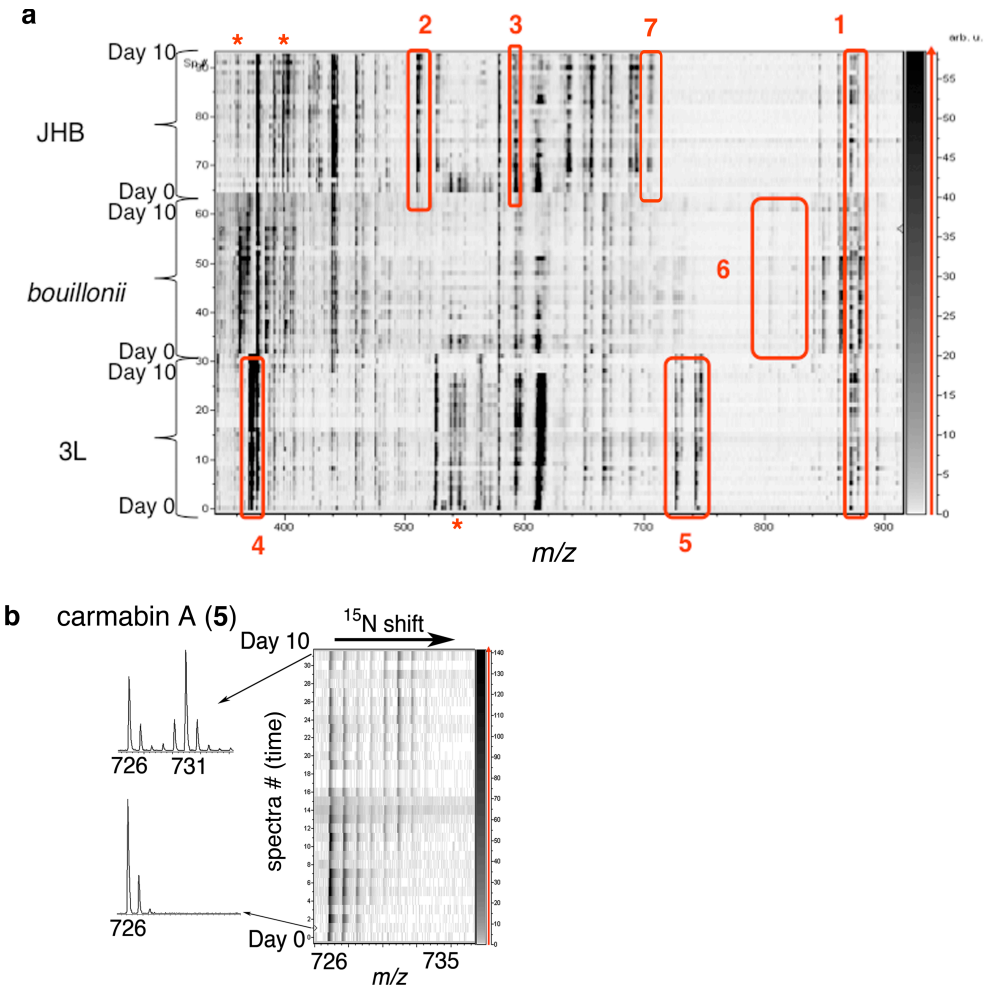

Figure 2.2. Comparison of percent 15N labeling of some known nitrogen-containing metabolites from Lyngbya majuscula 3L, JHB and Lyngbya bouillonii.
The culture conditions and time of inoculation were identical for all cultures of both species. (a) Isotope heat map view of m/z 300-950 MALDI spectra taken daily, with 4 replicates per day, during the course of a 10-day feeding experiment (days 0-5, 7, 10 shown). Shifting of the vertical spectral bands for each species indicates nitrogen-containing metabolites undergoing production and turnover. The red boxes and corresponding numbers highlight described metabolites, although many other metabolites can be seen undergoing nitrogen shifts. (b) Enlarged heat map showing region pertaining to carmabin A (5), the spectra for to Day 1 and Day 10 are shown on the left with the shift of 5 Da (pertaining to the 5 nitrogen atoms in carmabin A) being easily visible, the dark spots in the heat map correspond to the same isotopic peaks

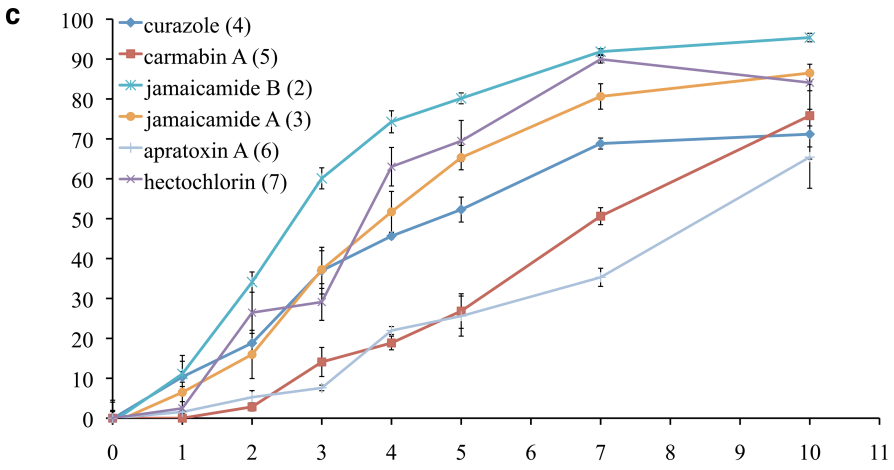

Figure 2.2 cont. (c) Percent ^{15}N labeling after 5 days for the compounds indicated by the red boxes, including the metabolite pheophytin a for all species and jamaicamide A and B from Lyngbya majuscula JHB, carmabin A and curazole in L. majuscula 3L, and apratoxin A in L. bouillonii. The percentage is calculated from weighted isotopic averages, N = 4.

2.2.2 Growth, and turnover of pheophytin *a* and jamaicamide B in *Lyngbya majuscula* JHB

Lyngbya majuscula JHB, a strain responsible for producing the jamaicamides, hybrid PKS/NRPS natural products with neurotoxic and ichthyotoxic activity,[40] was chosen for more detailed study due to its reliable growth and spectrum of produced metabolites. In order to further compare the turnover of selected compounds, the growth rate for JHB filaments was defined under typical culture conditions (figure 2.3a, and Supporting Information). Metabolite turnover was investigated by inoculating six *L. majuscula* JHB cultures from the same parent culture in a six-well culture plate with one control culture containing regular [^{14}N] $NaNO_3$ saltwater BG-11

medium and five with [^{15}N]$NaNO_3$ BG-11 saltwater medium. On days 0-5, 7 and 10, small samples (approximately 0.5 mg wet weight) were removed and frozen for future analysis. After day 10, the samples were analyzed using MALDI-TOF MS. The resulting spectra were analyzed with particular attention to the isotopic shifts of the nitrogen-containing molecules jamaicamide B and pheophytin *a*. Jamaicamide B was chosen for these comparisons due to its robust ionization and detection by MALDI, and because no matrix related ion peaks interfered with its analysis. Pheophytin *a,* a more stable breakdown product of chlorophyll *a*, was chosen for its role as a primary metabolite critical to energy production in these organisms (its only difference from chlorophyll *a* is that it lacks the central magnesium atom, likely removed during the acidic MALDI preparation).[41] A comparison of the control and experimental isotopic profiles for each molecule over 10 days is shown in figure 2.3b. The resulting

Figure 2.3. Comparison of growth, jamaicamide B and pheophytin *a* turnover during 10 days from small cultures of *Lyngbya majuscula* JHB grown in ^{15}N media. (**a**) Optical images (8x) show the growth of a single filament over the course of 10 days. (**b**) MALDI MS spectra from micro-extractions showing the relative changes in the pheophytin *a* (left) and jamaicamide B (right) isotope clusters over time. Top panels contain control spectra for each molecule. The decrease in the unlabeled, mono-isotopic peaks indicates the reduced abundance of the ^{14}N containing species, while the increase in other peaks is indicative of newly synthesized, ^{15}N labeled species. (**c**) Comparison of growth and percentage of ^{15}N labeling of jamaicamide B and pheophytin *a* over 10 days. At Day 6, approximately 50% of the growth is new and 50% of the pheophytin *a* present in the sample is labeled, whereas nearly 90% of the jamaicamide B is labeled, indicating significantly different rates of turnover between the two molecules. [Error bars are S.E.M. For ^{15}N labeling N = 5, for growth N = 16 (Day 2), 10 (Day 4), 7 (Day 6), 5 (Day 8), 3 (Day 10)]. Equation for percentage of new growth = $((L_x - L_0)*L_t^{-1}) * 100$, where $L_{x,0,t}$ = lengths at day x, 0, and total respectively.

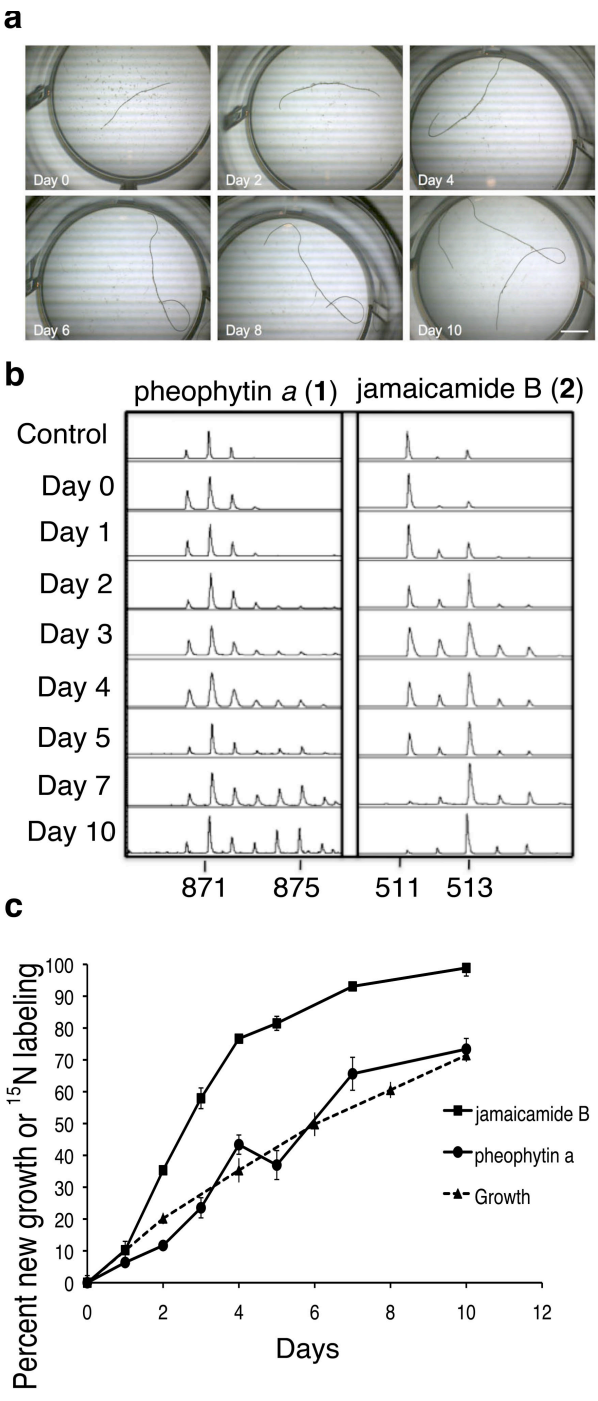
a
Day 0
Day 2
Day 4
Day 6
Day 8
Day 10
b
pheophytin a (1)
jamaicamide B (2)
Control
Day 0
Day 1
Day 2
Day 3
Day 4
Day 5
Day 7
Day 10
871
875
511
513
c
Percent new growth or 15N labeling
Days
jamaicamide B
pheophytin a
Growth

percentage of ^{15}N labeling over time, calculated from weighted isotopic averages[42] is shown in figure 2.3c, with comparison to new growth. Because the percentage of labeled molecule at any time point is a result of both newly biosynthesized ^{15}N-labeled molecules accumulating over the course of the experiment and elimination (via any mechanism, such as catabolism or excretion) of the older ^{14}N-labeled species, the combination of these values represents a measure of the net turnover of the metabolite. The average ratio of jamaicamide B to pheophytin *a* ^{15}N labeling during the 10 days was 2.1 ± 0.2 (S.E.M.), indicating that jamaicamide B is turned-over at twice the rate of pheophytin *a* in these cultures.

While the fate of jamaicamide B after biosynthesis was not clear from these experiments, the measured rates of turnover suggested that jamaicamide B is not accumulated within the cells, since by day 10, ^{15}N labeled (or newly biosynthesized) jamaicamide B represents nearly all of the molecule present. To determine whether jamaicamide B was being actively secreted from *L. majuscula* filaments into the culture medium, 6 mL of the media from a dense JHB culture maintained in a Petri dish for 17 days was extracted and analyzed by MALDI-TOF MS. Neither jamaicamide B nor any other known natural products from *L. majuscula* JHB were present in sufficient concentrations to be detected in this extract (S.I.).

The utility of the ^{15}N labeling / MALDI-TOF approach was further explored by manipulation of culture conditions and comparing the resulting effect on jamaicamide B and pheophytin *a* turnover. Reducing the available nitrate in the media

and exposure to UV light were two factors that showed appreciable impact, reducing the production of these metabolites (S.I. figure 2.1 and S.I. text and methods).

2.2.3 Comparison of ^{15}N labeling states of jamaicamide B with the brominated natural product jamaicamide A over 10 days

The consistent difference in the rates of ^{15}N labeling of jamaicamide B and pheophytin *a* was surprising and provoked a similar analysis of the related compound jamaicamide A from the data sets depicted in figure 2.3. Jamaicamide A (**3**) is the brominated analog of jamaicamide B (**2**), and the terminal alkynyl bromide of jamaicamide A is thought to be incorporated *via* an uncharacterized halogenase in the jamaicamide gene cluster.[43] Because the isotopic cluster for jamaicamide A in the MALDI spectra overlaps with another chlorophyll breakdown product (likely pheophorbide *a*[44]), calculating an accurate weighted average of the cluster was not possible. Instead, a different but common calculation strategy[45] was employed in order to examine the differences in the rate of ^{15}N incorporation between these molecules. Since both molecules contain only 2 nitrogens, it was possible to calculate the percentage of unlabeled vs. single, double, and total labeled molecules present at each time point by using only the first three peaks of both the jamaicamide A and B parent isotopic clusters (figure 2.4a and b).

The results in figure 2.4c show that jamaicamide A is turned over more slowly than jamaicamide B. There is a delay of approximately 1.5 days before the sharp increase in ^{15}N labeling of jamaicamide A when compared to jamaicamide B (T_{50} for jamaicamide B = 2.5 days, T_{50} for jamaicamide A = 4.0 days). One conceivable

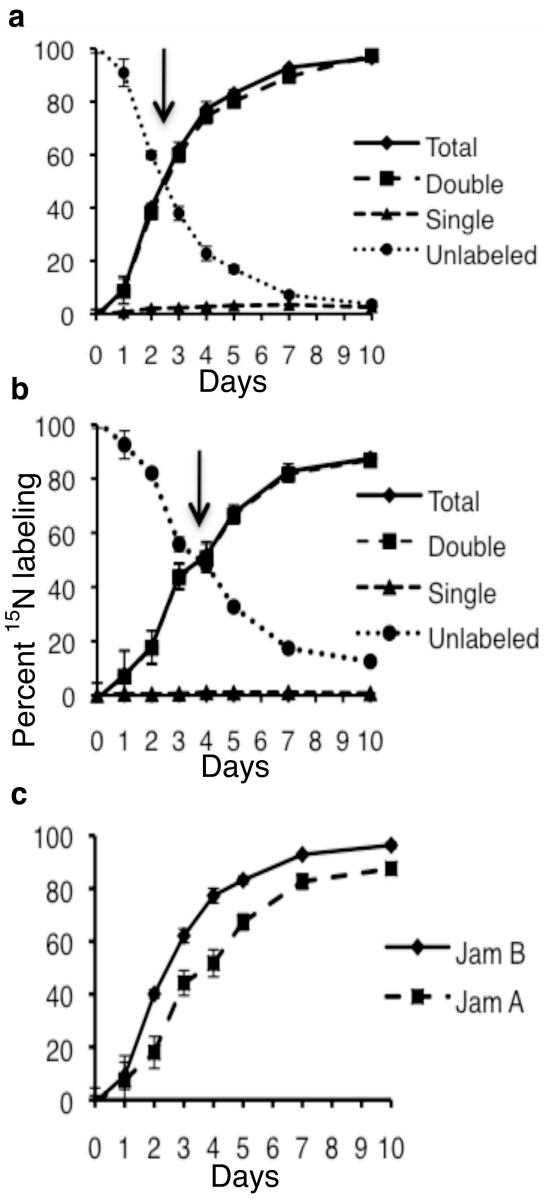

Figure 2.4. Different ^{15}N labeling states of jamaicamide B and A over 10 days in *L. majuscula* JHB. (a) Time course of single, double, total and unlabeled jamaicamide B over 10 days, calculated from same data as in figure 2B. The arrows points to T_{50}, or the time at which 50% of the molecules are ^{15}N labeled, which is 2.5 days. (b) Time course of single, double, total and unlabeled jamaicamide A over 10 days from the same data set. T_{50} here is equal to 3.9 days (arrow). (c) Comparison of total ^{15}N labeled jamaicamide B and A. At Day 6, approximately 78% of the jamaicamide A present in the sample is labeled, while nearly 95% of jamaicamide B is labeled, indicating considerably different rates of turnover between these molecules. The initiation of ^{15}N labeling in jamaicamide A is delayed by approximately 1.5 days when compared to jamaicamide B. (Errors are S.E.M., N = 5).

hypothesis to explain this observation is that the bromination reaction to form jamaicamide A occurs after the biosynthesis of jamaicamide B is completed.[46]

To further investigate the relationship between jamaicamide A and B biosynthesis, a series of ^{15}N feeding experiments were conducted with *L. majuscula* JHB using small cultures inoculated in 24 well plates. First, to determine if bromine might be a limiting nutrient in the biosynthesis of jamaicamide A, additional bromine was added to the ^{15}N culture media. The simple addition of NaBr to the media in either 0.5 g/L or 1.0 g/L resulted in a significant and step-wise increase in the percentage of ^{15}N labeled jamaicamide A (figure 2.5a), indicating that the concentration of bromine in seawater (65 ppm) is a limiting nutrient in jamaicamide biosynthesis. However, the addition of bromine still did not result in an equal ^{15}N labeling rate to that of jamaicamide B.

To support the possibility that the bromination of jamaicamide A occurs after the assembly of jamaicamide B,[47] an additional experiment was performed using a similar ^{15}N feeding time course with the inclusion of a dark phase. In preliminary trials, it was found that moving *L. majuscula* JHB cultures to a completely and continuously dark environment effectively stopped turnover of jamaicamide B and pheophytin *a,* a finding that supports the notion of light regulation of these pathways.[48] Two, 24-well culture plates were each inoculated with 8 *L. majuscula* JHB cultures in ^{15}N media supplemented with 1.0 g/L NaBr, and placed under typical light conditions and sampled on days 0-4. On the fourth day, one of the plates was placed in the dark, while the other reference plate remained in control 16 h light / 8 h

Figure 2.5. Further investigation of jamaicamide A and B biosynthesis. (**a**) Total percent ^{15}N labeling of jamaicamide A is enhanced by addition of NaBr to media. Bars indicate percent ^{15}N labeling of pheophytin a, jamaicamide A, and jamaicamide B in small *L. majuscula* JHB cultures incubated for 5 days in media containing 100% [^{15}N]$NaNO_3$ and either 0.5 g/L or 1.0 g/L NaBr (N = 6, error bars are S.E.M.). (**b**) Total percentage ^{15}N-labeled jamaicamide B (solid line) and A (dashed line) over 14 days in 16 h light / 8 h dark conditions. (**c**) New production (total ^{15}N labeling) is terminated for jamaicamide B (solid line) but continues for jamaicamide A (dashed line) when *L. majuscula* JHB is subjected to continuous dark for a 5-day period from day 4 to day 9 (opaque box) (N = 8, error bars are S.E.M.). (**d**) Ratio of jamaicamide A to jamaicamide B after 6 days in regular light conditions (16 h light / 8 dark) and continuous dark (24 h dark) from larger scale experiments. Ratios of jamaicamide A to jamaicamide B were determined after 6 days of culture in both cases. Quantities of jamaicamide A and B were determined using total ion count measurements from LC-MS analysis.

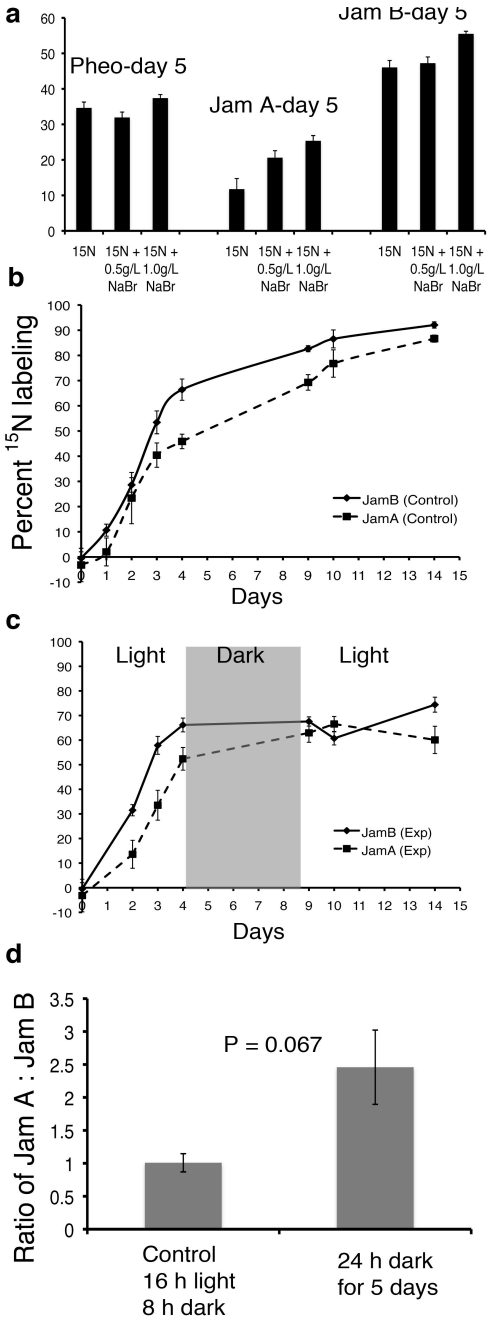
a
Jam B-day 5
Pheo-day 5
Jam A-day 5
15N
15N + 0.5g/L NaBr
15N + 1.0g/L NaBr
b
Percent 15N labeling
JamB (Control)
JamA (Control)
Days
c
Light
Dark
Light
JamB (Exp)
JamA (Exp)
Days
d
Ratio of Jam A : Jam B
P = 0.067
Control
16 h light
8 h dark
24 h dark
for 5 days

dark conditions. On the ninth day the experimental cultures were reverted to the control light cycle. Samples were taken from the reference and experimental cultures on days 9, 10 and 14. At the conclusion of the study, the samples were run by MALDI and the percentage of total ^{15}N of jamaicamides B and A was calculated for each sample (figure 2.5b (control) and c (experimental)). From this experiment, it is clear that production of jamaicamide A continues in the dark, whereas production of jamaicamide B is completely abrogated. These results support the hypothesis that jamaicamide A bromination occurs after the assembly of jamaicamide B, and implicates jamaicamide B as the substrate for bromination. This prediction of the timing of bromination is consistent with previously reported experiments that demonstrated the inclusion of only non-brominated substrates during the initial steps of jamaicamide biosynthesis.[49] This experiment was also repeated using a simpler design (S.I. figure 2.7), and those results also support the initial experiment with ^{15}N labeling of jamaicamide A continuing in the dark condition, while ^{15}N labeling of jamaicamide B is inhibited.

To confirm these MALDI results, a larger scale experiment was conducted for analysis by liquid chromatography – mass spectrometry (LC-MS). Two 6 well plates were fully inoculated with *L. majuscula* JHB cultures in regular [^{14}N] BG-11 media. The control plate was maintained in regular light conditions and the other was subjected to complete darkness (wrapped in aluminum foil). After six days the experimental plate was unwrapped, and vertically adjacent cultures in each plate were combined, to give three larger samples for each of the control and experimental plates.

Each of these six samples was extracted using a mixture of ethyl acetate and hexanes, and following a similar purification scheme to that originally used in jamaicamide isolation,[50] the extracts were each redissolved in MeOH/H_2O, run through separate solid phase extraction cartridges (C-18), and profiled using a MeOH/H_2O gradient by LC-MS. Elution peaks for jamaicamides A and B were identified using their associated chromatographic peaks and isotopic profiles, and the corresponding sum of the ion counts for all possible adducts of jamaicamide B and A [such as $(M+H)^+$, $(M+Na)^+$, and $(M+K)^+$] were obtained. The ratios of total jamaicamide A to jamaicamide B in each extract are shown in figure 2.5d, and indicate that while jamaicamide A biosynthesis persists in total darkness, the rate of jamaicamide B turnover drops considerably ($P = 0.067$).

2.3 Discussion

Isolation of natural products from sessile marine organisms for drug discovery or biotechnology applications, either from laboratory cultures or field collections, frequently results in the recovery of variable amounts of a metabolite from a parent extract. Many secondary metabolites are under strict environmental and epigenetic modes of regulation[51] while others are produced constitutively and can represent a large percentage of the harvested biomass.[52] The observation that the *Lyngbya* natural products included in this study had variable rates of ^{15}N labeling from [^{15}N]$NaNO_3$ feeding and MALDI analysis, and thus different turnover rates, is therefore not surprising. However, until now there has not been a consistent and robust approach to actually measure these production differences *in vivo*. Here, the use of MALDI-TOF

MS of crude preparations, in conjunction with ^{15}N feeding, has revealed itself to be a valuable approach, allowing the dynamics of biosynthesis of various metabolites in marine *Lyngbya* strains to be examined concurrently.

To better gain insight into the turnover rates of specific metabolites in marine organisms, it is important to understand how both growth and primary metabolism might be influenced by changes in culture conditions. Using *Lyngbya majuscula* JHB as a model organism, several factors were explored using filaments from the same parent culture. Under our typical culture conditions (see methods), the percent production of pheophytin *a* was found to directly parallel the growth rate calculated for single filaments (figure 2.3c), suggesting that pheophytin *a* turnover is a reasonable proxy for growth. More importantly, under these conditions pheophytin *a* turnover provides a useful measure of primary metabolic activity to which the turnover of specific natural products can be compared. A surprising observation in these cultures of *L. majuscula* JHB was that a greater percentage of ^{15}N labeled jamaicamide B was detected throughout the course of the experiments than ^{15}N labeled pheophytin *a*, indicating unequal rates of turnover for these two metabolites. It can be concluded that jamaicamide B is being produced significantly faster than chlorophyll in these cultures, and that the rate of its biosynthesis outpaces filament growth. Because of the predicted metabolic cost of natural product biosynthesis,[53, 54] variations in the relative rates of turnover for different natural products in the same organism may be indicative of their relative ecological importance under a given set of environmental parameters. Although jamaicamide B was previously found to have

sodium channel blocking activity and fish toxicity[55] its true ecological role has yet to be determined, and these results suggest that significant energy and resources are being devoted to its metabolism and turnover even in the absence of macroscopic predators. The possibility exists that its high turnover level is a result of microbial interaction/defense, as the polysaccharide sheath of *Lyngbya* strains tend to harbor various heterotrophic bacteria[56] or, equally plausible, evolution may have simply favored a robust, constitutive expression level for the jamaicamide B pathway.

One insight into the preferential expression of jamaicamide B was gained by measuring the ^{15}N labeling rate of both jamaicamide B and pheophtyin *a* under conditions where available ^{15}N nitrate was limiting. It is reasonable to expect that if the production of jamaicamide B was not favored, then available nitrogen should be preferentially shifted towards the production of chlorophyll (measured in terms of pheophytin *a*). The effect of reducing available nitrate on the turnover of jamaicamide B and pheophytin *a* is remarkably consistent between these two molecules, resulting in a parallel reduction for both compounds (SI figure 2.6a). However, providing nitrate in excess did not considerably affect the turnover rate of these nitrogen containing metabolites, indicating that the media concentration of nitrogen is not a limiting factor in the biosynthesis of these molecules.

In contrast, ultraviolet light exposure reduced the ^{15}N labeling rate of both jamaicamide B and pheophytin *a* (approximately 25 percent less turnover after 5 days). Since UV exposure in the environment is much more prevalent than in laboratory cultures, these data suggest that it may be an important factor in limiting

secondary metabolite production in *L. majuscula* JHB field populations. This would be contrary to other cyanobacterial natural products, such as the UV absorbing pigment scytonemin,[57] where expression levels increase upon UV exposure.

Jamaicamide B and the brominated analog jamaicamide A are most certainly products of the same PKS/NRPS biosynthetic gene cluster.[58] The unexpected finding that the two molecules have significant differences in their ^{15}N labeling rates (figure 2.4) led us to more carefully consider the resources being dedicated to the creation of each molecule, as well as the possible timing of bromination in jamaicamide A biosynthesis. One possible scenario is that the composition of the surrounding media defines the arsenal of secondary metabolites produced by *Lyngbya majuscula.* In the present case, bromine is a limiting element in the biosynthesis of jamaicamide A, as has been observed for the natural product phormidolide in the mat forming cyanobacterium *Phormidium sp.*[59] Another conceivable explanation for the observed production difference between jamaicamide A and B is that the halogenase required in the bromination of jamaicamide A may not be active in every round of jamaicamide biosynthesis, perhaps due to an additional energetic cost of halogenation that results in relatively fewer jamaicamide A molecules being created and turned over. A third explanation is that jamaicamide B represents an initial, shorter-lived and dynamic pool while jamaicamide A represents the end-product of the pathway and is metabolically a more stable molecule. Interestingly, this latter scenario provides a potential insight into an unknown aspect of jamaicamide biosynthesis. Although many features of the biosynthesis of the jamaicamides have been described,[60, 61] the timing, identity and

genomic location of the putative halogenase responsible for incorporation of bromine into jamaicamide A has been a source of speculation but has not yet been defined. Under normal culture conditions, the turnover rate of jamaicamide B occurs approximately 1.4 times faster than jamaicamide A. When the medium is supplemented with NaBr, the amount of ^{15}N-labeled jamaicamide A increases while that of jamaicamide B and pheophytin *a* do not, supporting the hypothesis that bromine is a limiting element in the biosynthesis of jamaicamide A. However, even with additional bromine the amount of total ^{15}N labeling for jamaicamide A remains lower than that of the other two molecules (figure 2.5a). Furthermore, when cultures are moved to a completely dark environment, thereby inhibiting photosynthesis, the turnover rate of jamaicamide B sharply decreases, while jamaicamide A turnover continues at a rate nearly comparable to JHB cultures in the light condition (figure 2.5 b,c,d). These data support the third scenario wherein a percentage of the newly biosynthesized jamaicamide B pool is converted to jamaicamide A by replacement of the alkynyl hydrogen with bromine, potentially catalyzed by the protein product of *jamD* from the jamaicamide biosynthetic pathway.[62] In this case, a previously expressed and functional halogenase could catalyze the enzymatic addition of bromine in the absence of light driven metabolism. Previous records show that jamaicamide A is often found in higher abundance than jamaicamide B in extracts of this strain (unpublished data). Given the above findings, it appears that jamaicamide B is only formed during daylight hours, whereas jamaicamide A is produced throughout a light/dark cycle, and accumulates to higher concentrations. We were able to observe

the same trends (figure 2.5d) when conducting larger scale experiments and analyzing them using more conventional methods (LC-MS), although the difference in the ratio of jamaicamide B to jamaicamide A between the dark and the light conditions was only marginally significant ($p = 0.067$). These results reinforce the utility of MALDI-MS for natural product turnover comparisons, as the increased sensitivity afforded by the MALDI instrument provided us with insights into the timing of jamaicamide biosynthesis that might otherwise have been overlooked.

The primary strength of the approach described in this report lies in the multiplex ability of MALDI-TOF MS to track the ^{15}N-labeling of multiple metabolites concurrently in a single experiment and within individual samples, thereby avoiding unknown variables that might influence metabolite turnover in separate experiments. This allows for careful measurements of the influence of abiotic and biotic factors on the production of individual metabolites, as well as the temporal relationships between metabolites, providing powerful insight into the origin of chemical variability in marine life forms and the *in vivo* metabolic processes of natural products. The marine genus *Lyngbya* provided an ideal system for measuring natural product turnover and the testing of specific ecologically relevant variables on culture conditions because small amounts of living material were easily manipulated and could be efficiently extracted using a MALDI matrix solution. Future experiments using these methods could help identify the main drivers of metabolite production, including possible factors leading to harmful cyanobacterial blooms, and thus assist in developing a better understanding of the biosynthesis of nitrogen containing molecules produced by

marine microalgae. In addition, this approach may find application in a variety of fields or in different organisms, including providing an experimental framework that could aid in assigning ecological roles to secondary metabolites, and represents a valuable tool in efforts aimed at increasing natural product yields from laboratory cultures of organisms with biomedical and biotechnological relevance.

2.4 Materials and Methods

2.4.1 Cyanobacteria strains and culture maintenance

Lyngbya majuscula strain JHB was originally collected in Hector's Bay, Jamaica in 2002. *L. majuscula* 3L was collected in Curaçao, Netherlands Antilles in 1996, and *L. bouillonii* was collected in Papua New Guinea in 2005. Pan (10 L) and Erlenmeyer flask (1 L) cultures of each strain were maintained at Scripps Institution of Oceanography, UCSD in SW BG-11 media[63] at 29°C, under 16 h light / 8 h dark cycles at approximately 5 μE m^{-2} s^{-1}. All experiments except those testing the effects of UV exposure and light cycles were also conducted using these temperature and light conditions. For all experimental cultures, SW-BG-11 was used, containing 5 g / L of either [^{14}N]$NaNO_3$ (controls) or [^{15}N]$NaNO_3$ (98%, Cambridge Isotopes).

2.4.2 Experimental culture conditions

2.4.2.*1 L. majuscula JHB, L. majuscula 3L* and *L. bouillonii* study

Approximately 10 milligram cultures of each species were inoculated in 6 well plates (Corning Life Sciences/ Costar) at the same time as follows: 2 experimental ([^{15}N]$NaNO_3$) and 1 control ([^{14}N]$NaNO_3$) well for each species and maintained at

standard culture conditions described above. On days 0-5, 7, and 10, two samples were taken from each well for each species, resulting in two technical replicates and two experimental replicates.

2.4.3 Sampling

Using aseptic technique and small tweezers, 2-4 filaments (0.2-0.4 μg wet weight) from small cultures were placed in a PCR tube and flash frozen with dry ice. Sampling intervals varied between experiments, as explained in each experimental description.

2.4.3.1 10-day experiment with *Lyngbya majuscula* JHB

Each well of a 6-well culture plate was inoculated with 10 mg wet weight of starting material from a parent culture of *Lyngbya majuscula* JHB. The filaments were cut using a razor blade into approximately 1 cm long clusters before starting the experiment. Five of the wells contained 10 mL of ^{15}N SW-BG-11, with 1 well of control (^{14}N) SW-BG-11.

2.4.3.2 Bromine Feeding in *Lyngbya majuscula* JHB

In a 24 well plate, 6 wells containing 2 mL regular [^{15}N]$NaNO_3$ medium, 6 containing the [^{15}N]$NaNO_3$ medium with 0.5 g / L NaBr, and 6 containing the [^{15}N]$NaNO_3$ medium with 1.0 g / L NaBr were inoculated with approximately 2.5 mg wet weight from a parent culture of *Lyngbya majuscula* JHB (filaments cut to 0.5-1.0 cm length). Samples were taken on day 0 and day 5.

2.4.3.3 Dark phase with bromine supplementation in *Lyngbya majuscula* JHB

Two 24-well culture plates were each inoculated with 8 small (2.5 mg) *L. majuscula* JHB (filaments cut to 0.5-1.0 cm length) cultures in 2 mL ^{15}N media containing 1.0 g/L NaBr, placed under the control culture conditions (above) and sampled on days 0-4. On the fourth day, one of the plates was wrapped completely with aluminum foil, while the other reference plate remained in control conditions. On the 9th day, the experimental plate was un-wrapped, with samples taken from the reference and experimental cultures on day 9 as well as days 10 and 14. At the conclusion of the study, the samples were run by MALDI and the percentage of total ^{15}N labeled jamaicamide B and A was calculated for each sample at each time point.

2.4.4 LC-MS comparison of jamaicamide B and A in 16 h light/8 h dark vs. 24 h dark

Two 6-well plates were inoculated with 6 small *L. majuscula* JHB cultures (10 mg) in regular ^{14}N BG-11 media. The control plate was maintained in regular light conditions and the other was completely wrapped in aluminum foil. After six days the experimental plate was unwrapped and the vertically adjacent cultures in both plates were combined, to give three, larger samples per plate. All of the samples were extracted with 80% EtOAC/hexanes for approximately 1 h with stirring at 25 °C. Each of these extracts were dried and redissolved in 80% MeOH/H_2O,[64] and run over C-18 solid phase extraction cartridges (Varian or Analytichem International, 100 mg) in the same solvent system. All extracts were dried under liquid nitrogen, weighed, and suspended in MeOH at a concentration of approximately 3 mg/mL. The extracts were profiled using a gradient program of 70-100% MeOH/H_2O with an analytical

column (Phenomenex Jupiter C-18, 5 μ 300 A) and LC-MS (Thermo-Finnigan Surveyor pump and PDA and LCQ Advantage Max). Retention times for jamaicamide A and B were identified by UV detection, and the total ion counts for all associated adducts (found to repeatedly include $(M+H)^+$, $(M+Na)^+$, (M+K)+ and $(M+45)^+$) of jamaicamide B and A were combined and integrated using Xcalibur software (Thermo Electron) to determine the ratio of jamaicamide A to jamaicamide B in each sample.

2.4.5 MALDI MS sample preparation

Approximately 1 μL of MALDI matrix solution (Per 1 mL: 35 mg α-cyano-4-hydroxycinnamic acid (*CHCA*), 35 mg 2,5-Dihydroxybenzoic acid (DHB) (Universal MALDI matrix, Sigma Aldrich), 750 μL acetonitrile, 248 μL milliQ H_20, 2 μL TFA) per 0.1 μg of biomass was mixed in a tube or well. After 20-30 seconds, 1 μL of this crude matrix solution was deposited on a well (spot) of the Bruker Microflex MSP 96 Stainless Steel Target Plate. After each spot had dried at room temperature, the plate was analyzed using a Bruker Microflex MALDI-TOF mass spectrometer equipped with flexControl 3.0.

2.4.6 Calculations

2.4.6.1 Weighted averages (percent 15N labeled)

For a particular compound in a sample, the mean mass was computed using the weighted average of the observed isotope cluster.[65]

2.4.6.2 For percent total, single, double and unlabeled ^{15}N jamaicamide

For comparisons of jamaicamide A and B (percent single, double, total and unlabeled, figures 2.4 and 2.5), calculations were performed as the percent contribution of ^{15}N nitrogen in each isotopic peak.[66]

2.5 CHAPTER 2 ACKNOWLEDGEMENTS

We thank Dr. Hyukjae Choi for assistance in analyzing LC-MS data. Support was provided by a graduate fellowship to EE from the National Institutes of Health Training Program in Marine Biotechnology (T32GM067550), a graduate fellowship to ACJ from the Los Angeles Chapter of the Achievement Rewards for College Scientists (ARCS) Foundation, and NOAA Grant NA08OAR4170669, California SeaGrant College Program Project SG-100-TECH-N, through NOAA's National Sea Grant College Program, US Department of Commerce. The statements, findings, conclusions, and recommendations provided here are those of the authors and do not necessarily reflect the views of the National Institutes of Health, California Sea Grant or the US Department of Commerce.

Author Contributions

E.E and A.J. performed research. T.B. maintained cultures. E.E. A.J. P.C.D. and W.H.G. designed research and wrote the manuscript.

The authors declare no conflicts of interest.

Chapter 2, in essence, includes a part that has been submitted to the Proceedings of the National Academy of Sciences in 2010. Eduardo Esquenazi, Adam Jones, Tara Byrum, Pieter C. Dorrestein and William H. Gerwick. The dissertation author is the primary investigator and author of this paper.

2.6 CHAPTER 2 SUPPORTING INFORMATION

The Impact of Nitrate Concentration and UV Exposure on the Rate of ^{15}N Labeling of Jamaicamide B and Pheophytin *a* in *L. majuscula* JHB

To study the relationship between pheophytin *a* and jamaicamide B production, the impact of the reduction of nitrate in the media was evaluated by combined [^{15}N]$NaNO_3$ feeding and MALDI analysis. *L. majuscula* JHB cultures were incubated in 1.0, 0.1, 0.01 and 0.001 times the normal nitrate concentration using [^{15}N]$NaNO_3$ (4 cultures per condition) for 7 days. The percentage of ^{15}N labeling for jamaicamide B and pheophytin *a* was calculated from the weighted average of the isotope clusters. A parallel stepwise reduction of labeling, and thus turnover, was seen for both metabolites (S.I. figure 2.6a). When cultures were grown in media containing twice the amount of [^{15}N]$NaNO_3$ compared to control cultures, no appreciable difference in the percent ^{15}N labeling was observed (1X [^{15}N]$NaNo_3$ control: 67.4 ± 2.8 for jamaicamide B and 43.4 ± 2.4 for pheophytin *a*; 2X [^{15}N]$NaNo_3$ experimental: 61.2 ± 2.8 for jamaicamide B and 36.5 ± 2.1 for pheophytin*;* N = 5, errors are S.E.M.), indicating that at 5 g/L, NO_3^- is not a limiting nutrient in these cultures.

Next, the effect of UV light on the production of jamaicamide B and pheophytin *a* in *Lyngbya majuscula* JHB was explored. A set of 5 cultures in [^{15}N]$NaNO_3$ media were exposed to UV light (see S.I. methods section) for 5 days, at which time the percentage of ^{15}N labeled molecules was determined (S.I. figure 2.6b). The percent labeling of both jamaicamide B and pheophytin *a* were significantly lower

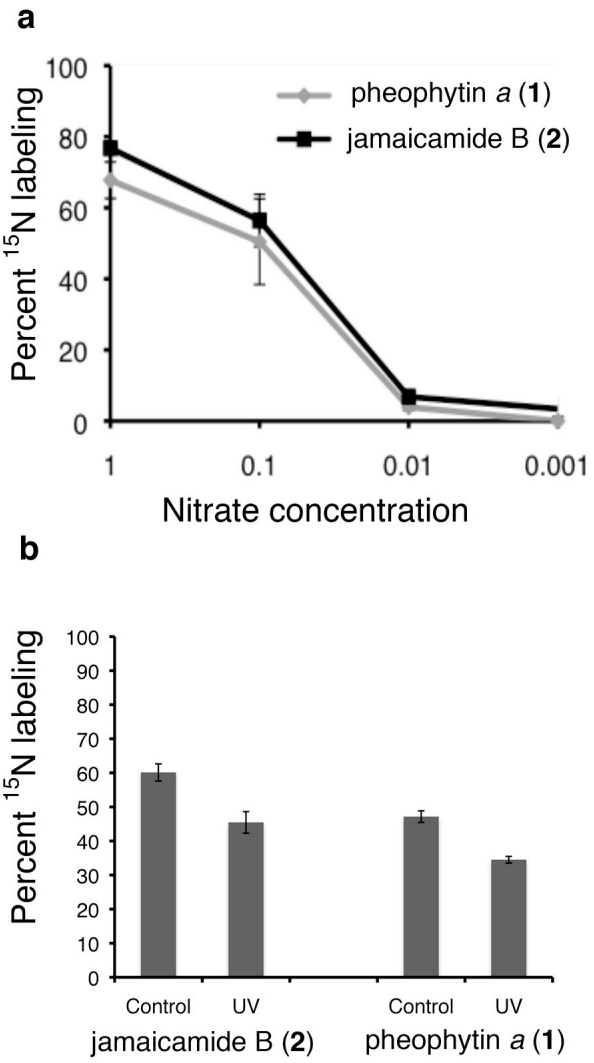

Figure 2.6. Effect of nitrate concentration and UV light on percent ^{15}N labeling of jamaicamide A and pheophytin *a*.
(a) Percent ^{15}N labeling at day 7 for jamaicamide B (solid line) and pheophytin *a* (dashed line) under different nitrate concentrations (control is equal to 1.0 or 5 g/L $NaNO_3$, N = 4) (**b**) Effect of 5 days of exposure to UV light on the percent ^{15}N labeling for jamaicamide B (left bars) and pheophytin *a* (right bars) (N = 5, errors are S.E.M).

between the experimental and the control cultures after the UV light treatment. However, for both the UV light exposure and variable nitrate concentration experiments described above, the ratio between jamaicamide B and pheophytin *a* remained constant between the control and the experiment samples (S.I. Table 2.1), suggesting that the biosynthesis of both molecules may share a similar regulatory mechanism.

Table 2.1. The Impact of UV Exposure and Two-Fold Nitrate Concentration in the Media on the Production of Pheophytin A And Jamaicamide B in L.majuscula JHB

Experiment	Metabolite	% Labeling	Std. error	Ratio (Jam B / Pheo a)
UV	Jam B (control)	60.11316555	2.524971072	1.274723048
	Pheo (control)	47.15782433	1.696386669	
	Jam B (exp)	45.45144582	3.161929934	1.317116039
	Pheo (exp)	34.50830792	0.990046453	
2X NaNO3	Jam B (control)	67.36767869	2.759420468	1.553752815
	Pheo (control)	43.35804128	2.400706583	
	Jam B (exp)	61.23058640	2.843221840	1.676021014
	Pheo (exp)	36.53330470	2.003388766	

2.7 Supplemental Information: Methods

2.7.1 Growth rates

Because the filament width of *L. majuscula* remains constant at approximately 50-60 μm, all observed growth over this time period was due to increases in filament length (figure 2.3a). The growth rate for *Lyngbya majuscula* JHB filaments was determined by recording the changes in length of a subset of individual filaments

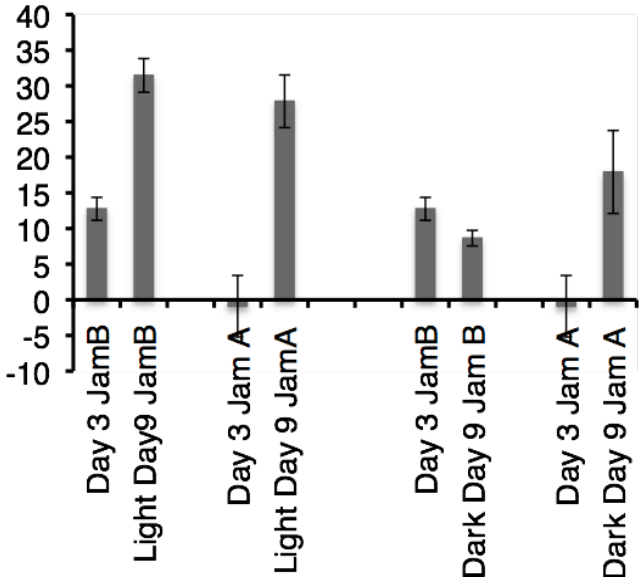

Figure 2.7. Y-axis is percent labeling.
In this experiment, 16 cultures were inoculated in ^{15}N media containing 1.0 g/L NaBr under typical light conditions. After three days, reference samples were taken, and eight of the cultures were placed in continuous dark for 5 days, with the other eight remaining in the regular light cycle. On the ninth day, the sixteen cultures and the reference samples were subjected to MALDI mass spectrometry and the percent ^{15}N labeling was calculated. There was no significant labeling of jamaicamide B in the dark (Day 3 JamB and Dark Day 9 JamB) while jamaicamide A showed robust and continued labeling in the dark. (Day 3 JamA and Dark Day 9 JamA)

grown in ^{15}N SW-BG-11 media. Twenty individual filaments were each placed in a separate well of a 24-well culture plate with 2 mL of media. Using a dissecting scope equipped with a camera (XLiCap V. 17, XL Imaging 3M Camera MK2), images were captured at (8X) magnification at 0 hours and every 48 hours thereafter. The filaments in the images for each time point were measured using ImageJ software.[67] At each 48 h time point, 4 filaments were removed, flash frozen using dry ice and kept frozen for MALDI analysis at the completion of the study. Because of the removal of these

subset of filaments for MALDI analysis, and because a few filaments died during the course of the experiment (removed from the study altogether) each subsequent time point contained a reduced numbers of replicates. Thus, from Day 0-Day 2, N = 16 filaments measured; for Day 2-4, N = 10; for Day 4-6, N = 10; for Day 6-8, N = 5; Day 8-10 N=3. Filament length was measured in each image using ImageJ software.[68] Individual filaments were found to have a doubling rate of 6 days (figure 2.3c), which is somewhat faster than rates observed previously in other *L. majuscula* cultures.[69]

2.7.2 Media extracts

Six mL of medium was removed from a 17 day old, dense culture of *Lyngbya majuscula* JHB growing in a petri dish. This media was filtered to remove any filament or cell material, and extracted at room temperature with 12 mL of ethyl acetate. The ethyl acetate partition was removed with a separatory funnel, evaporated until dry in a 5 mL glass vial under nitrogen, the resulting extract was prepared with the same matrix used previously and subjected to MALDI-MS.

Decreasing nitrate concentration: In a 24 well plate, 5 wells for each of the conditions (1.0X, 0.1X, 0.01X, 0.001X of control concentration of [^{15}N]$NaNO_3$) and 4 control wells were inoculated using 2 mL of the media and approximately 2.5 mg wet weight from a parent culture of *Lyngbya majuscula* JHB (filaments cut to 0.5-1.0 cm length). Samples were taken on days 0 and 7. Light and culture conditions were the same as described above.

Two-fold nitrate study in *Lyngbya majuscula* JHB: Experimental and controls were inoculated as described for the 10 day study (N =5), with the experimental

condition receiving media containing twice the amount of [^{15}N]$NaNO_3$ (0.5 g / L control and 1g / L experimental). Cultures were kept at the conditions described above and sampled on days 0 and 5.

UV study of *Lyngbya majuscula* JHB: Both UV and control plates were inoculated as described above for the 10 day experiment (N = 5). Both plates were kept at 33 μE m^{-2} sec^{-1} light intensity (measured with a ILT-1400A light meter, International Light Technologies, Peabody, MA). The UV levels were 165.7 μw cm^{-2} UVA (Omega Engineering, Stamford, CT) and 400 μw cm^{-2} UVA+B (Solarmeter 5.0, Solartech, Inc., MI). Other than these light factors, cultures were kept in the same conditions described above and sampled on days 0 and 5.

2.7.3 MALDI-TOF settings

The instrument and program settings for these experiments were as follows: *General*: Flex-Control Method- RP_pepmix.par. *Processing*: Flexanalysis Method- none, Biotools MS method- none. **Laser Power**: 25-55 %. **Sample Carrier**: nothing. **Spectrometer**: On, Ion Source 1- 19.0 0 mV, Ion Source 2- 16.40 mV, Lens- 9.45 mV, Reflector 20.00, Pulsed Ion Extraction- 190 ns, Polarity- Positive. Matrix Suppression: Deflection, Suppress up to: *m/z* 300. **Detection**: Mass Range- 300-1600, Detector Gain- Reflector 3.7- 4.2 X. Sample Rate- 2.00 GS/s, Mode- low range, Electronic Gain-Enhanced, 100 mV. Real time Smooth- Off. Spectrometer, Size: 81040, Delay 42968. **Processing Method**: Factory method RP_2465. **Setup**: Mass Range- Low. Laser Frequency- 20 Hz, Autoteaching- off. Instrument Specific Settings: Digitizer- Trigger Level- 2000 mV, Digital Off Linear- 127 cnt, Digital Off,

Reflector- 127 cnt. Detector Gain Voltage Offset, Linear- 1300 V, Reflector- 1400 V. Laser Attenuator, Offset -23 %, Range- 50 %, Electronic Gain Button Definitions, Regular: 100 mv (offset lin) 100 mV (offset ref) 200mV/full scale. Enh: 51 mV (offset lin), 51 mV (offset ref) 100 mV/full scale. Highest: 25 mV (offsetlin) 25 mV (offset ref) 50 mV/full scale. **Calibration**: Calibration was done using Bruker's peptide Calibration Mixture # 4. Zoom Range +-1.0%, Peak Assignment Tolerance- User Defined-500 ppm

2.8 CHAPTER 2 REFERENCES

1. M. Donia and M. T. Hamann, "Marine Natural Products and Their Potential Applications as Anti-Infective Agents," *Lancet Infect. Diseases* 3 (2003): 338–48.

2. J. W. Blunt, B. R. Copp, W. P. Hu, M. H. Munro, P. T. Northcote, and M. R. Prinsep, "Marine Natural Products," *Nat. Prod. Rep.* 26 (2009): 170–244.

3. D. Tillett, E. Dittmann, M. Erhard, H. van Döhren, T. Börner, and B. A. Neilan, "Structural Organization of Microcystin Biosynthesis in *Microcystis Aeruginosa* PCC7806: An Integrated Peptide-Polyketide Syntetase System," *Chem. Biol.* 7 (2000): 753–64.

4. Ibid.

5. M. Kaebernick, E. Dittmann, T. Börner, and B. A. Neilan, "Multiple Alternate Transcripts Direct the Biosynthesis of Microcystin, a Cyanobacterial Nonribosomal Peptide," *Appl. Environ. Microbiol.* 68 (2002): 449-55.

6. M. C. Moffitt and B. A. Neilan, "Characterization of the Nodularin Synthetase Gene Cluster and Proposed Theory of the Evolution of Cyanobacterial Hepatotoxins," *Appl Environ Microbiol* 70 (2004): 6353–62.

7. Z. Chang, P. Flatt, W. H. Gerwick, V-A. Nguyen, C. L. Willis, and D. H. Sherman, "The Barbamide Biosynthetic Gene Cluster: A Novel Marine Cyanobacterial System of Mixed Polyketide Synthase (PKS)-Non-Ribosomal Peptide Synthetase (NRPS) Origin Involving an Unusual Trichloroleucyl Starter Unit," *Gene* 296 (2002): 235–47.

8. Z. Chang, N. Sitachitta, J. V. Rossi, M. A. Roberts, P. M. Flatt, J. Jia, D. H. Sherman, and W. H. Gerwick, "Biosynthetic Pathway and Gene Cluster Analysis of Curacin A, an Antitubulin Natural Product from the Tropical Marine Cyanobacterium *Lyngbya majuscula*," *J. Nat. Prod.* 67 (2004): 1356–67.

9. D. J. Edwards and W. H. Gerwick, "Lyngbyatoxin Biosynthesis: Sequence of Biosynthetic Gene Cluster and Identification of a Novel Aromatic Prenyltransferase," *J. Amer. Chem. Soc.* 126 (2004): 11432–33.

10. A. V. Ramaswamy, C. M. Sorrels, and W. H. Gerwick, "Cloning and Biochemical Characterization of the Hectochlorin Biosynthetic Gene Cluster from the Marine Cyanobacterium *Lyngbya majuscula," J. Nat. Prod.* 70 (2007): 1977–86 .

11. D. J. Edwards, B. L. Marquez, L. M. Nogle, K. McPhail, D. E. Goeger, M. A. Roberts, and W. H. Gerwick, "Structure and Biosynthesis of the Jamaicamides, New Mixed Polyketide-Peptide Neurotoxins from the Marine Cyanobacterium *Lyngbya majuscula*," *Chem. Biol.* 11 (2004): 817–33.

12. Z. Chang, P. Flatt, W. H. Gerwick, V-A. Nguyen, C. L. Willis, & D. H. Sherman, "The Barbamide Biosynthetic Gene Cluster: A Novel Marine Cyanobacterial System of Mixed Polyketide Synthase (PKS)-Non-Ribosomal Peptide Synthetase (NRPS) Origin Involving an Unusual Trichloroleucyl Starter Unit," *Gene* 296 (2002): 235–47.

13. L. Gu, T. W. Geders, B. Wang, W. H. Gerwick, K. Håkansson, J. L. Smith, and D. H. Sherman, "GNAT-like strategy for polyketide chain initiation," *Science* 318 (2007): 970–4.

14. L. Gu, B. Wang, A. Kulkarni, T. W. Geders, R. V. Grindberg, L. Gerwick, K. Håkansson, P. Wipf, J. L. Smith, W. H. Gerwick, and D. H. Sherman, "Metamorphic Enzyme Assembly in Polyketide Diversification," *Nature* 459 (2009): 731–5.

15. E. Dittmann and T. Börner, "Molecular Biology of Peptide and Polyketide Biosynthesis in Cyanobacteria," *Appl. Microbiol. Biotechnol.* 57 (2001): 467–73.

16. A. C. Jones, L. Gerwick, D. Gonzalez, P. C. Dorrestein, and W. H. Gerwick, "Transcriptional Analysis of the Jamaicamide Gene Cluster from the Marinecyanobacterium *Lyngbya majuscula* and Identification of Possible Regulatory Proteins," *BMC Microbiol.* 9 (2009): 247.

17. G. M. Cragg, D. J. Newman, and K. M. Snader, "Natural Products in Drug Discovery and Development: The United States National Cancer Institute Role," in *Phytochemicals in Human Health Protection, Nutrition, and Plant Defense*, ed. J. T. Romeo (New York: Kluwer Academic/Plenum Publishers, 1999).

18. Jones et al.

19. J. V. Rossi, M. A. Roberts, H-D Yoo, and W. H. Gerwick, "Pilot Scale Culture of the Marine Cyanobacterium *Lyngbya majuscula* for its Pharmaceutically-Useful Natural Metabolite Curacin A," *J. Appl. Phycol*. 9 (1997): 195–204.

20. H-S Yoon and J. W. Golden, "PatS and Products of Nitrogen Fixation Control Heterocyst Pattern," *J. Bacteriol.* 183 (2001), 2605–13.

21. O. A. Koksharova and C. P. Wolk, "Genetic Tools for Cyanobacteria," *Appl. Microbiol. Biotechnol.* 58 (2002): 123–37.

22. L. T. Tan, "Bioactive Natural Products from Marine Cyanobacteria for Drug Discovery," *Phytochem.* 68 (2007): 954–79.

23. K. Tidgewell, B. R. Clark, and W. H. Gerwick, "The Natural Products Chemistry of Cyanobacteria," in *Comprehensive Natural Products II Chemistry and Biology*, eds. L. Mander and H.-W. Lui (Oxford: Elsevier, 2010).

24. Edwards et al.

25. Rossi et al.

26. D. Vavilin, D. C. Brune, and W. Vermaas, "^{15}N-labeling to Determine Chlorophyll Synthesis and Degradation in *Synechocystis* sp. PCC6803 Strains Lacking One or Both Photosystems," *Biochim. Biophys. Act. Bioenerg.* 1708 (2005): 91–101.

27. D. Vavilin, D. Yao, and W. Vermaas, "Small Cab-Like Proteins Retard Degradation of Photosystem II-Associated Chlorophyll in *Synechocystis* sp. PCC6803," *J. Biol. Chem.* 282 (2007): 37660–8.

28. Y. Chikaraishi, K. Matsumoto, N. O. Ogawa, H. Suga, H. Kitazato, and N. Ohkouchi, "Hydrogen, Carbon, and Nitrogen Isotopic Fractionations During Chlorophyll Biosynthesis in C3 Higher Plants," *Phytochem.* 66 (2005): 911–20.

29. E. Esquenazi, C. Coates, L. Simmons, D. Gonzalez, W. H. Gerwick, and P. C. Dorrestein, "Visualizing the Spatial Distribution of Secondary Metabolites Produced by Marine Cyanobacteria and Sponges Via MALDI-TOF Imaging," *Mol Biosyst* 4 (2008): 562–70.

30. T. L. Simmons, R. C. Coates, B. R. Clark, N. Engene, D. Gonzalez, E. Esquenazi, P. C. Dorrestein, and W. H. Gerwick, "Biosynthetic Origin of Natural Products Isolated from Marine Microorganism-Invertebrate Assemblages," *Proc. Nat. Acad. Sci. USA.* 105 (2008): 4587–94.

31. M. Erhard, H. von Döhren, and P. Jungblut, "Rapid Typing and Elucidation of New Secondary Metabolites of Intact Cyanobacteria Using MALDI-TOF Mass Spectrometry," *Nat. Biotechnol.* 15 (1997): 906–9.

32. K. Hollywood, D. R. Brison, and R. Goodacre, "Metabolomics: Current Technologies and Future Trends," *Proteomics* 6 (2006): 4716–23.

33. Erhard, von Döhren, and Jungblut

34. M. L. Kahn, A. Parra-Colmenares, C. L. Ford, F. Kaser, D. McCaskill, and R. E. Ketchum, "A Mass Spectrometry Method for Measuring ^{15}N Incorporation into Pheophytin," *Anal. Biochem.* 307 (2002): 219–25.

35. Y. Chikaraishi, K. Matsumoto, H. Kitazato, and N. Ohkouchi, “Sources and

Transformation Processes of Pheopigments: Stable Carbon and Hydrogen Isotopic Evidence from Lake Haruna, Japan,” *Org. Geochem.* 38 (2007): 985–1001.

36. Rossi et al.

37. Edwards et al.

38. Kahn et al.

39. Ibid.

40. Edwards et al.

41. Kahn et al.

42. Ibid.

43. Edwards et al.

44. R. B. Van Breemen, F. L. Canjura, and S. J. Schwartz, “Identification of Chlorophyll Derivatives by Mass Spectrometry,” *J. Agricul. Food Chem*. 39 (1991): 1452–6.

45. K. Biemann, *Mass Spectrometry: Organic Chemical Applications* (New York: McGraw-Hill, 1962), 223-231.

46. Edwards et al.

47. Ibid

48. Jones et al.

49. P. C. Dorrestein, J. Blackhall, P. D. Straight, M. A. Fischbach, S. Garneau-Tsodikova, D. J. Edwards, S. McLaughlin, M. Lin, W. H. Gerwick, R. Kolter, C. T. Walsh, and N. L. Kelleher, “Activity Screening of Carrierdomains within Nonribosomal Peptide Synthetases Using Complex Substrate Mixtures and Large Molecule Mass Spectrometry,” *Biochemistry* 45 (2006): 1537–46.

50. Edwards et al.

51. B. Humair, N. Gonzalez, D. Mossialos, C. Reimmann, & D. Hass, “Temperature-Responsive Sensing Regulates Biocontrol Factor Expression in *Pseudomonas fluorescens* CHA0,” *ISME J*. 3 (2009): 955–65.

52. M. E. Hay, “Marine Chemical Ecology: What’s Known and What’s Next?” *J. Exp. Mar. Biol. Ecol.* 200 (1996): 103–34.

53. P. D. Coley, J. P. Bryant, and F. S. Chapin III, “Resource Availability and Plant Herbivore Defense,” *Science* 230 (1985): 895–9.

54. D. A. Herms and W. J. Mattson, “The Dilemma of Plants: To Grow or Defend,” *Quart. Rev. Biol.* 67 (1992): 283–335.

55. Edwards et al.

56. Simmons et al.

57. C. M. Sorrels, P. J. Proteau, and W. H. Gerwick, “Organization, Evolution, and Expression Analysis of the Biosynthetic Gene Cluster for Scytonemin, a Cyanobacterial UV-Absorbing Pigment,” *Appl. Environ. Microbiol*. 75 (2009): 4861–9.

58. Edwards et al.

59. F. A. Vulpanovici, “Biosynthesis, Production and Structural Studies of Secondary Metabolites in Cultured Marine Cyanobacteria” PhD diss., Oregon State University, 2004.

60. Edwards et al.

61. Gu et al.

62. Edwards et al.

63. R. W. Castenholz, “Culturing of Cyanobacteria,” *Meth. Enzymol.*167 (1988): 68–93.

64. Edwards et al.

65. Kahn et al.

66. Biemann

67. M. D. Abramoff, P. J. Magelhaes, and S. J. Ram, “Image Processing with ImageJ,” *Biophotonics Internat. 11* (2004): 36–42.

68. Ibid.

69. Rossi et al.

2.9 CHAPTER 2 APPENDIX

Other ^{15}N feeding studies and results

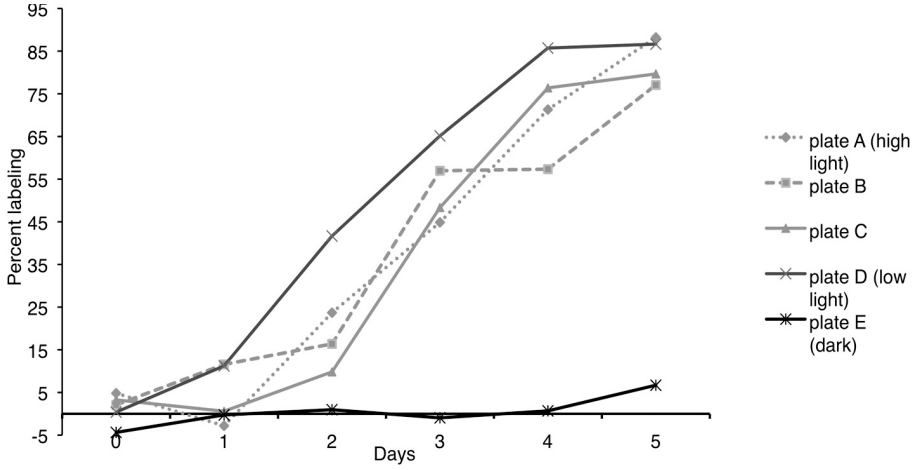

Figure 2.8. Effect of light intensity on jamaicamide B ^{15}N labeling.
Highest light level (plate A) corresponds to 30 μE m^{-2} sec^{-1}, plate B is 20 μE m^{-2} sec^{-1}, plate C is 10 μE m^{-2} sec^{-1} (closest to control conditions), plate D is 2 μE m^{-2} sec^{-1}, and plate E is complete darkness. The differences between plates A-D are not significant. Most notably, there appears to be no new production of jamaicamide B in the dark, hence no ^{15}N labeled compound is present. This finding was replicated in the final set of experiments discussed in chapter 1. N = 5

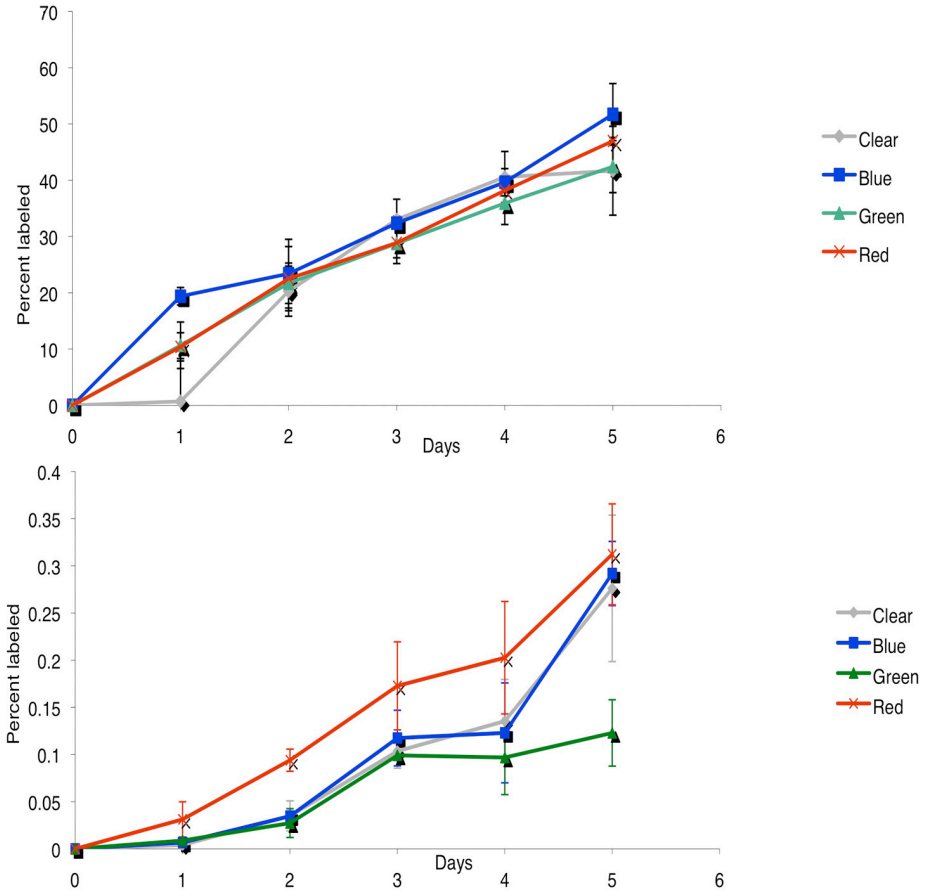

Figure 2.9. Effect of different visible wavelengths on jamaicamide and pheophytin labeling. The hypothesis here is that the wavelength of ambient light might have an effect on the regulation of jamaicamide biosynthesis. This was idea was hatched by Adam Jones when he realized a putative jamaicamide B regulatory protein shares sequence identity with RcaD. The RcaD protein is involved in chromatic adaptation in *Tolypothrix* and responds to red light. These results indicate that there is no significant difference in the labeling or production of jamaicamide B (top graph) under different wavelengths (Clear, Red, Blue, Green) however, the amount of labeled pheophytin (bottom graph) appears to decrease, hinting that there might be measurably different allocation of light energy to jamaicamide B biosynthesis and prompting repeat experiments. All cultures kept under light level of 10 μE m^{-2} sec^{-1}, N = 5 errors are S.E.M.

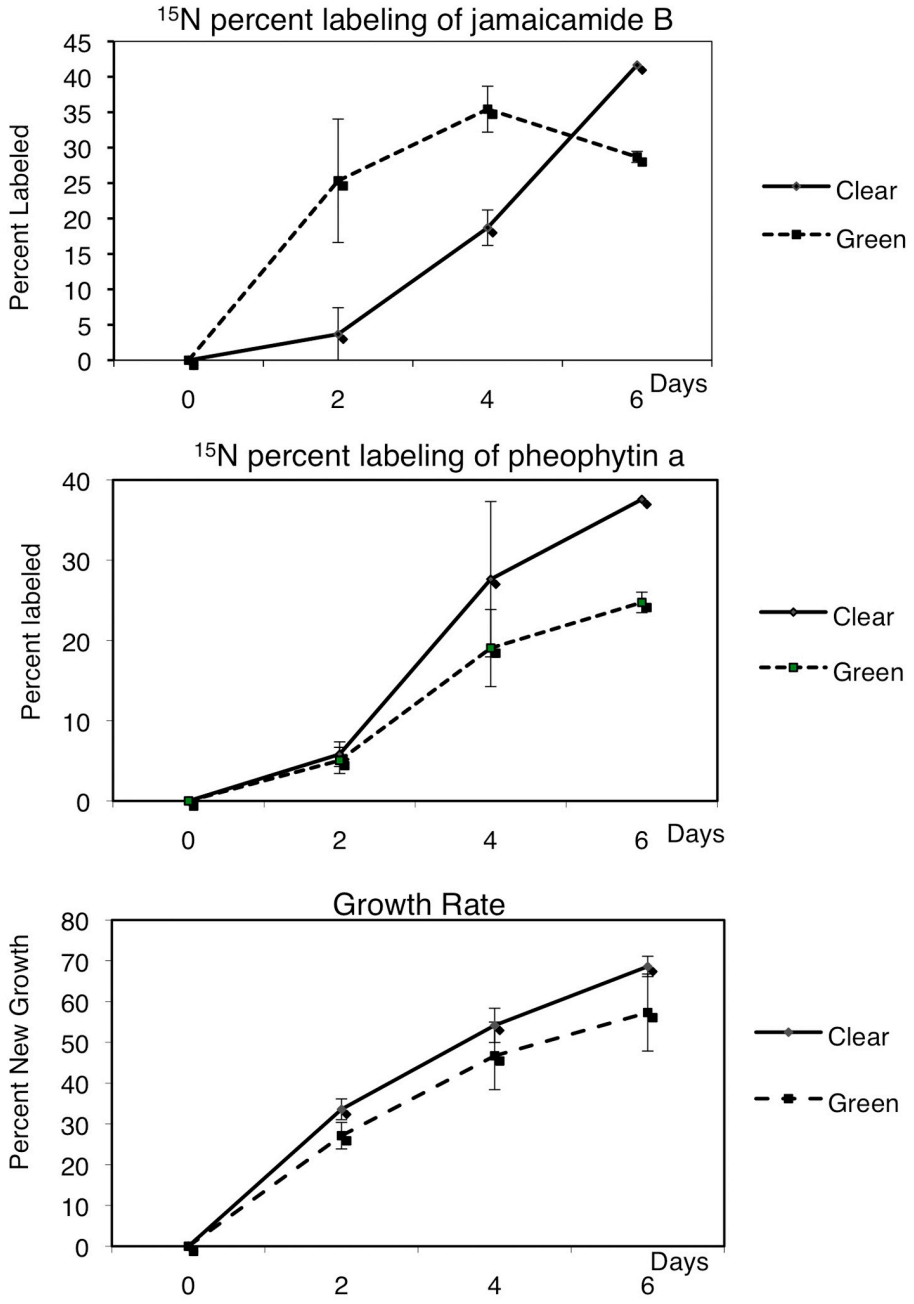

Figure 2.10. Further experiments into the effect of green wavelength on *L.majuscula* JHB. Comparison between green and full spectrum light on ^{15}N labeling of jamaicamide B (top), pheophytin (middle) and growth (bottom). These results are inconsistent with the previous set (figure x) and suggest a much preferred allocation of resources to the production of jamaicamide B initially under the green condition. This is assumed because the production of pheophytin and growth stayed the same or decreased while jamaicamide B increased, at least during the first two time points. N = 5 errors are S.E.M.

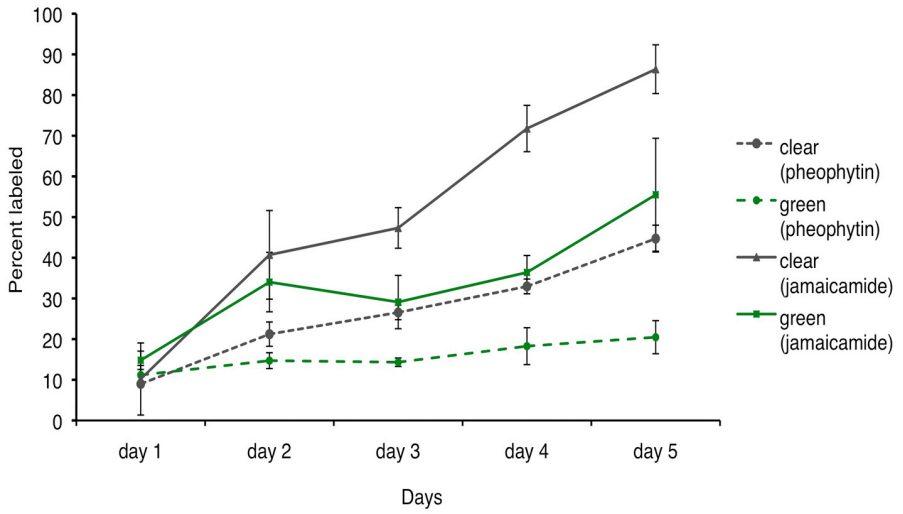

Figure 2.11. The previous (figure 2.10) experiment was repeated, this time using foil to block out all other light. These results are easier to interpret. It appears that the green light simply decreases both ^{15}N labeleling of both pheophytin *a* and jamaicamide B and does not support the initial hypothesis of wavelength dependent regulation of the jamaicamide pathway. However, it does support one of the growing hypothesis from these studies that the ratio of turnover of jamaicamide B to pheophytin *a* is somehow related. N =5 errors are S.E.M.

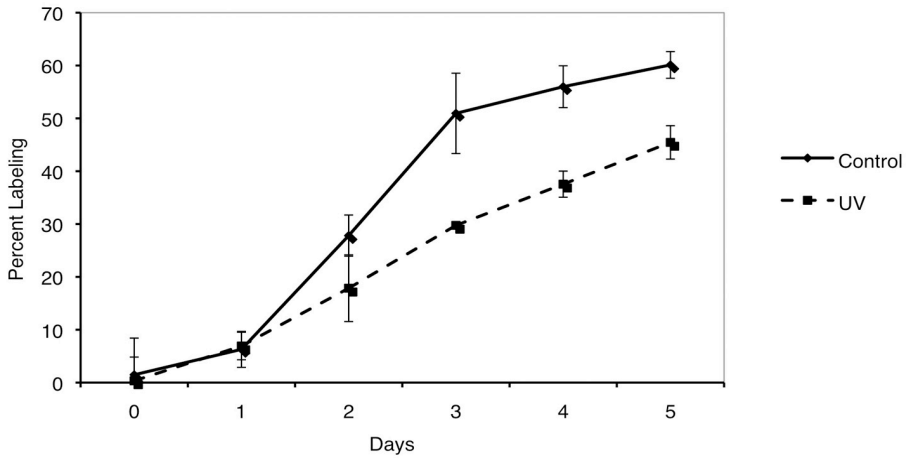

Figure 2.12. Effect of UV light on the ^{15}N labeling rate of jamaicamide B. This is the full result set from the experiment shown in figure x of the supporting information of chapter 1. UV exposure at the same light intensity (33 μE m^{-2} sec^{-1}) reduces the turnover of jamaicaimide B. N = 5 errors are S.E.M.

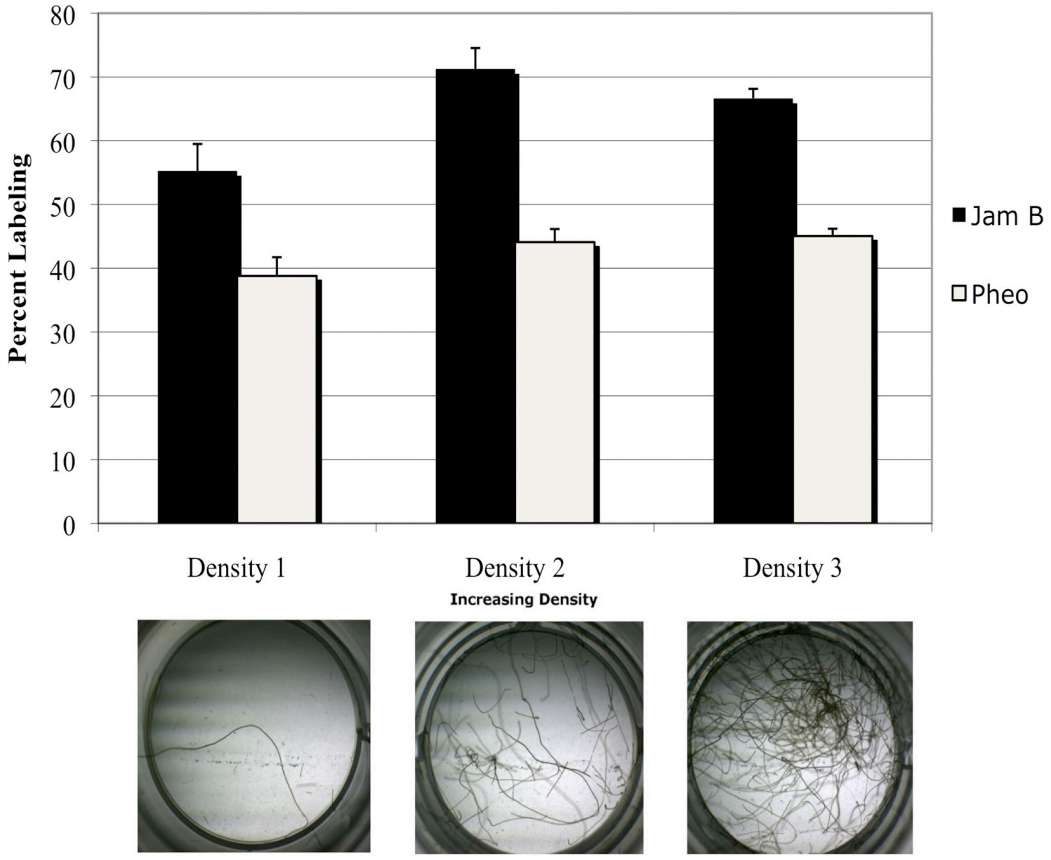

Figure 2.13. Effect of filament density on percent ^{15}N Labeling of jamaicamide B and pheophytin a after 5 days. The top graph indicates the amount of 15N labeling for both jamaicamide B (black) and pheophytin a (white) after 5 days for each condition. The bottom panel shows an image of each of the conditions (the culture density) after 5 days. Filament density appears to have a slightly different impact on pheophytin a than jamaicamide B and suggests possible quorum control of jamaicamide B production. Further studies here might reveal that there is an optimal culture density for natural product production and could provide insight into ecology of toxic cyano blooms.

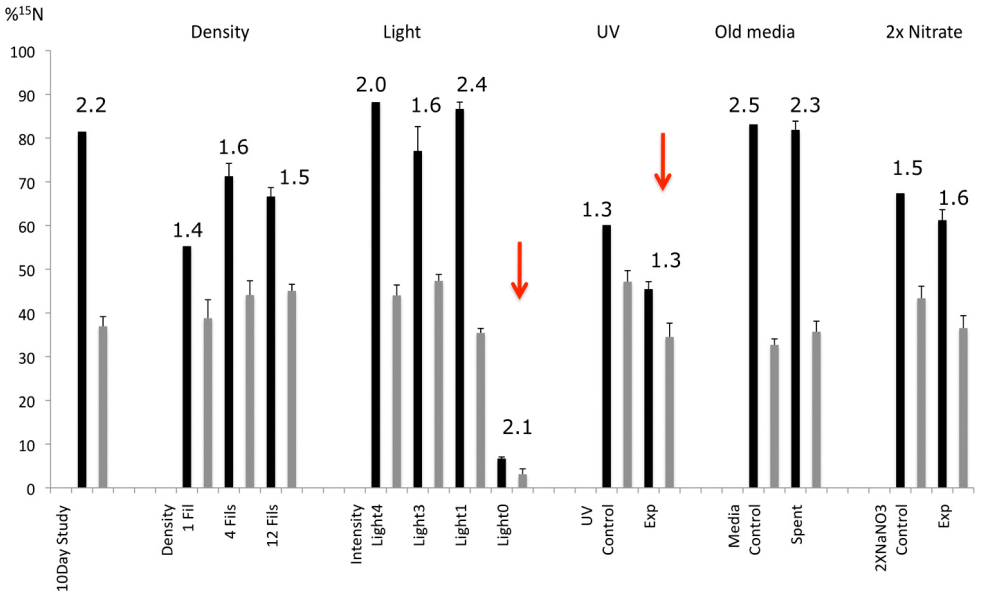

Figure 2.14. Summary- Impact of all the different culture conditions tested on the ^{15}N labeling of jamaicamide B (black) and pheophytin *a* (grey). Comparison of percent labeling after 5 days (bars) the numbers above indicate the ratio of labeled jamaicamide B to pheophytin a. With one exception (Light 3), these ratios are remarkably consistent within each experiment, suggesting a relationship between the production of jamaicamide B and the production of chlorophyll (measured as pheophytin a)

<u>The story of cryptomaldamide.</u>

The ^{15}N feeding studies with L.majuscula JHB had a pleasant by-product. During the course of a large scale study (Figure 2.1 and 2.14 and 2.15) the presence of an abundant and unknown peak with a molecular weight of m/z 400 was detected undergoing a 5 Da shift. This shift is important for several reasons- it allowed this signal to stand out from the rest of matrix associated and small molecule adduct signals present in the sub *m/z* 450 region, it also indicated active biosynthesis and finally the presence of 5 nitrogens.

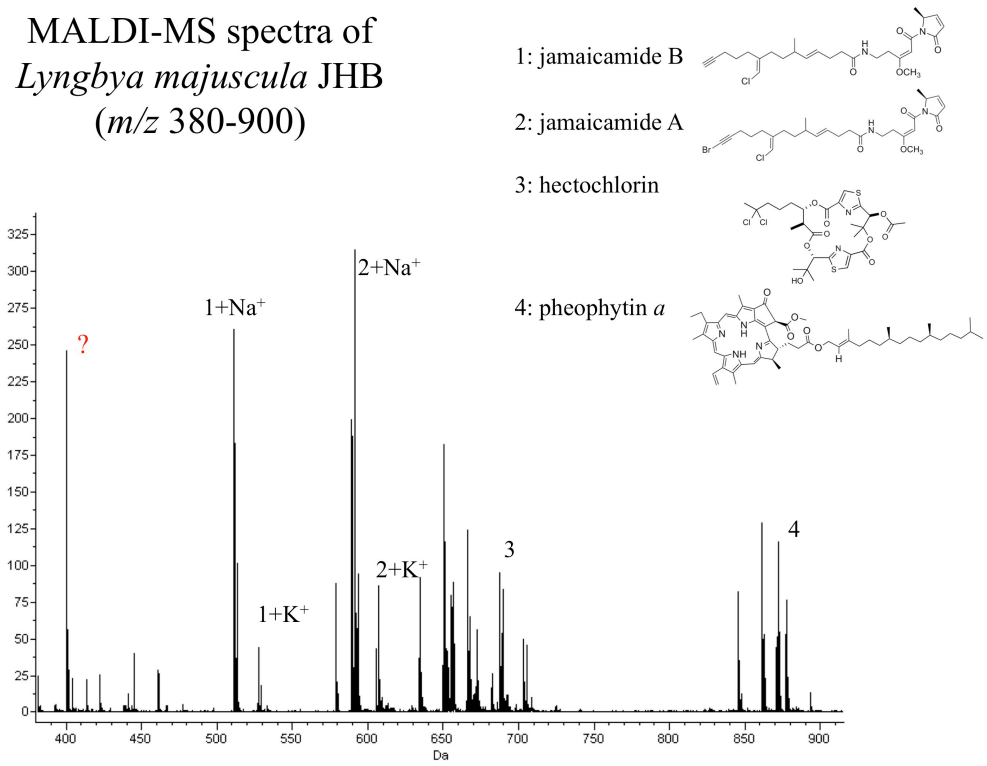

Figure 2.15. MALDI spectrum of *Lyngbya majuscula* JHB showing the presence the known metabolites jamaicamides A and B, hectochlorin and pheophytin *a*, as well as an unknown peak at *m/z* 400.

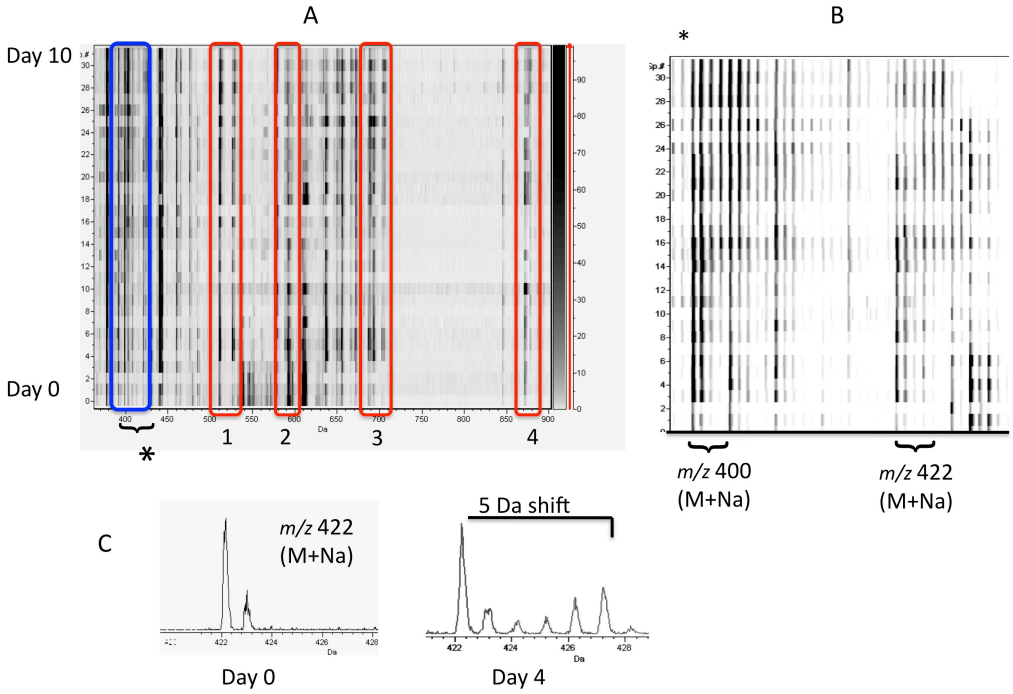

Figure 2.16. Large scale ^{15}N feeding study in *Lyngbya majuscula* JHB showing shifts of known and unknown metabolites. A. Heatmap representation of the global nitrogen containing metabolome shifting over 10 days. Red boxes and numbers indicate the known metabolites in Figure 2.14, the blue box is the unknown metabolite at m/z 400. B. Enlarged area (*m/z* 395-440) showing the presence of a Na^+ adduct at *m/z* 422. C. Spectrum view of Na^+ adduct at *m/z* 422 showing 5 Da shift.

The *Lyngbya majuscula* JHB culture was scaled up and the biomass extracted and fractionated (Figure 2.16), with the resulting fractions checked by MALDI TOF MS dried droplet (see methods in Chapter 2) as the compound was not detected by ESI-LCMS. Further purification was MALDI guided and performed in conjunction with Dr. Robin Kinnel, the compound was found in the aqueous fractions (Figure 2.16), the structure elucidation of cryptomaldamide was performed by Dr. Kinnel. The structure is shown in Figure 2.17.

Cultured *Lyngbya majuscula* JHB: Robin Kinnel's Purification and elucidation

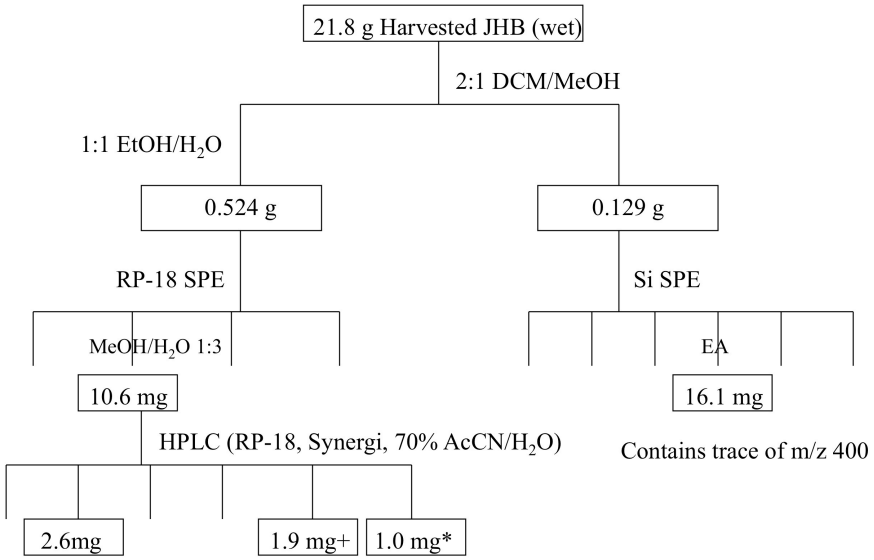

* Pure material, m/z 400.

+Pure peak, but unknown

Figure 2.17. Purification tree following the *m/z* 400 compound, cryptomaldamide performed by Robin Kinnel. (Figure courtesy of W.H.Gewick and R. Kinnel).

Structural Comparison of Cryptomaldamide and the Anticancer Lead Hemiasterlin

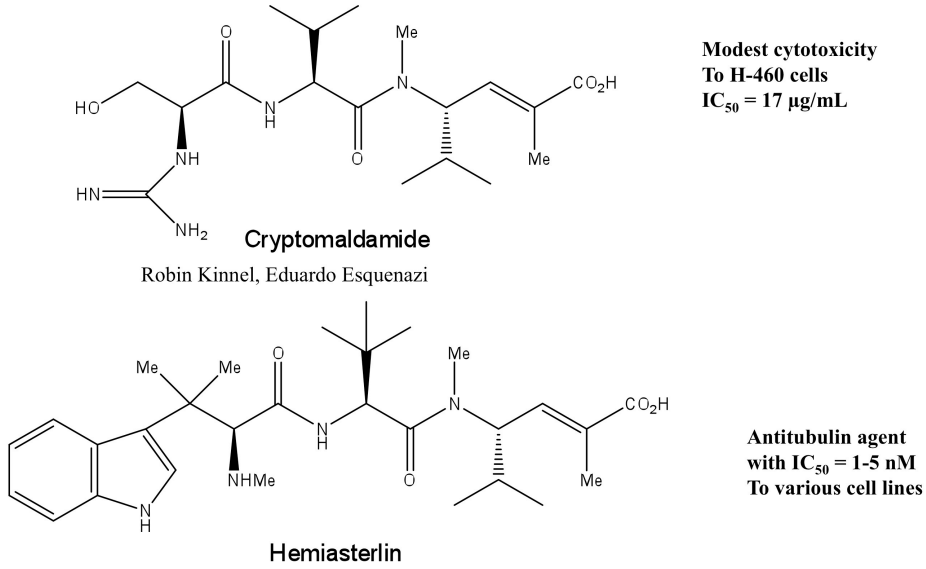

Kashman et al, TL, 1994, 4453; Andersen et al, Tetrahedron 1995, 10653

Figure 2.18. Structure and bioactivity comparison between cryptomaldamide and the anticancer lead compound hemiasterlin (Figure courtesy of W.H.Gewick).

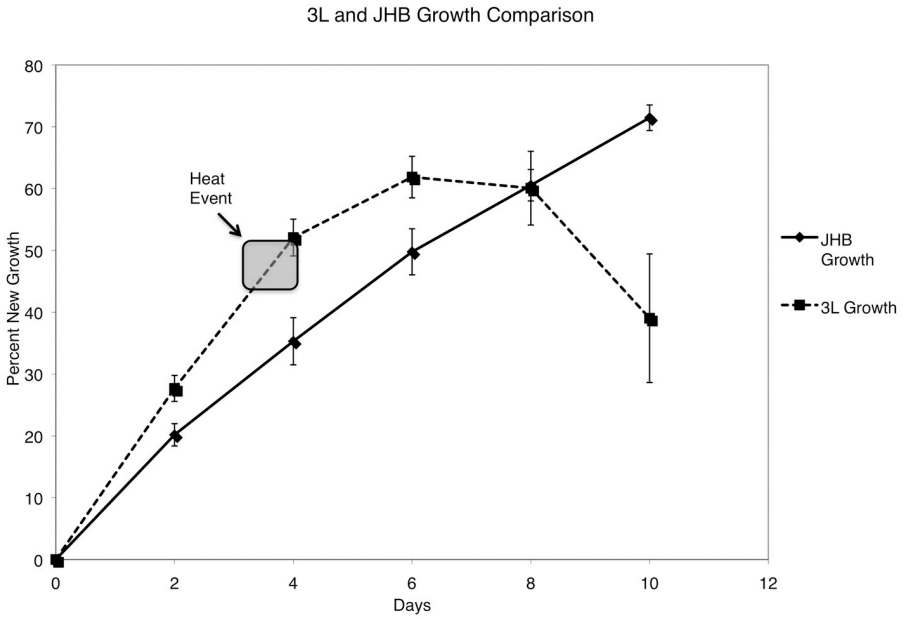

Figure 2.19. Comparison of *L.majuscula* JHB and 3L growth rates.
The two strains appear to have similar growth rates under the same culture conditions, with 3L perhaps having slightly faster rate. During the night of day 3, the culture room experienced an unexpected heat event to above 31C, the impact of this event is shown- having a delayed but large effect on the health of the 3L culture (JHB was run at previous to the heat event.) N = 12

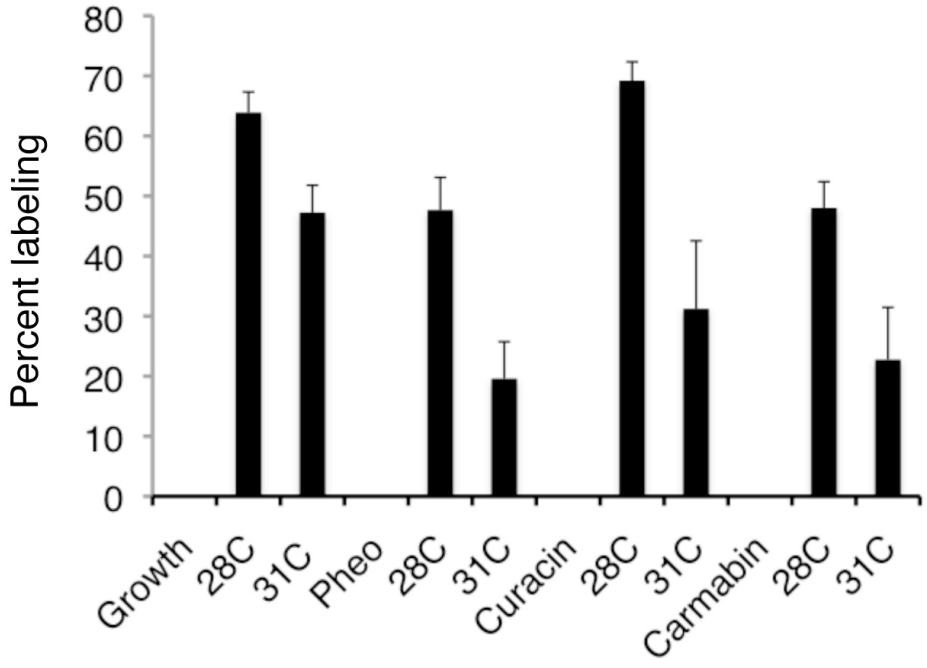

Figure 2.20. Impact of increased temperature on the ^{15}N labeling after 5 days of various metabolites and growth in *Lyngbya majuscula* 3L. An increase of 3C in culture room temperature (from 28C to 31C) for 5 days results in a greater than 50% decrease in the production of pheophytin a, curacin A, and carmabin A as well as a significant reduction in growth.

A

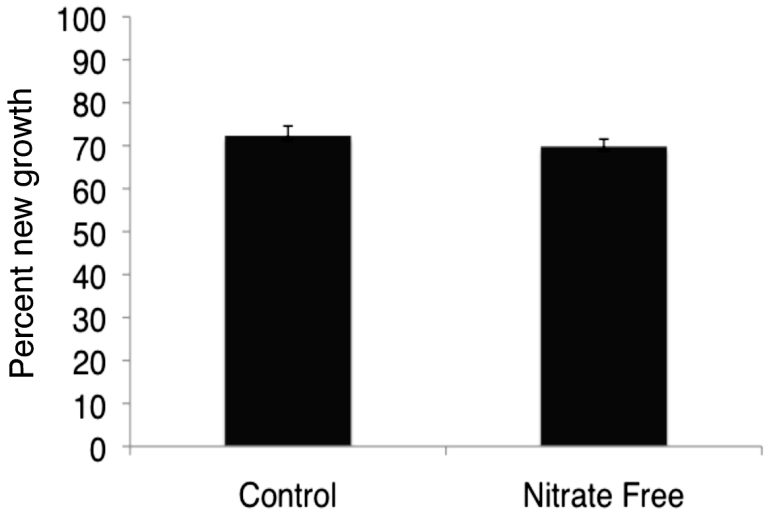

B

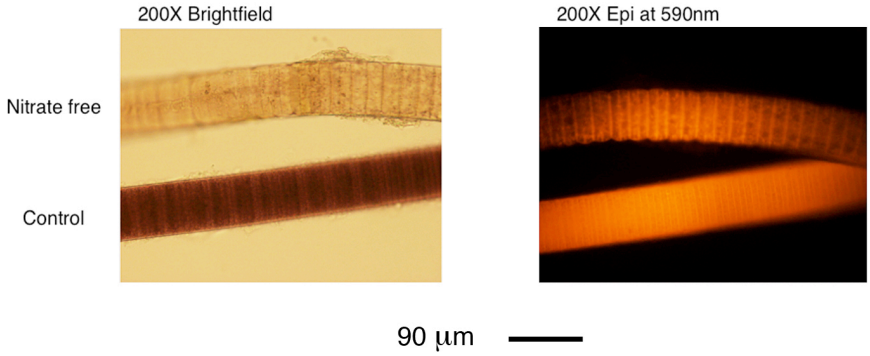

Figure 2.21. Effect of nitrate-free media on *L.majuscula* 3L growth and morphology. A. Percent new growth after 10 days in both control and nitrate free media (as measured by ImageJ software, N = 6). B. Comparison of gross cellular morphology between both conditions.

Table 2.2. Effect of 10 days in Nitrate-Free Media on Number of Cells Per Unit Length of Filament, Cell Width and Filament Width.

	cells/1000pix	Cell Width (pix)	Filament Width (pix)
Control	31.0	209	250
Nitrate free 1	18.5	198	240
Nitrate free 2	12.0	180	228

3.0 CHAPTER 3

VISUALIZING THE SPATIAL DISTRIBUTION OF SECONDARY METABOLITES PRODUCED BY MARINE CYANOBACTERIA AND SPONGES VIA MALDI-TOF IMAGING

3.0.1 Abstract

Marine cyanobacteria and sponges are prolific sources of natural products with therapeutic applications. In this paper we introduce a mass spectrometry based approach to characterize the spatial distribution of these natural products from intact organisms of differing complexities. The natural product MALDI-TOF-imaging (npMALDI-I) approach readily identified a number of metabolites from the cyanobacteria *Lyngbya majuscula 3L and JHB*, *Oscillatoria nigro-viridis*, *Lyngbya bouillonii*, and a *Phormidium* species, even when they were present as mixtures. For example, jamaicamide B, a well established natural product from the cyanobacterium *Lyngbya majuscula* JHB, was readily detected as were the ions that correspond to the natural products curacin A and curazole from *Lyngbya majuscula* 3L. In addition to these known natural products, a large number of unknown ions co-localized with the different cyanobacteria, providing an indication that this method can be used for dereplication and drug discovery strategies. Finally, npMALDI-I was used to observe the secondary metabolites found within the sponge *Dysidea herbacea*. From these sponge data, more than 40 ions were shown to be co-localized, many of which were halogenated. The npMALDI-I data on the sponge indicates that, based on the differential distribution of secondary metabolites, sponges have differential chemical

micro-environments within their tissues. Our data demonstrate that npMALDI-I can be used to provide spatial distribution of natural products, from single strands of cyanobacteria to the very complex marine assemblage of a sponge.

3.1 Introduction

Today, nearly 50% of all anti-cancer agents and 75% of all antimicrobial agents in use are, or have origins from, natural products.[1] Even so, the pharmaceutical industry has gone through a series of ebbs and flows with respect to their reliance on naturally derived or inspired compounds, in more recent times almost entirely depending on combinatorial chemistry for leads because of its cost effectiveness. However, in the last decade the interest in natural products has gained renewed interest.[2] The lack of novel chemistry coming from combinatorial approaches, the growing body of knowledge and availability of genome sequencing, and the increase (at least in public awareness) in diseases such as cancer or drug resistant pathogenic microorganisms, suggests that secondary metabolites could be the source of many significant breakthroughs in therapeutics, and underscores the importance of developing new approaches to characterize and observe secondary metabolites.

Historically, most natural product research has been directed towards terrestrial organisms, mainly plant, fungi and microbes. Among these important discoveries are the plant related anti-tumor agents taxol and colchicine, and numerous antibiotics including amphotericin B, tetracycline, erythromycin and vancomycin.[3, 4] Alternatively, the marine environment remains a largely unexplored resource for novel bioactive natural products, despite the fact that our planet is composed of 70% water

and that life has evolved for a much longer time in the marine environment.[5] Nevertheless, there are a few marine natural products that have been approved by the FDA, including cytarabine in 1969 to the conotoxins and bryostatins of today, and a number of others that have entered clinical trials and hold promise for a variety of diseases.[6–9] It is clear, however, that we still stand to uncover a wealth of new therapeutic agents from the marine environment, especially if we can streamline the bio-discovery process and combine and maximize the efforts of marine biologists and chemists with the power of genomics and bioinformatics.

One tool that has bridged marine biologists with chemists is MALDI-TOF mass spectrometry. MALDI-TOF is a method that can be used to analyze cyanobacterial extracts with minimal work-up.[10] This approach involves extraction of the cyanobacteria, mixing the extract with matrix and subsequent analysis for peptides and other structural classes by MALDI-TOF mass spectrometry. This approach is an excellent complement to standard LC-MS approaches, and is easier to implement.[11] Using MALDI-TOF, several new cyanopeptides were observed and characterized. Recently, MALDI-TOF was used to directly analyze cyanobacteria for the presence of cyanopeptides and toxins from 850 individual colonies.[12] In this study, a small colony of the cyanobacterium was placed on a MALDI-TOF-plate and covered with a small amount of 2,5-dihydroxybenzoic acid matrix before they were analyzed by MALDI-TOF mass spectrometry. A total of 90 individual peptides were identified from these 850 individual cyanobacteria colonies, including 18 that appear to be unique from their masses. Finally, MALDI-TOF mass spectrometry has also been used to observe

sponge derived metabolites from sponge bacterial isolates or even a homogenized sponge tissue itself.[13–15]

In this communication we expand upon the approaches described above which were primarily developed by the von Dohren lab, and demonstrate that MALDI-TOF-imaging can be applied to the detection of natural products even from very complex marine systems such as sponges. In this paper we show that MALDI-TOF imaging is a valuable tool in the de-replication of cyanobacteria for low intensity signals, allowing the detection of a broad range of known and unknown metabolites in both homogenous and heterogeneous assemblages. This approach provides not only the mass information on the ions analyzed but also the spatial localization of these metabolites. Such an imaging approach has been used to identify biomarkers of disease as well as the accumulation of drugs in whole animals but has not yet been applied to the analysis of natural products.[16–18] The visualization and spatial information this technique provides could allow the identification and enrichment of specific organisms, allowing the isolation and characterization of genomes via single cell genomic sequencing. It could also become an important tool in the study of host-microbe interactions, such as those involving complex assemblages of species (e.g. sponges, tunicates). Finally the new MALDI-TOF-imaging approach outlined in this paper could aid in the discovery of new therapeutic agents as numerous uncharacterized ions are detected in these experiments.

3.2 Results and Discussion:

3.2.1 MALDI-TOF-imaging of natural products from single cyanobacterial filaments

We first needed to establish the reasonableness of our goal to determine the presence and localization of natural products from samples of marine origin with MALDI-TOF-imaging. Because the lower *m/z* region is typically obscured from ions deriving from matrix, it is usually not recommended that MALDI-TOF mass spectrometry be used when the ions under examination are in the low *m/z* region of the spectrum. Unfortunately, most natural products are observed in this region. The observations of matrix clusters within the lower *m/z* window is particularly problematic when small amounts of material are analyzed, as would be expected from single cyanobacterial filaments.[19, 20] To demonstrate that secondary metabolites can be observed from intact marine organisms, *Lyngbya majuscula* JHB was analyzed via MALDI-TOF-imaging, referred to here as Natural Product MALDI-TOF-imaging or npMALDI-I throughout the rest of the manuscript. *Lyngbya majuscula JHB* is known to produce several bioactive natural products with masses below *m/z* 600. For example, jamaicamides A-C are sodium channel blockers (figure 3.1A).[21] Therefore, this strain serves as an excellent example to demonstrate that npMALDI-I can be utilized to show the location of secondary metabolites even when the molecular species is less than *m/z* 600,(the $M+H^+$ of jamaicamide B has a mass of 489 Da).

To image natural products from intact cyanobacteria, a small colony of *Lyngbya majuscula JHB* was grown for ~20 days. Single filaments were removed, washed in distilled water to remove most of the salty growth media and placed on top

Figure 3.1. MALDI-TOF-imaging of the intact marine cyanobacterium Lyngbya majuscula JHB filament. (A) The molecular structures of jamaicamide A, B and yanucamide B. (B) The average mass spectrum of a 0.6 x1.5 mm area of the MALDI imaging experiment. The colors indicate the regions visualized in C. (C) The differential localization of the indicated masses with respect to the cyanobacterial filament, **a** shows the raster points in this experiment. (D) Comparison of the theoretical isotopic distribution of jamaicamide B and yanucamide B indicated by the black dots with the observed average spectrum in this experiment. (E) The spatial distribution for several molecular ions co-localized with Lyngbya majuscula JHB.

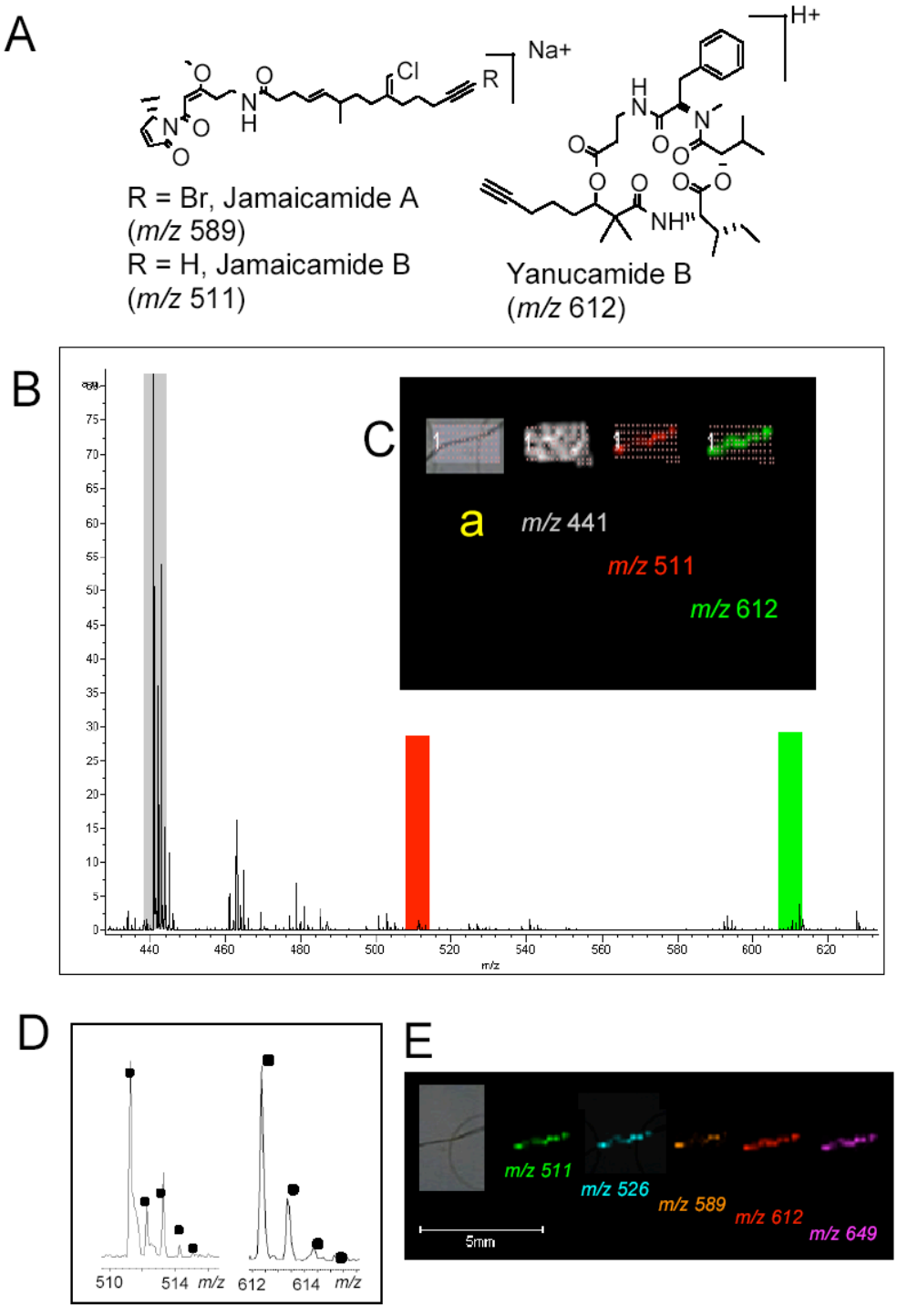
A
R = Br, Jamaicamide A
(m/z 589)
R = H, Jamaicamide B
(m/z 511)
Yanucamide B
(m/z 612)
B
C
a
m/z 441
m/z 511
m/z 612
D
510
514 m/z
612
614 m/z
E
m/z 511
m/z 526
m/z 589
m/z 612
m/z 649
5mm

of the MALDI plate. The plate was dried and a matrix (composed of a-cyano-4-hydroxycinnamic acid, 2,5 dihydroxybenzoic acid) was airbrushed on the plate until a uniform crystalline layer appeared. This matrix composition was deemed to be optimal for minimizing the crystal size and therefore increased our spatial resolution, while retaining enough ionization so that a mass spectrum can be obtained directly from a single filament (we estimate that we are only analyzing 25-40 individual cyanobacterial cells at one time as the cells are 20-50 μm in width and 2-4 μm in length).

To demonstrate the npMALDI-I approach, a 0.6 *1.5 mm area that contained a section of a single *Lyngbya majuscula* JHB filament was imaged with a 100*100 μm raster area (figure 3.1B and 3.1C). At each of those raster points, a single MALDI spectrum from *m/z* 350 to 1000 was obtained. Following the acquisition of all the spectra, an average spectrum was generated from all the individual spectra. The individual masses can then be displayed on a pre-imported image of the cyanobacterial filament by designating a specific color to an *m/z* window (figure 3.1C). The higher the relative intensity of a specific species with respect to other ions at any one raster point, the darker the color. Manual scanning at *m/z* 0.5-3.0 windows revealed that several masses co-localized with the cyanobacterial filament, while others were localized throughout the entire sample. Once a particular isotope peak is shown to co-localize with the filament, the *m/z* window is expanded to include the neighboring peaks as long as they show the same co-localization pattern. Keeping in mind the resolution of the instrument- R, by the FWHM method, is determined to be about 5000

for each individual raster point and closer to 4000 for the average spectrum, it is difficult to distinguish between different metabolites with similar masses, however the isotopic signatures combined with the localization pattern is usually enough to suggest if there is more than one compound present in a particular *m/z* window. For example, the ions *m/z* 511 and 612 are localized with the filament while other ions such as *m/z* 441, originating from the matrix, are localized throughout the sample (figure 3.1C). The masses and the isotopic distributions at *m/z* 511 and 612 are in agreement with the natural products jamaicamide B and yanucamide, and demonstrate that even low molecular weight natural products can be observed by npMALDI-I of intact marine cyanobacterial filaments (figure 3.1D).[22] In addition to ions that are in agreement with jamaicamide B and yanucamide B, other ions at *m/z* 589 (jamaicamide A), 526, 629 were also observed and co-localized with the cyanobacterium (figure 3.1E.). It is not yet known what molecular entities are represented by the ions at *m/z* 526 and 629.

Following the detection of ions with the same isotopic profile that correspond to the expected mass of jamaicamide A and B, and yanucamide B in the *Lyngbya majuscula* JHB*,* it was important to demonstrate that npMALDI-I would work on other marine cyanobacteria, to establish that this may in fact be a general method for observing natural products from these organisms. To demonstrate the generality of this approach, the marine cyanobacteria, *Lyngbya majuscula 3L*, *Oscillatoria nigro-viridis*, *Lynbya bouillonii*, and *Phormidium* species were investigated in a similar fashion as *Lyngbya majuscula JHB* described in the previous section. Imaging showed that some of the ion intensities co-localized with the cyanobacteria and a

selection is shown in figure 3.2. Some of the masses that co-localized to the *Lyngbya majuscula* 3L filament were observed at *m/z* 372, 374, 592 and 610. The *m/z* 372 and *m/z* ions are in agreement with the natural products curazole and curacin (Fig. 3.2).[23] Ions *m/z* 592 and 610 are unknown but have to come from the filament as they are co-localized. Among the ions that were observed to co-localize with the image of the cyanobacteria *Oscillatoria nigro-viridis* were *m/z* 593, 871 and 885. Of these masses, *m/z* 871 and 885 are in agreement with the unpublished natural products viridamides A and B (Fig. 3.1E), demonstrating that this approach could be used to discover new natural products (Gerwick, unpublished results). The *m/z* 593 ion represents an unknown that is associated with this cyanobacteria and similar ions of this mass were detected in a previous MALDI-TOF study of cyanobacteria.[24]

Phormidium sp. and *Lynbya bouillonii*, just like the previous cyanobacteria, showed a large number of associated unidentified ions. Because there are a large number of ions observed (e.g. 24 unique ions were observed for *Phormidium*), only some representative co-localizations are shown in Figure 3.2 F and G, demonstrating that npMALDI-I of intact cyanobacterial species can be used to detect metabolites in a spatial fashion. In some cases additional information can be gleaned from just analyzing the mass spectrum alone. For example, the *m/z* 364 ion is halogenated, judged from the isotopic pattern that this ion displays (Fig. 3.2H). Since none of these metabolites could be correlated to specific natural products, it underscores the untapped therapeutic potential that the ocean represents.

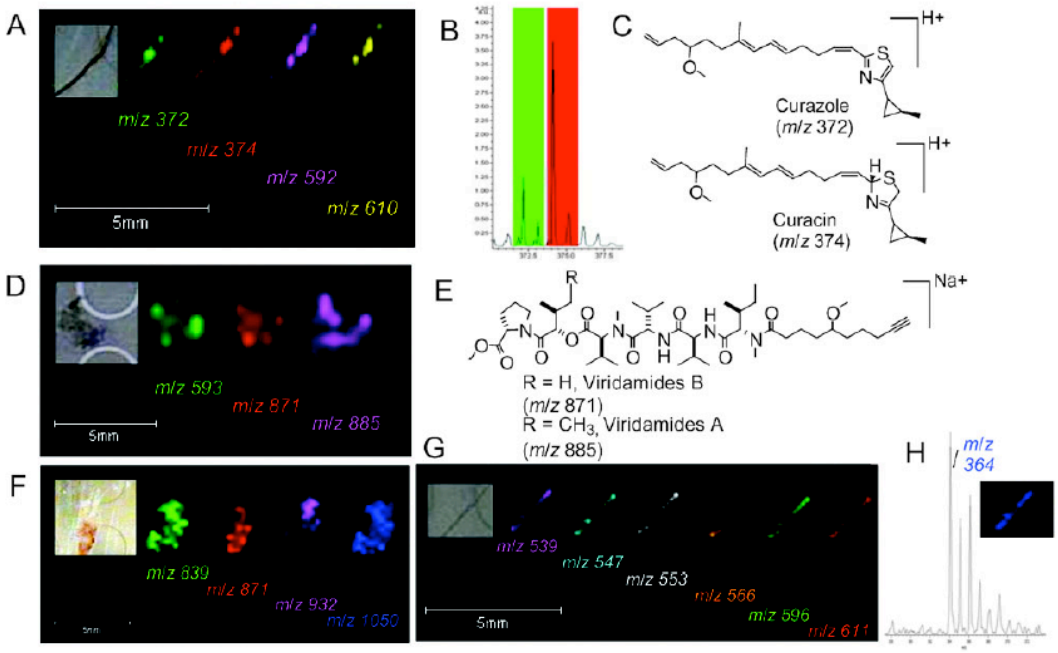

Figure 3.2. The spatial distribution of selected ions observed to co-localize with *Lyngbya majuscula 3L* (A), *Oscillatoria nigro-viridis* (D), a *Phormidium* species (F), and *Lyngbya bouillonii* (G). The average mass spectral trace showing curacin and curazole and the respective colors indicated is shown in B. The structures of curacin, curazole (C) and viridamides (E) are also shown. (H) The isotopic distribution for the 364 m/z molecular ion.

One of the main challenges with the npMALDI-I approach is the spatial resolution of the instrument and sample preparation. Currently our technique is limited to about 100-200 µM resolution, hinging on the size of the matrix crystals applied to the specimens. While the size of the crystals is one of the factors in determining resolution, the N_2-laser used for these experiments is also a limitation. A typical N_2 laser has a diameter of 50-100 µM, although in the near future it should be possible to get 10 µm resolution.[25] Many laboratories are still developing new

approaches to matrix application and, undoubtedly, future implementation of these techniques will greatly improve the resolution in our experiments.[26–28]

Even though npMALDI-I has this inherent spatial resolution, npMALDI-I can indeed identify ions for which the masses are in agreement with unique natural products even at low *m/z* regions (we have shown ions as low as *m/z* 372 can be observed by this approach). We currently do not see the low *m/z* as a major limitation for npMALDI-I as we can confidently say that the ions detected are associated with the cyanobacteria via co-localization. Therefore, the npMALDI-I approach is applicable in dereplication or taxonomic strategies.

3.2.2 Using MALDI-TOF imaging for the dereplication of individual marine cyanobacteria from mixed assemblages

Thus far, we have only demonstrated that the npMALDI-I approach works on single cyanobacteria but if the analysis from heterogeneous mixtures or the ability to dereplicate individual cyanobacteria is desired, it is important to show that the spatial information is not lost when multiple organisms are present in one image. Therefore, a mixture of *Lyngbya majuscula* 3L *and* JHB, *Oscillatoria nigro-viridis*, *Lyngbya bouillonii*, were laid down on the MALDI-plate and imaged using MALDI-TOF in an identical fashion described for the individual cyanobacteria. The ions at *m/z* 511 (*Lyngbya majuscula JHB*), 592 (*Lyngbya majuscula 3L*), 611 (*Lyngbya bouillonii*), and 885 (*Oscillatoria nigro-viridis*) were displayed with a different color. npMALDI-I could readily distinguish these known ion masses known to be associated with each

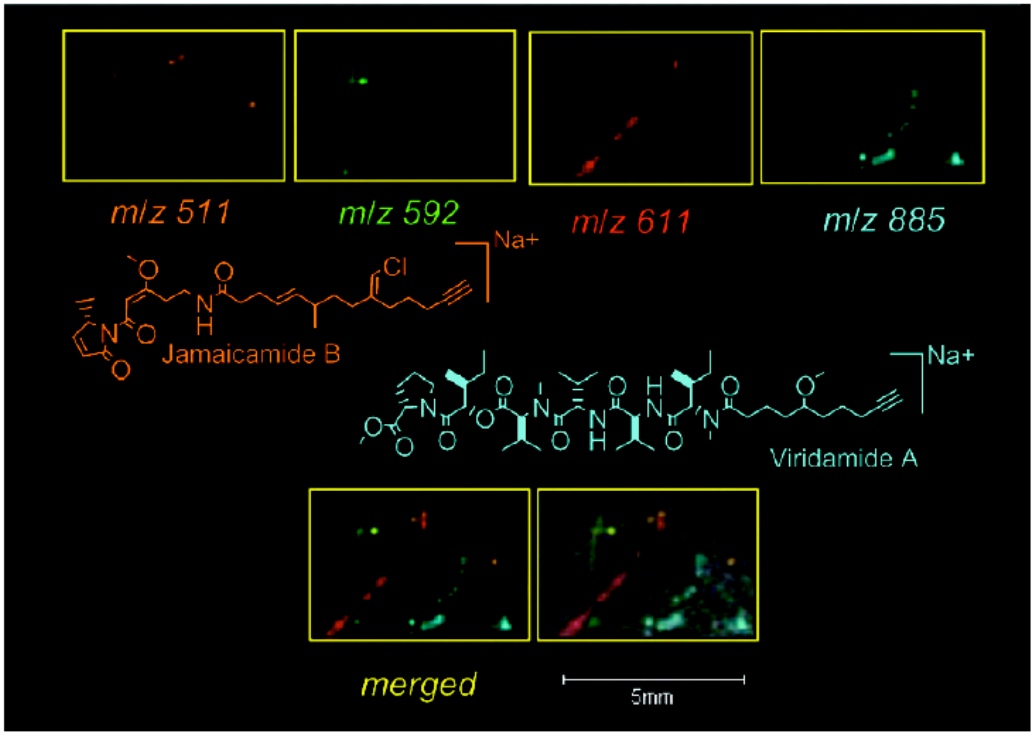

Figure 3.3. npMALDI-I of a complex mixture of cyanobacteria: a single npMALDI-I run on a mixture of Lyngbya majuscula JHB (orange), and 3L(green), Lynbya bouillonii (Red) Oscillatoria nigro-viridis (Blue). The top panels represent detection of two known masses-Jamaicamide B (orange structure shown) and viridamide A (blue-structure shown) as well as two unknown masses (red and green), each specifically and differentially locates to a particular organism. The bottom panels emphasizes the scale and spatial resolution, as well as the ability to visualize various different secondary metabolites from multiple organisms.

cyanobacteria. This proof-of-principle experiment demonstrates that we can observe natural products in a spatial fashion within mixed assemblages.

3.2.3 Spatial distribution of secondary metabolites within the marine sponge, *Dysidea herbacea*

Sponges are often regarded as one of the oldest, most successful and most complex assemblages in the marine environment, with some species often comprised

of a several species of cyanobacteria, red algae, and many other microorganisms. Up to 40% of a sponge's mass is widely thought to be attributed to coexisting organisms.[29, 30, 31] This observation, combined with the fact that sponges are a rich source of new natural products with potent bioactivities, leads us to the question as to which organisms are responsible for the observed bioactive compounds. Our goal was to determine if npMALDI-I could be accomplished on a sponge and if the resulting data could provide us with insight regarding not only the presence of natural products, but their localization as well. We choose to study the sponge, *Dysidea herbacea,* because it is known to be rich in cyanobacteria and numerous natural products have been isolated from this sponge.[32-35] To accomplish the imaging on the sponge, a 14 μM thick section was prepared using a cryo-microtome and mounted onto a MALDI plate, the sample was then dessicated and covered with a uniform crystalline matrix and subjected to npMALDI-I. Using this approach, at least 40 ions localized specifically to the sponge, many of which are halogenated judging from the isotopic profile (figure 3.4A). In addition, differential localization of ions throughout is observed. The relative variation in the MALDI-TOF signal from region to region can be directly observed from the individual spectra. Three mass spectral traces from the indicated raster points as shown in figure 3.4B indicate that they have dramatically different ion concentration profiles, these abundances are then reflected by the use of colors on those relative (but not absolute) ion intensities to provide a spatial localization. Some representative ions we have observed with differential localization are shown in figure 3.4C (and supporting information figure 3.5). The data in figure

Figure 3.4. npMALDI-I on the sponge *Dysidea herbacea*. (A) The average mass spectrum. The colors indicate all the ions that specifically localized to the sponge section, the colors themselves have no meaning other than that they are a means to show the differential localization. (B) An image of the *Dysidea* section with the laser raster points and selected masses shown. In this image we show the relative ion intensities in the region from 560 to 660 m/z for three different areas of the sampling area. This image shows the different ion localizations and ion clusters associated with the matrix. Ions indicated with a # are co-localized throughout the sponge, ions that are localized near the edges of the sponge are indicated with a ^ and ions found on the inner section of the sponge are shown with a *. (C) Some representative differential localizations and ion masses associated with the sponge, suggesting differential chemical microenvironments. ‘‘a’’ shows the raster on the image. ‘‘b’’ shows the photomicrograph of the sponge-section itself.

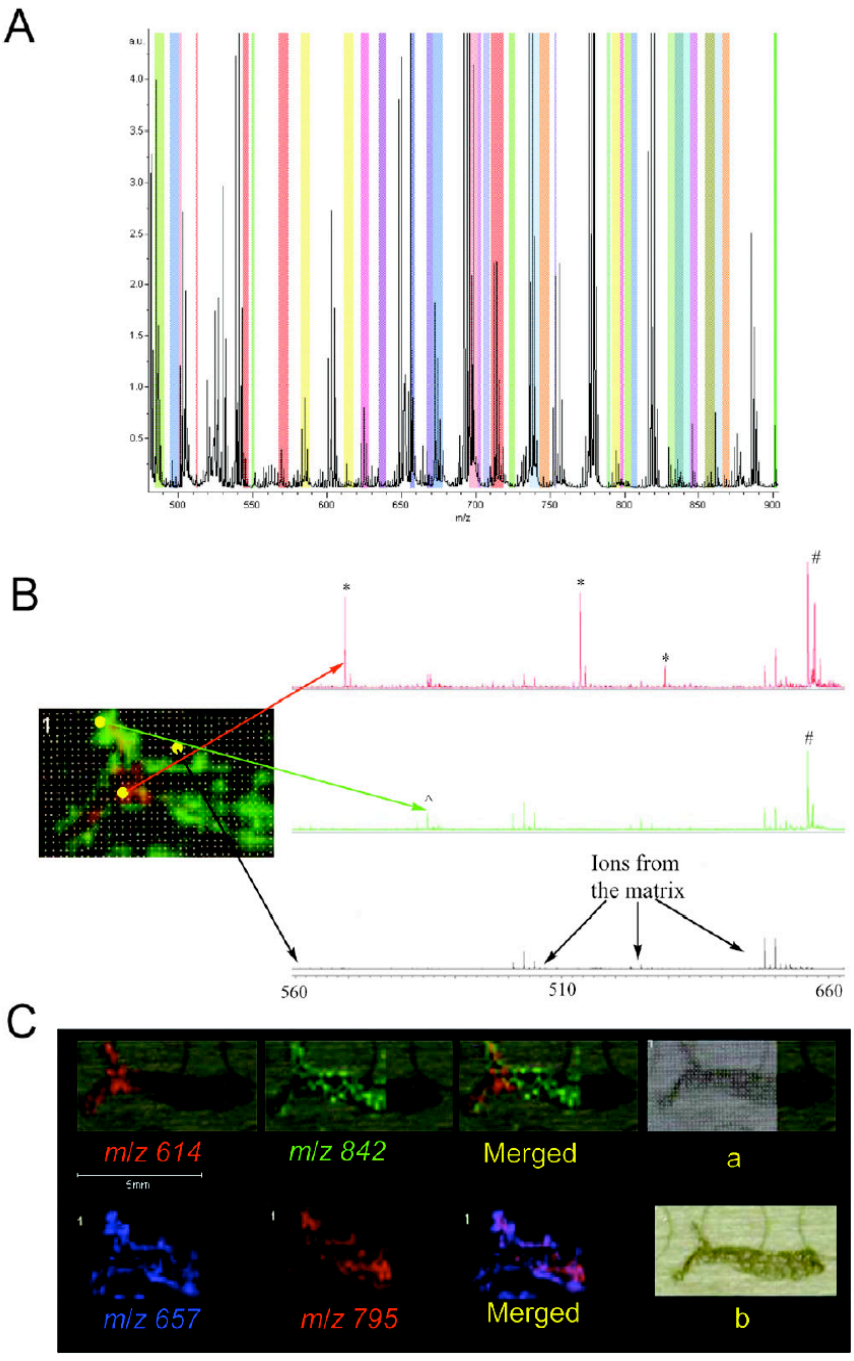
A
a.u.
4.0
3.5
3.0
2.5
2.0
1.5
1.0
0.5
500
550
600
650
700
750
800
850
900
m/z
B
*
*
*
#
#
^
1
Ions from
the matrix
560
510
660
C
m/z 614
5mm
m/z 842
Merged
a
1
m/z 657
1
m/z 795
1
Merged
b

3.4C clearly provides evidence that there is a differential distribution of secondary metabolites within a cross section of the sponge. Some ions are localized on the outer edges, tentatively the pinacoderm and edges of the ostia, while others have a more complete and uniform distribution, and others appear to have distinct, internal localization concentrated in what appears to be possibly the mesohyl. The idea that secondary metabolites have different spatial distributions within the sponge tissue is not surprising given that it has been shown that co-existing microorganism tend to populate specific regions of sponge tissue and that it is becoming increasingly clear that these same microorganisms are at least responsible for the biosynthesis of some of the secondary metabolites.[36–39] A detailed report on npMALDI-I, combined with microscopy studies, single cell genomics and LC-MS analysis of the *Dysidea* sponge is forthcoming (Gerwick, Dorrestein unpublished).

3.3 Conclusions

In this paper we have introduced npMALDI-I to observe, in a spatial fashion, natural products from intact marine organisms such as cyanobacteria and heterogenous assemblages such as the *Dysidea herbacea* sponge. We have demonstrated that it can be used to observe these metabolites from intact cyanobacterial filaments and sponges with high spatial resolution even though the ions are in the low *m/z* window. In addition, npMALDI-I has advantages over traditional MALDI-TOF screening because we can say with confidence that even the very low intensity ions are originating from the sample because of the specific co-localization with the target tissue. The data on the sponge *Dysidea herbacea* indicates that, based on the differential distribution of

secondary metabolites, sponges have differential (chemical) micro-environments within their tissues. Our laboratories are planning to use npMALDI-I to localize previously described specific natural products with potent therapeutic properties from heterogeneous marine assemblages, a step towards allowing us to collect the genetic material and pinpoint the specific gene clusters responsible for their synthesis. Finally, the approach outlined in this paper should be readily adapted to secondary metabolomic studies, the chemical communication of symbionts or therapeutic discovery programs.

3.4 Materials and Methods

3.4.1 Cyanobacteria cultures

3L Lyngbya was collected at Las Palmas beach near the CARMABI Research Station in Curacao, Netherlands. JHB was collected in Hector's Bay, Jamaica. *Oscillatoria nigroviridis* was isolated as a contaminant of the 3L *Lyngbya majuscula* strain *Lyngbya bouilonii* was collected on Pigeon Island in Papau New Guinea. *Phormidium sp*. was collected in Indonesia. All cultures were subsequently isolated to a monoclonal culture using standard microbiological isolation techniques (Rossi et al 1997, Edwards *et al* 2004). Approximately 3 g of each strain were inoculated into 2-L Fernbach flasks containing 1 L of SWBG11 medium. These static cultures were grown at 28°C under uniform illumination (4.67 µmol photon s^-1 m^-2) with a 16hr/8hr light/dark cycle for 30 days. About 10-20 individual filaments were transferred to 50ml polystyrene tissue culture flasks.

3.4.2 Filament sample preparation

Using blunt-tip tweezers, a single filament was removed from the small colonies in the 50ml flasks and transferred to a petri dish containing distilled water to remove excess salt water attached to the cyanobacterial filaments. Again, using blunt-tip tweezers, the filament was removed and carefully laid out onto a Bruker MSP 96 anchor plate, making sure that the filament laid flat against the plate. Any excess liquid on the surface was absorbed using the corner of a Kimwipe ®. If multiple filaments were being examined, particular attention was given to the orientation and location of the filaments on the plate. The plate was then placed in a desiccator at 38^0C for 5-10 minutes or until visibly dry. Prior to matrix application, a photograph (Nikon Coolpix, 1-3 mp image) of the plate was taken to use as teach reference for the Bruker MALDI MS.

3.4.2.1 MALDI matrix deposition

After the desiccation and image capture, matrix composed of 35mg/ml a-cyano-hydroxycinnamic acid, 15 mg/ml DHB, 78% ACN and 0.1% TFA was coated onto the MALDI MSP 96 plate using an airbrush (**Error! Hyperlink reference not valid.**) and repeated side to side strokes until an even, thin crystalline layer occluded the background of the plate The Bruker MSP 96 anchor plate containing the sample and matrix was placed in an empty Petri dish until analysis.3.4.2.2 MALDI MS and imaging

The Bruker MSP 96 anchor plate containing the sample was inserted into a Microflex Bruker Daltonics mass spectrometer outfitted with Compass 1.2 software

suite (Consists of FlexImaging 2.0, FlexControl 3.0, and FlexAnalysis 3.0). The sample was run in positive mode, with 100μm raster intervals in XY and roughly 35-62% laser power. Briefly, a photomicrograph of the sample to be imaged by mass spectrometry was loaded onto the *Fleximaging* command window. Three teach points were selected in order to align the background image with the sample target plate. After the target plate calibration was complete, the *AutoXecute* command was used to analyzed the samples. The settings under the FlexControl panel where as follows: For the **Autoexecute**. **Method**: Our own. Consisting of the following settings: *General*: Flex-Control Method- RP_pepMix.par. *Laser*: Fuzzy Control-On, Weight - 1.00; Laser Power- varied between 35-62%; Matrix Blaster- 0. *Evaluation*: Peak Selection- Masses from *m/z* 350-3000, mass control list- Off. Peak Exclusion-Off. Peak Evaluation- Processing Method- Default, Smoothing-Off, Baseline Subtraction-On, Peak- Resolution higher than 100. *Accumulation*: Parent Mode: On, Sum up to 20 satisfactory shots in 20 shots, Dynamic Termination- Off. *Movement*: Random Walk- 2 shots at raster spot. Quit sample after- 2 subsequent failed attempts. *Processing*: Flexanalysis Method- none, Biotools MS method- none. **Sample Carrier**: nothing **Spectrometer**: On, Ion Source 1- 19.00mV, Ion Source 2- 16.40mV, Lens- 9.45mV, Reflector 20.00, Pulsed Ion Extraction- 190ns, Polarity- Positive. Matrix Suppression: Deflection, Suppress up to: *m/z* 350. **Detection**: Mass Range- 350-1000, Detector Gain- Reflector 3.7X. Sample Rate- 2.00 GS/s, Mode- low range, Electronic Gain- Enhanced, 100mV. Real time Smooth- Off. Spectrometer, Size: 81040, Delay 42968. **Processing Method**: Factory method RP_2465. **Setup**: Mass Range- Low. Laser

Frequency- 20Hz, Autoteaching-off. Instrument Specific Settings: Digitizer- Trigger Level- 2000mV, Digital Off Linear- 127 cnt, Digital Off Reflector- 127cnt. Detector Gain Voltage Offset, Linear- 1300V, Reflector- 1400V. Laser Attenuator, Offset -12%, Range- 30%, Electronic Gain Button Definitions, Regular: 100mv (offset lin) 100mV (offset ref) 200mV/full scale. Enh: 51mV (offset lin), 51mV (offset ref) 100mV/full scale. Highest: 25mV (offsetlin) 25mV (offset ref) 50 mV/full scale.

Calibration: Calibration was accomplished using a BSA digest as external standard. Zoom Range +-1.0%Peak Assignment Tolerance- User Defined-500ppm.

After data acquisition, the data was analyzed using the FlexImaging software. The resulting mass spectrum was filtered manually in 0.5-3.0 Da increments with individual colors assigned to the specific masses associated with the filaments.

3.4.3 Dysidea herbacea preparation

3.4.3.1 Sample collection and storage

Dysidea herbacea (Collection code 02158) was collected in Papua New Guinea in 2002 by Phil Crews lab (UCSC). It was stored and frozen in EtOH/Sea water (1:1)

3.4.3.2 Cryosectioning of sponge tissue

The sample was thawed and precut then embedded in 1X Dulbecco's PBS and placed in the cryostat at -20C. Once the tissue and embedding block had frozen completely, 14-20 μm thick coronal sections were cut and mounted on to a semi-thawed MALDI MSP 96 plate. The plate was desiccated at 38^0C for 10 minutes. Prior

to matrix application, a photograph (Nikon Coolpix, 3mp image) of the plate is taken as teach reference for the Bruker MALDI MS.

3.4.3.3 MALDI imaging of Dysidea herbacea.

The Data acquisition, Flex control settings and data processing was performed as described for the analysis of single filaments with a few notable exceptions. The sample was run in positive mode, with 100 μm raster intervals in XY and 55-65% laser power. **Autoexecute**. **Method**: *Movement*: Random Walk- 3 shots at raster spot. Sum up to 30 satisfactory shots in 30 shots.

3.5 CHAPTER 3 ACKNOWLEDGEMENTS

We thank P. Crews and K. Tenney (UC Santa Cruz) for samples of the sponge *Dysidea herbaceae*, We thank T. Matainaho and the captains/crews of the Golden Dawn and Teleta Dive Boats for their assistance with cyanobacterial collections, and the governments of Papua New Guinea, Curaçao, and Indonesia for permission to make these collections. We thank Mark Ellisman, Tom Deerinck, John Crum and Andrea Thor at The National Center for Microscopy and Imaging Resource for their support and expertise in cryo-sectioning. This work was supported by grants NIH CA52955, CA100851, American Cancer Society for maintenance of the instrumentation (IRG-70-002-29) and funding to the Skaggs school of pharmacy and pharmaceutical sciences.

Chapter 3, in part, includes a reprint as it appears in Molecular Biosystems 2008, 4(6): 562-570. Eduardo Esquenazi, Cameron Coates, T. Luke Simmons, David Gonzales, Pieter C. Dorrestein and William H. Gerwick. The dissertation author was the primary investigator and author of this paper.

3.6 CHAPTER 3 REFERENCES

1. D. J. Newman and G.M. Cragg, "Natural Products as Sources of New Drugs over the Last 25 Years," *Journal of Natural Products* 70 no. 3(2007): 461-477.

2. B. H. Bode and R. Mueller, "The impact of bacterial genomics on natural product research," *Angewandte Chemie* [International Edition] 44, no. 42 (2005): 6828-46.

3. J. Dubois, D. Guenard, and F. Gueritte, « Recent Developments in Antitumour Taxoids," *Expert Opinion on Therapeutic Patents* 13 no. 12 (2003): 1809-23.

4. A. L. Demain, "Pharmaceutically Active Secondary Metabolites of Microorganisms," *Applied.Microbiology and Biotechnology* 52 (1999): 455-63.

5. M. W. Taylor, R. Radax, D. Steger, and M. Wagner Sponge, "Associated Microorganisms: Evolution, Ecology, and Biotechnological Potential," *Microbiology and Molecular Reviews* 71 no. 2 (2007): 295–347.

6. J. Jimeno, G. Faircloth, J. M. Fernandez Souse-Faro, P. Scheuer, and K. Rinehart, "New Marine Derived Anticancer Therapeutics - A Journey from the Sea to Clinical Trials," *Marine Drugs* 2 no. 1 (2004): 14-29.

7. A. M. Grant, K. Shanmugasundaram, and A. C. Rigby, "Conotoxin Therapeutics: A Pipeline for Success?" *Expert Opinion on Drug Discovery* 2 no. 4 (2007): 453-68.

8. S. Sudek, N. B. Lopanik, L. E. Waggoner, M. Hildebrand, C. Anderson, H. Liu, A. Patel, D. H. Sherman, and M. G. Haygood, "Identification of the Putative Bryostatin Polyketide Synthase Gene Cluster from 'Candidatus Endobugula sertula,' the Uncultivated Microbial Symbiont of the Marine Bryozoan Bugula neritina," *Journal of Natural Products* 70 no. 1 (2007): 67-74.

9. H. Burkhard, "Drugs From the Deep: Marine Natural Products as Drug Candidates," *Drug Discovery Today* 8 no. 12 (2003): 536-44.

10. M. Erhard, H. von Dohren, and P. Junblut, "Rapid Typing and Elucidation of New Secondary Metabolites of Intact Cyanobacteria Using MALDI-TOF Mass Spectrometry," *Nature Biotechnology* 15 (1997): 906-9.

11. M. Welker and M. Erhard, "Consistency Between Chemotyping of Single Filaments of Planktothrix Rubescens (Cyanobacteria) by MALDI-TOF and the Peptide Patterns of Strains Determined by HPLC-MS," *Journal of Mass Spectrometry* 42 (2007): 1062–8.

12. M. Welker, B. Marsalek, L. Sejnohova, and H. von Dohren, "Detection and Identification of Oligopeptides in Microcystis (Cyanobacteria) Colonies: Toward an Understanding of Metabolic Diversity," *Peptides* 27 (2006): 2090–103.

13. R. Dieckmann, I. Graeber, I. Kaesler, U. Szewzyk, and H. von Döhren, "Rapid screening and Dereplication of Bacterial Isolates from Marine Sponges of the Sula Ridge by Intact-Cell-MALDI-TOF Mass Spectrometry (ICM-MS)," *Applied Microbiology and Biotechnology* 67 (2005): 539–48.

14. C. T. Pabel, J. Vater, C. Wilde, P. Franke, J. Hofemeister, B. Adler, G. Bringmann, J. Hacker, and U. Hentschel, "Antimicrobial Activities and Matrix-Assisted Laser Desorption/Ionization Mass Spectrometry of Bacillus Isolates from the Marine Sponge Aplysina aerophoba," *Journal of Marine Biotechnology* 5 (2003): 424–34.

15. T. Maierb, M. Kostrzewab, and M. Kocka, "MS-Guided Fractionation as a Fast Way to the Identification of New Natural Products – MALDI-TOF-MS Screening of the Marine Sponge Stylissa caribica Achim Grubea," *Zeitschrift für Naturforschung* 62b (2007): 600–4.

16. D. S. Cornett, M. L. Reyzer, P. Chaurand, and R. M. Caprioli, "MALDI Imaging Mass Spectrometry: Molecular Snapshots of Biochemical Systems," *Nature Methods* 4, no. 10 (2007): 828-33.

17. L. A. McDonnell and R. M. A. Heeren, "Imaging Mass Spectrometry," *Mass Spectrometry Reviews* 26, no. 4 (2007): 606-43.

18. M. Stoeckli, D. Staab, A. Schweitzer, J. Gardiner, and D. Seebach, "Imaging of a b-Peptide Distribution in Whole-Body Mice Sections by MALDI Mass Spectrometry," *Journal of the American Society for Mass Spectrometry* 18, no. 11 (2007): 1921-4.

19. S. Vaidyanathan, S. Gaskell, and X. Royston, "Matrix-Suppressed Laser Desorption/Ionisation Mass Spectrometry and Its Suitability for Metabolome Analyses," *Rapid Communications in Mass Spectrometry* 20 (2006): 1192–8.

20. D. S. Peterson, "Matrix Free Methods for Laser Desorption/Ionization Mass Spectrometry," *Mass Spectrometry Reviews,* 26 (2007): 19–34.

21. D. J. Edwards, B. L. Marquez, L. M. Nogle, K. McPhail, D. E. Goeger, M. A. Roberts, and W. H. Gerwick, "Structure and Biosynthesis of the Jamaicamides, New Mixed Polyketide-Peptide Neurotoxins from the Marine Cyanobacterium Lyngbya majuscula," *Chemistry & Biology* 11 (2004): 817–33.

22. N. Sitachitta, T. R. Williamson, W. H. Gerwick, "Yanucamides A and B, Two New Depsipeptides from an Assemblage of the Marine Cyanobacteria Lyngbya majuscula and Schizothrix Species," *Journal of Natural Products* 63 no. 2 (2000): 197-200.

23. Z. Chang, N. Sitachitta, J. V. Rossi, M. A. Roberts, P. M. Flatt, J. Jia, D. H. Sherman, and W. H. Gerwick, "Biosynthetic Pathway and Gene Cluster Analysis of Curacin A, an Antitubulin Natural Product from the Tropical Marine Cyanobacterium Lyngbya majuscula," *Journal of Natural Products* 67 (2004): 1356-67.

24. Erhard, von Dohren, and Junblut

25. P. Chaurand, K. E. Schriver, and R. M. Caprioli, "Instrument Design and Characterization for High Resolution MALDI-MS Imaging of Tissue Sections," *Journal of Mass Spectrometry* 42 no. 4 (2007): 476-89.

26. N. Y. R. Agar, H. W. Yang, R. S. Carroll, P. M. Black, and J. N. Agar, "Matrix Solution Fixation: Histology-Compatible Tissue Preparation for MALDI Mass Spectrometry Imaging," *Analytical Chemistry* 79 no. 19 (2007): 7416-23.

27. J. A. Hankin, R. M. Barkley, and R. C. Murphy, "Sublimation as a Method of Matrix Application for Mass Spectrometric Imaging," *Journal of the American Society for Mass Spectrometry* 18 no. 9 (2007): 1646-52.

28. S. A. Schwartz, M. L. Reyzer, and R. M. Caprioli, "Direct Tissue Analysis Using Matrix-Assisted Laser Desorption/Ionization Mass Spectrometry: Practical Aspects of Sample Preparation," *Journal of Mass Spectrometry* 38 (2003): 699–708.

29. R. W. Hacker and S. Starnes, "Host Specificity of the Symbiotic Cyanobacterium Oscillatoria Spongeliae in Marine Sponges, Dysidea spp," *Marine Biology* 142 no. 4 (2003): 643-8.

30. W. C. Dunlap, C. N. Battershill, C. H. Liptrot, R. E. Cobb, D. G. Bourne, M. Jaspars, P. F. Long, and D. J. Newman, "Biomedicinals from the Phytosymbionts of Marine Invertebrates: A Molecular Approach," *Methods* 42 (2007): 358–76.

31. M. D. Unson. N. D. Holland, and D. J. Faulkner, "A Brominated Secondary Metabolite Synthesized by the Cyanobacterial Symbiont of a Marine Sponge And Accumulation of the Crystalline Metabolite in the Sponge Tissue," *Marine Biology* 119 (1994): 1-11.

32. N. Dumrongchai, C. Ponglimanont, B. L. Stapleton, and M. J. Garson, "Chemical Diversity in the Tropical Marine Sponge Dysidea herbacea," *ACGC Chemical Research Communications* 13 (2001): 17-22.

33. P. M. Flatt, J. T. Gautschi, R. W. Thacker, M. Musafija-Girt, P. Crews, and W. H. Gerwick, "Identification of the Cellular Site of Polychlorinated Peptide Biosynthesis in the Marine Sponge Dysidea (Lamellodysidea) herbacea and Symbiotic Cyanobacterium Oscillatoria spongeliae by CARD-FISH Analysis," *Marine Biology* 147 no. 3 (2005): 761-74.

34. J. D. Deschamps, J. T. Gautschi, S. Whitman, T. A. Johnson, N. C. Gassner, P. Crews, and T. R. Holman, "Discovery of Platelet-Type 12-Human Lipoxygenase Selective Inhibitors by High-Throughput Screening of Structurally Diverse Libraries," *Bioorganic & Medicinal Chemistry* 15 no. 22 (2007): 6900-8.

35. A. E. Flowers, M. J. Garson, R. I. Webb, E. J. Dumdei, and R. D. Charan, "Cellular Origin of Chlorinated Diketopiperazines in the Dictyoceratid Sponge Dysidea herbacea (Keller)," *Cell Tissue Research* 292 (1998), 597-607.

36. Taylor et al.

37. Deschamps et al.

38. Dunlap et al.

39. Unson et al.

3.7 CHAPTER 3 APPENDIX

Other MALDI Imaging Results and Pilot Studies

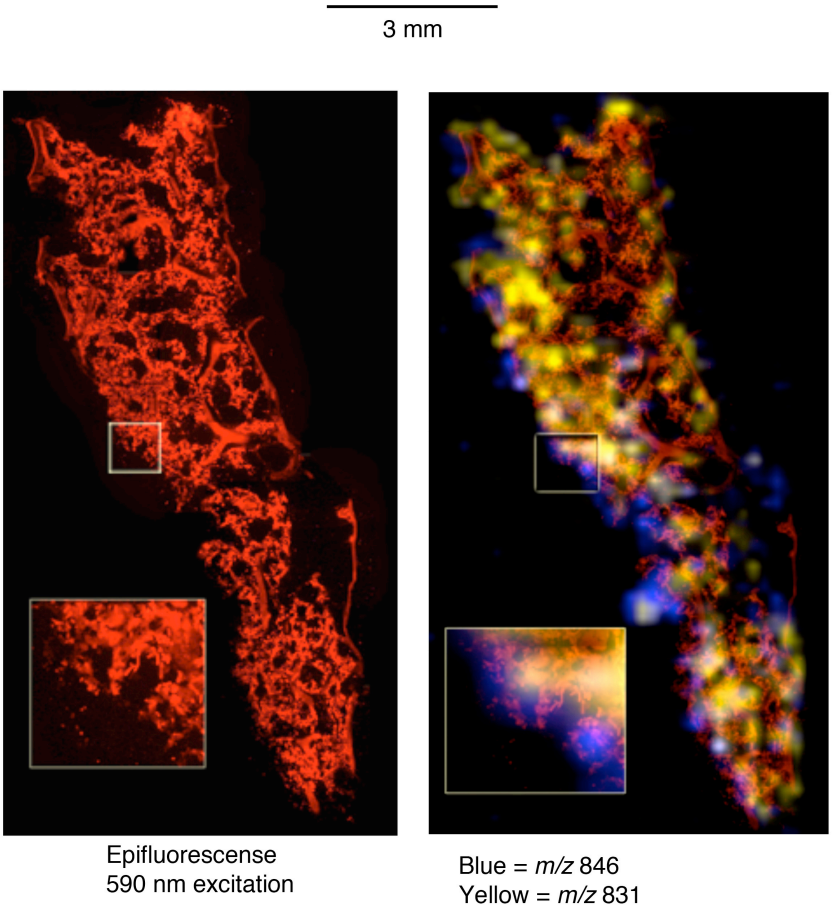

Figure 3.5. Large scale MALDI imaging of *Dysidea herbacea* combined with epiflourescence images. Left Panel: a broad scale composite image of approximately 20 epiflourescene images taken at 20X (590nm filter) capturing the entire 14 um thick cryotome section of a *Dysidea herbacea* sample. The images were stitched together with Adobe photoshop (CS4). Inset shows blown up region inside white box, present are numerous red, rod-shaped organisms, most likely *Oscillatoria spongelia*, a known cyanobacterial symbiont of this sponge. Right Panel: MALDI imaging results showing two unknown ions that co-localize to the sponge tissue but have different distributions. The blue ion (*m/z* 846) appears to be found on the lower half and periphery of the sponge section, while the yellow ion (*m/z* 831) is found in areas with dense sponge tissue. These results support the initial findings that there are different chemical microenvironments within *Dysidea herbacea* and likely other marine tropical sponges.

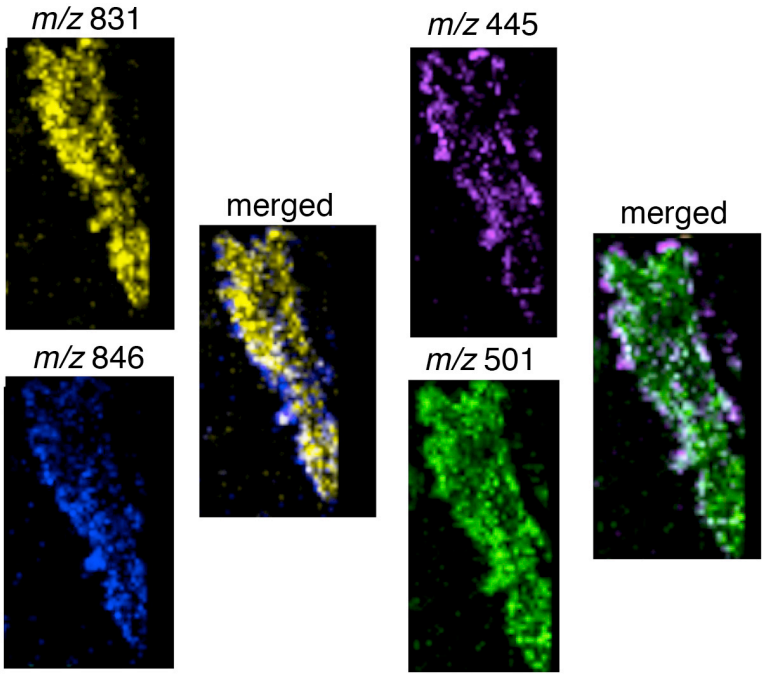

Figure 3.6. More MALDI imaging results from the *Dysidea herbacea* sample shown in figure 3.5. The distribution of the ions at *m/z* 846 and 831 is more clearly apparent in the unmerged results. The purple ion at *m/z* 445 has an almost entirely peripheral distribution while the green at *m/z* 501 is found in dense amounts throughout the section.

Pilot Study: Elysia and Kahalalide

Background and methods

Kahalalide F is large, marine depsipeptide originally isolated from the nudibranch Elysia rufescens. There has been much excitement regarding this compound since it isolation in 1993 (1) as it is a strong cytotoxic compound to numerous different cancer cell lines, with preferential activity. More specifically it has IC_{50} values ranging from 0.07 MM (PC3) to 0.28 MM (DU145, LNCaP, SKBR-3, BT474, MCF7) while non-tumor human cells (MCF10A, HUVEC, HMEC-1, IMR90) were up to 40 times less sensitive to the drug (2,3). Although not yet fully established,

the mechanism of action leads to severe disruption of crucial organelles while leaving the nuclear structure intact. The compound is in various stages of clinical trials for several cancers (3,4) and has been licensed by Pharmamar.

This compound is a classic example of how complex and nuanced the field of marine natural products is. The compound has been isolated from Elysia rufescens, however there is no evidence that the organism actually biosynthesizes the entire molecule. More to the point, its main diet the green alga Bryopsis pennata, which has been shown to produce very similar peptides (kahalalide G and F among others). At this point it has been hypothesized that the mollusk sequesters the algae's peptides either as different isoforms, which are then converted, or directly as kahalalide F (3), as well as several other kahalalides (5). There's also been suggestions that the molecules are originating from a microbial symbiont of both the species (5).

A MALDI imaging and dried droplet analysis was performed on frozen samples of *Bryopsis sp*. and *Elysia rufescens* given to us by Mark Hamann. The results are shown below. The methods for the MALDI imaging and dried droplet experiments were performed as described in chapter 1 (for dried droplet) and Chapter 2 (for imaging). Although some insight was obtained, it is my opinion that a fresher specimen of Elysia would result in better, more insightful results.

Figure 3.7. Coronal cryotome section of the nudibranch *Elysia rufescens*. Left panel: Image of a nudibranch on reef, white line shows approximate location of coronal section (right panel). Right panel: epiflourescent (ex 590 nm) image of a 20 um thick section on a MALDI target plate. Small red dots scattered throughout (dorsal and ventral) are likely chloroplasts accumulated by the nudibranch from photosynthetic food sources (*Bryopsis*), the large red spots are mantle dermal formations.

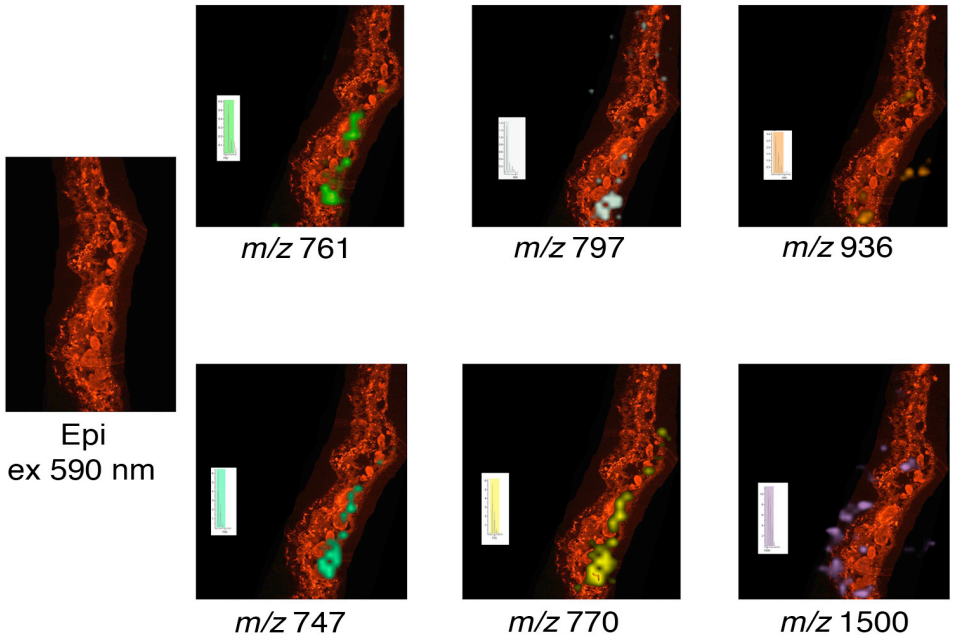

Figure 3.8. MALDI imaging results of section in far left panel (see figure 3.7). The ions at m/z 761, 747, 770, 797 and 936 all appear to localize on the mid-ventral (bottom) of the nudibranch. The ion at m/z 1500 (is consistent with kahalalide F, no other kahalalide variant was seen by imaging) and localizes to the mid-dorsal (top) area of the sample.

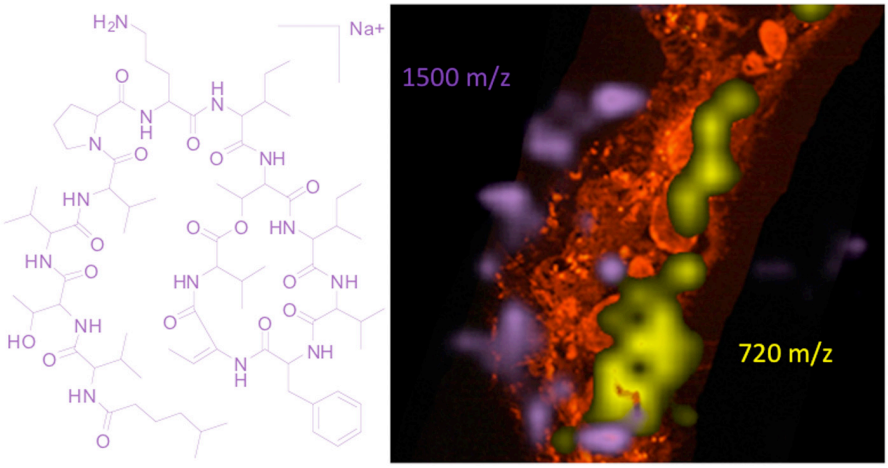

Figure 3.9. kahalalide F structure and distribution on *Elysia rufescens*.
Left panel: shows the large, 1500 Da molecule kahalalide F- the target molecule that has shown very strong anti-cancer properties in clinical trials. Right panel: the distribution of the mass consistent with kahalalide F and the unknown ion at m/z 720 overlaid on the epiflourescent image of a crytome section of *Elysia rufescens.*

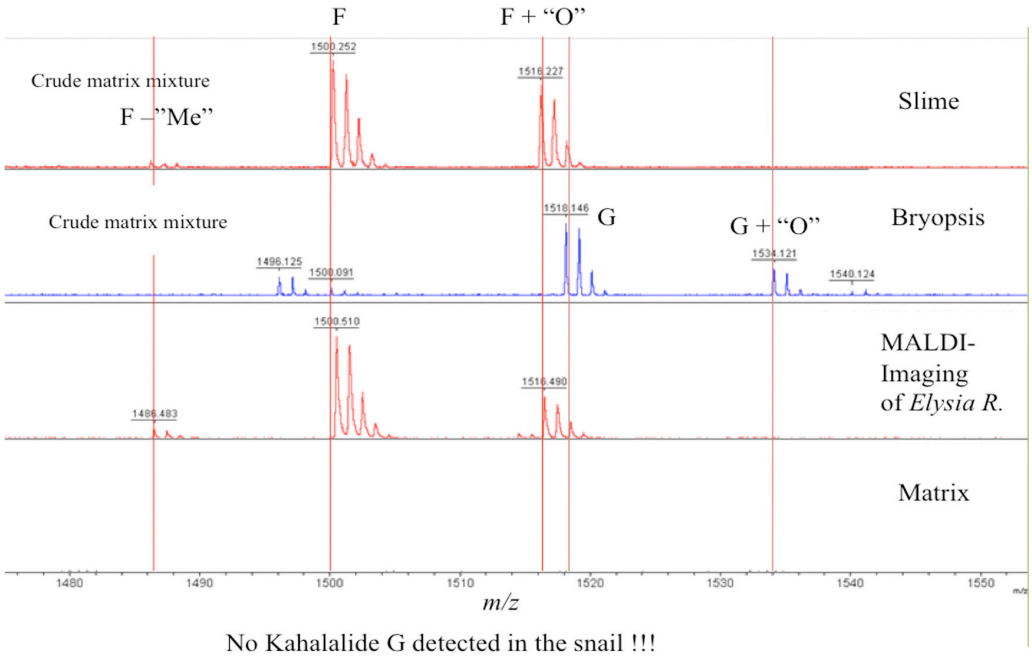

Figure 3.10. Dried droplet MALDI analysis (*m/z* 1480-1550) of the various players in the kahalalide story. The top red spectrum shows the ions found in the coating of the slime associated with *Elysia rufescens*. Here we see kahalalide F, along with a plus oxygen mass, and a minus methyl mass. The middle, blue spectrum, shows the ions associated with its foodsource, a *Bryopsis sp*. This spectrum shows the presence of kahalalide G, G plus oxygen, a trace amount the F variant as well as trace of two lesser analogs. The bottom red spectrum shows the results of the MALDI imaging of the section of *Elysia r*. which is consistent with the the results from the slime dried droplet results- showing the presence of F, F+O, and F-Me. From these results, it is unknown whether the valuable kahalaide F is truly found within the nudibranch, or possibly just found in the slime.

Pilot experiment: Differential distribution of natural products in marine cyanobacteria.

Background and methods

Whether or not there is homogenous production of secondary metabolites in cultures of cyanobacteria is unknown. There have been studies supporting heterogenous production of certain metabolites in agar cultures of soil bacteria using GFP tagged natural product clusters. However, because the majority of the target marine cyanobacteria (*Lyngbya*, *Phormidium*, etc) are still genetically intractable, the same experiments cannot be performed on these organisms. The following MALDI studies were performed with these ideas in mind.

The MALDI imaging of filaments was performed as described in Chapter 2, the imaging of the agar culture was prepared using the sieve method and dry universal matrix (Sigma) as described in reference 7. The dried droplet was performed as described in Chapter 1.

These initial experiments support the idea that there is a heterogenous distribution of natural products in marine cyanobacteria. These results are also consistent with the single cell results in Chapter 4 which indicate that different individual cells of *Lyngbya majuscla* 3L either express only certain metabolites, or have undetectable concentrations of some metabolites with high concentrations of others.

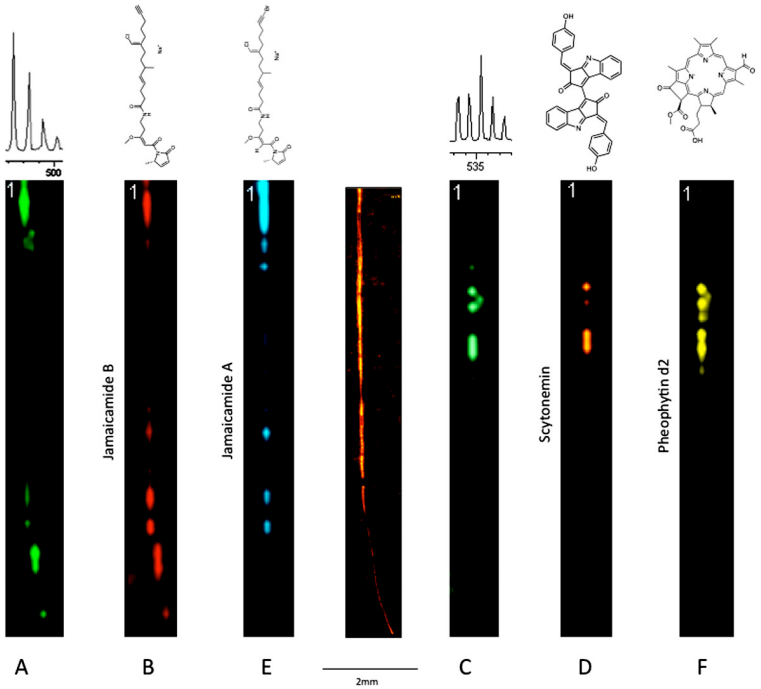

Figure 3.11. Evidence of differential distribution of metabolites in a filament of *L.majuscula* JHB. The central image is a series of epifluorescent (ex 590) micrographs taken at 100X an tiled together with photoshop and shows presence of chlorophyll, this image serves as the alignment of the MALDI results. This 10 mm filament was subjected to MALDI imaging and is the longest one successfully imaged. A. spatial distribution of an unknown metabolite at *m/z* 497. B jamacamide B C. unknown D. consistent with scytonemin (unverified) E. jamaicamide A F. pheobarbide.

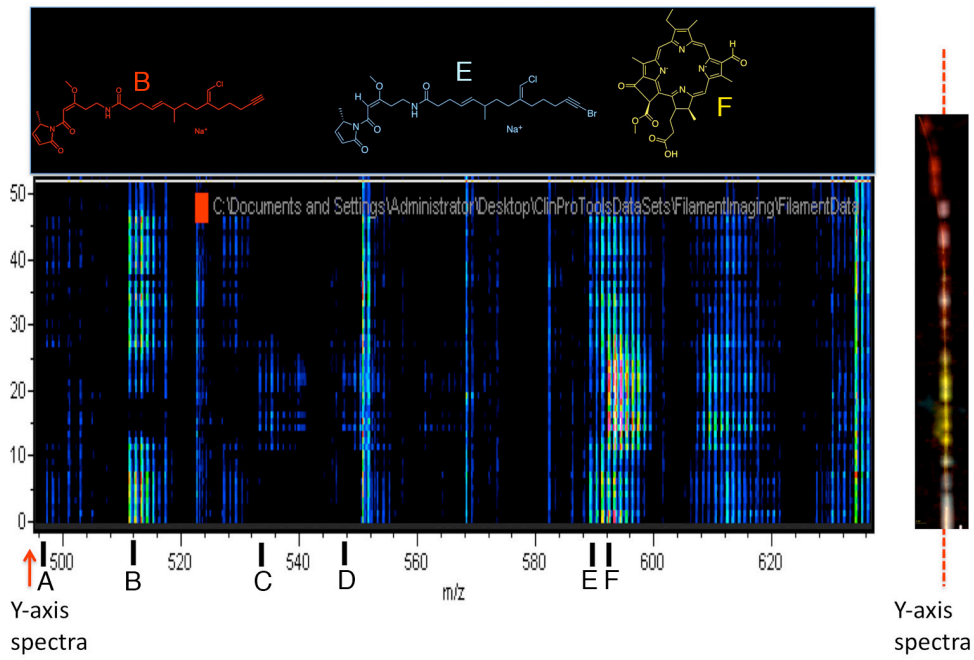

Figure 3.12. Heat map representation of MALDI imaging data of a filament of *L majuscula* JHB. The right panel shows the merged distributions of the compounds in the top panel. The y-axis spectra line indicates how the individual spectra were picked for the heat map- the image is aligned with the results on the left. The letters (A-F) are indicative of the compounds in figure x (previous). Adding a spatial dimension to the heatmap is a powerful way to visualize imaging data, allowing all the compounds which colocalize (A,B,E and C, D, F) to be quickly determined, and also reveal two unknown compounds (A and C).

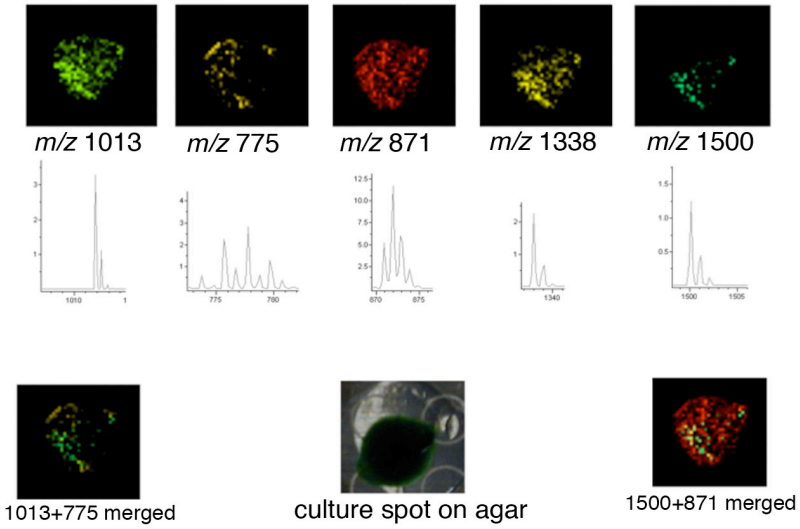

Figure 3.13. *Nostoc punctiforme* spatial distribution of metabolites.
This culture of *Nostoc p* was grown on BG-11 saltwater agar (bottom middle) and prepared for MALDI using the sieve method (ref). *m/z* 871 is consistent with pheophytin a, the rest of the metabolites are unknown.

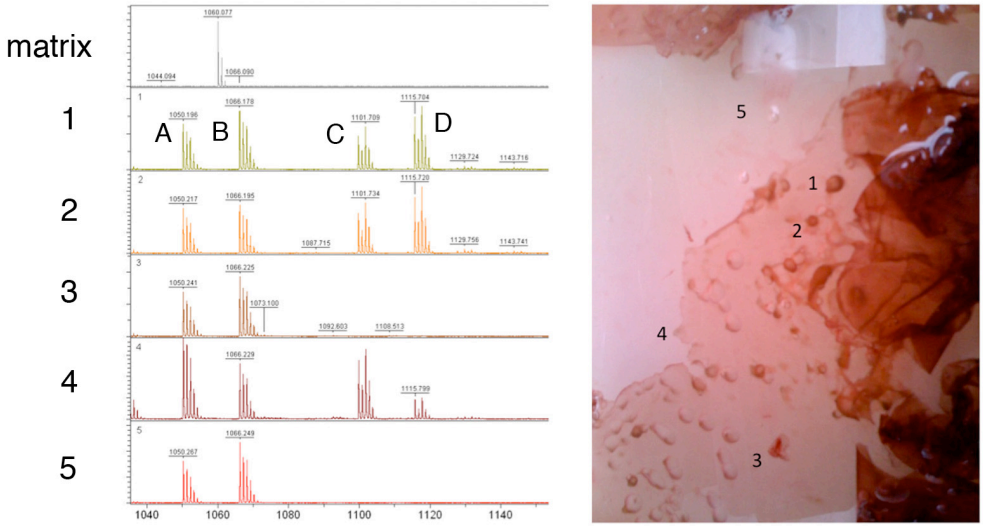

Figure 3.14. Dried droplet MALDI analysis of different areas of a pan grown *Phormidium sp.* culture. The numbers 1-5 on the right image are different samples taken from the culure. 1,2,4 were all found growing on the bottom of the pan while 3 and 5 were floating on the surface. The spectra on the left correspond to the numbers. Compounds A and B are unknown, but are often found in MALDI preparation of algal biomass (perhaps pigments) compounds C and D are likely phormidamide and an adduct (O). From this data it appears that phormidamide is only found on biomass growing on the bottom of the pan- perhaps indicating an older constituent of the culture or different heterotroph composition.

4.0 CHAPTER 4

BIOSYNTHESIS OF MAJOR METABOLITES IN SINGLE CYANOBACTERIAL CELLS

4.0.1 Abstract

Marine organisms are a prolific and largely untapped source of medically relevant natural products. Many of these secondary metabolites are the focus of isolation, purification and bioassay efforts that often reveal tantalizing chemistry with novel mechanisms of action. However two factors prevent further sourcing of these compounds, impeding more thorough development into clinically viable drug leads; the potential organisms to which they are often attributed live in complex association with a multitude of microorganisms, making identification of the biosynthetic machinery difficult, and synthetic chemistry of the compounds is often too complex and expensive to be a viable option. Organisms of the genus *Lyngbya*, giant filamentous marine cyanobacteria, typically exist in close association with heterotrophic bacteria and other micro and macro organisms, and are reported to be the source of scores of bioactive natural products. Reported here is an approach that relies on Matrix Assisted Laser Desorption Ionization Mass Spectrometry (MALDI-MS) to detect abundant natural products in the metabolomes of single *Lyngbya* cells, providing further evidence of their origin of biosynthesis. Furthermore, single cells from cultures inoculated with ^{15}N-nitrate show evidence of ^{15}N incorporation into known secondary metabolites, confirming active biosynthesis.

4.1 Introduction

Marine organisms have consistently been shown to be the source of many powerfully bioactive, clinically and commercially important secondary metabolites (natural products). A look through the literature suggest the range of bioactive compounds isolated from marine organisms is stunning, with at least 20 marine derived natural products currently or recently in clinical trials for the treatment of cancer, with many more discovered with potent anti-bacterial, anti-fungal and anti-inflammatory activity [1,2]. Many of these structures and chemistries are novel when compared to their terrestrial counterparts, probably stemming from competition and evolution in a marine environment that likely has very different selection pressures.[3]

Several long-standing issues have hindered the full development of the marine natural products field. Many of these secondary metabolites exist in small amounts and require large collections of biomass from remote and sensitive environments only to yield a small amount of purified compound. In order to generate enough material for assessing the true capacity of these compounds, the field has had to rely on culturing of these organisms, which works in only small percentage of attempts, and is further complicated by slow growth or on very difficult and expensive synthetic chemistry [4]. To truly maximize the promise of marine natural products, this supply issue needs to be resolved. At this point, heterologous expression of the known gene clusters for these compounds in a suitable host system is the most promising solution to the supply issue, but one that depends on knowing the locus of the biosynthetic

genes. Thus, knowing the true origin of the biosynthesis of these molecules will not only help solve the sourcing of these compounds but also provide insight into the evolution of chemical defense and communication, and our environmental and ecological understanding of the marine environment.

As was the case with paclitaxel in the terrestrial environment [5], the true biosynthetic origin of these marine natural products can be easy to incorrectly assume. A typical collection, be it a sponge, algae or cyanobacterial mat, is rarely a single organism and most often an intricate and poorly understood mixture of several species [6,7]. Even in a collection of a relatively pure sample, such as the nudibranch responsible with kahalalide [8] the residence of the actual biosynthetic capability is elusive to pinpoint. Thus, the true biosynthetic source of the compounds can only be vaguely determined and even then, is sometimes subsequently shown to be wrong [9]. Intimate knowledge of the architecture of many of these compounds, and the pathways from which they arise, can help preclude certain species as possible origins. [6,7] However, it is not uncommon for organisms housing similar biosynthetic capabilities to live in close association and produce similar molecules.

Marine cyanobacteria, especially of the genus *Lyngbya*, are thought to be the source of a large number of bioactive and clinically interesting metabolites; between 2001 and 2006, a total of 128, mainly mixed PKS/NRPS, nitrogen containing, bioactive molecules have been isolated from marine cyanobacteria [10]. All of the reported cyanobacteria live in close association with heterotrophic bacteria, (often a-proteobacter) and in certain cases a reported natural product is attributed to a mixed

assemblage of two or more cyanobacterial species [11-15]. Work supporting the ability of Matrix Assisted Laser Desorption Ionization Time of Flight Mass Spectrometry (MALDI-TOF-MS) to identify and dereplicate natural products in cyanobacteria is well documented [16-18]. Because of its ease of preparation, ability to deal with complex mixtures and high sensitivity, MALDI-TOF has also been used to assay single cells, as has been reported by Sweedler et al. with peptide queries in mammalian neuronal cells [19, 20] as well as reported success for analyzing metabolites in yeast [21]. Described here is a single cell isolation with subsequent MALDI-TOF-MS analysis for *Lyngbya* specimens that are reported to be the source of many important biomedically relevant natural products but are commonly found as assemblages of marine micro-organisms [11-15]. These preparations allowed the metabolomes of single cells to be analyzed and compared, yielding the locus of abundant known and unknown natural products to be more clearly defined then ever before. Furthermore, inoculating cultures of these strains in media in which the available nitrate has been replaced with ^{15}N-nitrate resulted in ^{15}N incorporation into known metabolites, providing the ability to verify both active biosynthesis and relative age of metabolite content.

4.2 Results and Discussion

An individual cell from a filamentous cyanobacteria, especially from the *Lyngbya majuscula* varieties, can be up to 70 μm and larger in diameter and thus can be manipulated with a micro-manipulator under a dissecting microscope. The single cell process is depicted in Figure 4.1 and 4.2, briefly a filament of cyanobacteria is mechanically disrupted and single cells are forced out of the polysaccharide sheath.

Once freed from the sheath, a micropipette is used to pick a single cell that is then immediately placed on the MALDI target plate. At this point the excess media is aspirated and 0.5 µl of MALDI matrix is placed on top of the cell. Once dry, the preparation is ready to be analyzed.

Figure 4.1

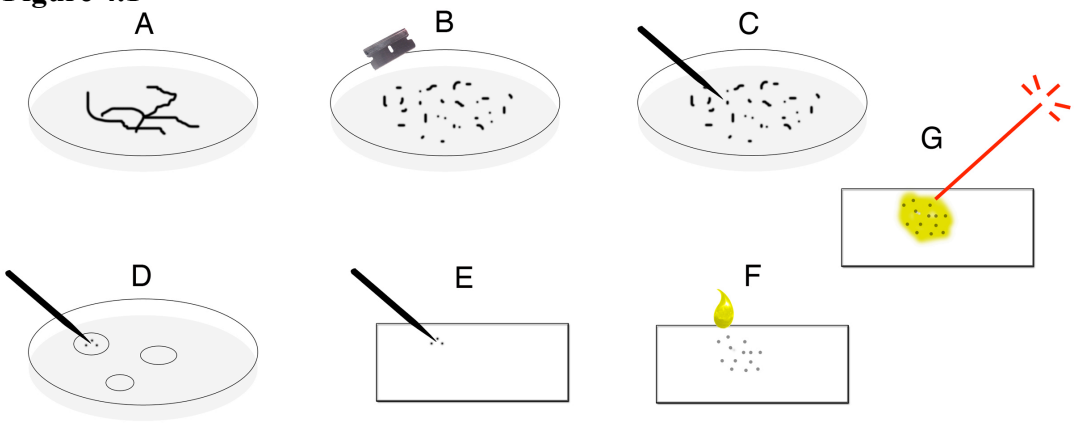

Figure 4.1. The marine filamentous cyanobacteria single cell isolation and MALDI target plate preparation. A. A few filaments are transferred to a petri dish containing regular growth media. B. Using a razor blade, the filaments are chopped finely (0.5 cm pieces) C. Using a glass micropipette (or 40 gauge needle) single cells are dislodged from the small filament fragments and sheath, and then aspirated individually. D. The individual cells are transferred to a drop of fresh media in a new petri dish containing 3-4 isolated drops of fresh media. The cells are transferred to a new drop of media 3-4 times (can be done in groups) resulting in a sequentially cleaner preparation. The cells can be examined using a microscope at this point to check for contamination. E. The clean cells are transferred to a MALDI target plate (small amounts of media are ok). F. After the media has dried, the desired matrix is applied in small amounts over the cells (0.3-0.5 uL). G. The plate and cells are ready for insertation into the MALDI-TOF instrument. Depending on the system, a raster of the laser over a broad area containing the cells can be successful or a visual targeting of the laser onto the individual cells, which are sometimes visable in the matrix, can be performed.

The results suggest that the combination between the sensitivity of the instrument with high metabolite concentration is strong enough to generate mass data on the most abundant metabolites found in single cells, especially ones from larger species of filamentous cyanobacteria. It can also be concluded that the detected metabolites are being stored inside the cell in sufficient concentration, about 1-100 nM, to be detected by our instrument.

Figure 4.2

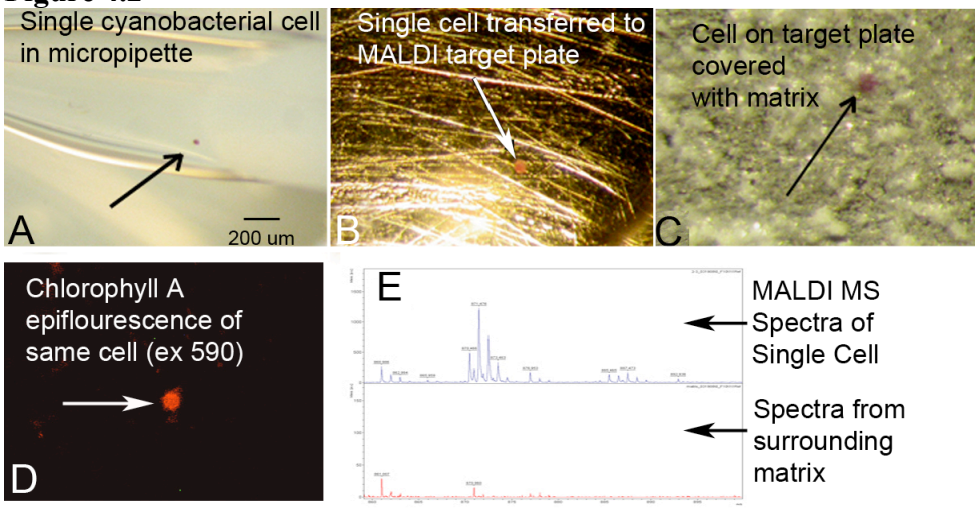

Figure 4.2. Actual single cell preparation from *Lyngbya majuscula 3L*. A. Dissociated, single cell in micropipette. B. Same cell on MALDI target plate. C. Cell covered with matrix. D. Confirmation of presence of chlorophyll a by epifluorescence. E. MALDI spectra of single cell, with signal consistent with pheophytin a (breakdown product of chlorophyll a).

The single cell MALDI approach becomes even more attractive for pinpointing the origin of natural products when one considers the common presence of various heterotrophic bacteria residing on the polysaccharide sheath of the cyanobacteria. Figures 4.3A and 4.3B shows a DAPI stained single filament of *Lyngbya majuscula*

3L, the stain is specific to bacterial DNA and confirms the presence of heterotrops. Although it has yet to be demonstrated, these heterotrophs could be responsible for the biosynthesis of at least some of the molecules reported in the literature. The aim of the single cell isolations performed thus far has been to disengage and separate the cell from the sheath material on which the heterotrophs reside. Figures 4.3C and 4.3D show DAPI staining of live single cell preparations, confirming the dissociation of heterotrophs from the cyanobacteria. This would suggest that the MALDI signal and any metabolite contained within are either originating from the isolated cell or finding their way into the cell in very high concentrations.

Figure 4.3

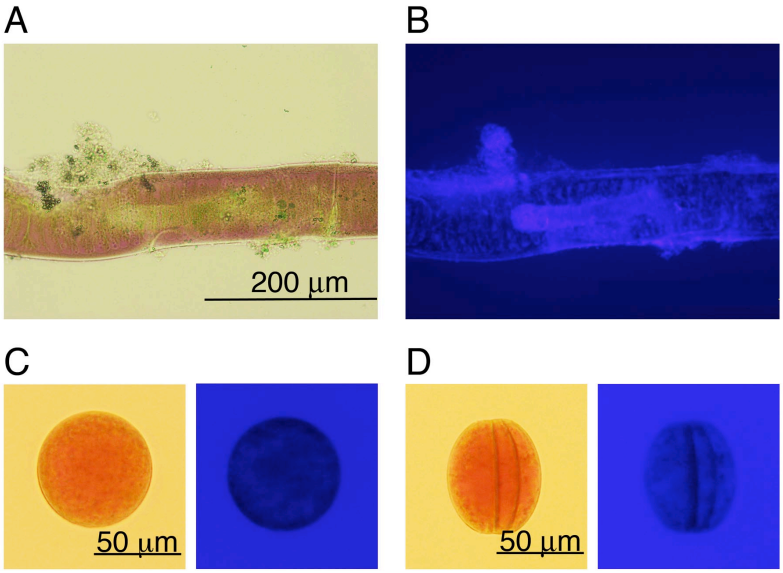

Figure 4.3. Photo micrographs of DAPI staining of live intact filaments and single cells of *L.majuscula* 3L. A. Live intact filament, with polysaccharide sheath, showing presence of foreign material (greenish moss-like). B. Same filament after DAPI staining and viewed at ex. 358 nm, lighter areas show presence of bacterial DNA, likely highlighting the location of heterotrophs. C and D. Isolated live, single cell (C) and dividing cells (D) with DAPI staining under regular light (lefts panel) and at 358 nm (right panels). There is no sign of any staining on the surface of the cells, indicating absence of foreign DNA in the preparation.

In order to further explore the idea that these single cells are actively producing the detected metabolites, a culture of *L.majuscula* 3L was grown in media in which all the available nitrate has been replaced with isotopically labeled [^{15}N]NaNO3. After 4 days, filaments were removed from this culture and 6 single cells were isolated and subjected to MALDI mass spectrometry along with 5 whole filaments to serve as a baseline (Figure 4.4A). Of the 6 cells, all contained signals consistent with curacin A (m/z 372) and the percent ^{15}N incorporation calculated into the curacin pool was very

similar among each cell (15-24%) and to the percentage determined for the whole filament sample (15%). For the chlorophyll breakdown product pheophytin a (m/z 871), 3 of the cells yielded a detecable signal, with the percentage of ^{15}N incorporation ranging between 7-14% which is comparable to the whole filament average of 17%. For carmabin A only 2 of the cells yielded a detectable signal, with the percentage of ^{15}N incorporation ranging between 41-42%, which is consistent with the whole filament average of 41%. These signals all showed evidence of significant levels of ^{15}N isotopic labeling consistent with the nitrogen content of each molecule (Figure 4.4B). This numbers indicate active biosynthesis of these molecules, and makes the possibility that these metabolites are simply accumulating inside the cells and originating from foreign sources much less likely, as the isotopic labeling would be would not be prevalent.

Figure 4.4

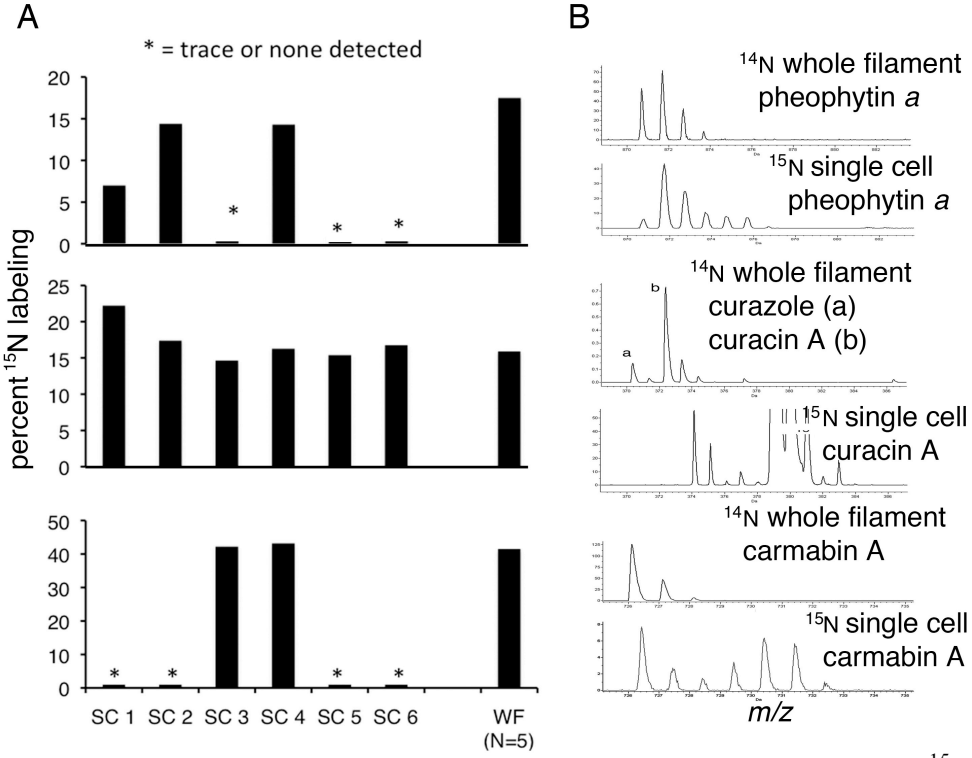

Figure 4.4. Single cells from an *L.majuscula* 3L culture incubated with [^{15}N]NaNO3 suggest active biosynthesis of metabolites.
A Six cells were successfully analyzed (labeled SC 1-6). The presence and percent ^{15}N incorporation was calculated for pheophytin a (top graph), curacin A (middle graph) and carmabin A (bottom graph). Whole filaments of the same cultures were also analyzed for presence and percent ^{15}N incorporation of the same metabolites (labeled WF). The panels in B shows representative spectra for each of the metabolites with labeled and unlabeled. Top panel shows MALDI spectra consistent with pheophytin a in a whole filament, while bottom panel is from a single cell of a culture grown in media in which the available nitrate is ^{15}N labeled, the spectra shows evidence of incorporation of ^{15}N into the pheophtyin a molecule (m/z 871 contains 4N). B and C show further evidence of ^{15}N labeling into other molecules and were generated from the same data sets, with B showing curazole (a- m/z 372 contains 1N) and curacin (b- m/z 374 contains 1N) and C showing carmabin A (m/z 726 contains 5N).

Both the endogenous role of these and many other secondary metabolites and the nature of the symbiosis between cyanobacteria and other marine organisms is so complicated and poorly understood that the possibility remains that a molecule present

in a cell did not originate from it. If such cases exist, the only way to truly confirm the biosynthetic capacity for a secondary metabolite is to sequence the genome of the organism in question, identify the responsible gene cluster, and heterogeneously express it in the appropriate host. However, the reported approach is a useful in that it strongly suggests origin and provides evidence of active biosynthesis of abundant metabolites associated with marine filamentous cyanobacteria. The results here indicate that pheophytin a, carmabin A, curazole and curacin are all actively produced in single vegetative cells of *L.majuscula* 3L, a finding which is supported by the recent annotation of this organism's genome (Monroe and Jones, in-progress).

4.3 Materials and Methods

4.3.1 Cyanobacteria strains and culture maintenance

Lyngbya majuscula strain JHB was originally collected in Hector's Bay, Jamaica in 2002. *L. majuscula* strain 3L was collected in Curaçao, Netherlands Antilles in 1996. Pan (10 L) and Erlenmeyer flask (1 L) cultures of each strain were maintained at Scripps Institution of Oceanography, UCSD in SW BG-11 media [22] at 29°C, under 16 h light / 8 h dark cycles at approximately 5 μE m-2 s-1. All experiments were conducted using these temperature and light conditions. For all experimental cultures, SW-BG-11 was used, containing 5 g / L of either [^{14}N]NaNO3 or for ^{15}N labeling studies, [^{15}N]NaNO3 (98%, Cambridge Isotopes).

4.3.2 Media

For all cultures, SW-BG-11 was used (22). For the experimental ^{15}N studies the entire $NaNO_3$ component of the SW-BG-11 media was replaced with [^{15}N]NaNO3 from Cambridge Isotopes Laboratories (98%+ purity).

4.3.3 Single Cell Isolations

Following aseptic procedure and using small tweezers, 2-4 filaments (5-10 μg wet weight) were removed from the parent culture placed in a sterile Petri dish containing clean 2-3 ml of media (either regular or ^{15}N). Under a dissecting microscope the filaments are chopped into small pieces using a razor blade, single cells will become dislodged from the sheath and become free floating. Individual cells are then vacuumed into a pulled glass micropipette (puller, etc) or a pipette-man and a 10 μl tip. These cells are then transferred to a separate Petri dish containing a drop of clean media. This transfer of cells into clean drops of media can be repeated until the individual cell suspension is free from any extraneous sheath material or ruptured cells. Once enough cells (5-10) have been gathered into a droplet of media, the entire contents can be pipetted onto a MALDI target (Bruker MSP 96 stainless steel plate).

4.3.4 DAPI staining

Instead of transfer to MALDI target plate (see above), once isolated and cleaned, the cells were transferred to a glass microscope slide into a drop of media. The same was done for whole filaments. Reference images were captured at 200 X under brighfield lighting. A drop of DAPI stain was then added to the two preparations (whole filament and single cells) and images captured at 200X with brightfield lighting and with an excitation filter of 358 nm.

4.3.5 MALDI MS Sample preparation

Once the droplet has been transferred to the target plate, the excess liquid must be aspirated carefully with a small pipette tip or thin glass micropipette, this should leave individual cells scattered in a small area of the target plate. Alternately, if the accompanying volume of media is small, the plate can be left to dry at room temperature. A small amount (0.3-0.5 µl) of matrix (see below) is then deposited on the area(s) containing the cells and allowed to dry at room temperature.

Matrix- Per 1ml: 70 mg HCCA/DHB (Universal MALDI matrix from Sigma), 750 µl Acetonitrile, 248 µl milliQ H20, 2 µl TFA.

After each spot has dried, the plate is ready to be run by MALDI –TOF (Bruker Microflex MALDI-TOF mass spectrometer equipped with flexControl 3.0).

4.3.6 MALDI-TOF acquisition and settings

Using the camera view, the laser was targeted at areas containing visible cells or areas marked previously (useful to note were cells are found on the target plate with a dissecting scope prior to insertion in the mass spectrometer). The number of laser shots per cell area was set at 30 at a frequency of 20 Hz. The laser was manually moved within the area containing an individual cell.

The instrument and program settings for these experiments were as follows: General: Flex-Control Method- RP_pepmix.par. Processing: Flexanalysis Method- none, Biotools MS method- none. Laser Power: 70-80 %. Sample Carrier: nothing. Spectrometer: On, Ion Source 1- 19.0 0mV, Ion Source 2- 16.40 mV, Lens- 9.45 mV, Reflector 20.00, Pulsed Ion Extraction- 190 ns, Polarity- Positive. Matrix Suppression: Deflection, Suppress up to: m/z 350. Detection: Mass Range- 350-1600, Detector Gain- Reflector 3.7X. Sample Rate- 2.00 GS/s, Mode- low range, Electronic Gain- Enhanced, 100 mV. Real time Smooth- Off. Spectrometer, Size: 81040, Delay 42968. Processing Method: Factory method RP_2465. Setup: Mass Range- Low. Laser Frequency- 20 Hz, Autoteaching- off. Instrument Specific Settings: Digitizer- Trigger Level- 2000 mV, Digital Off Linear- 127 cnt, Digital Off, Reflector- 127 cnt. Detector Gain Voltage Offset, Linear- 1300 V, Reflector- 1400 V. Laser Attenuator, Offset -23 %, Range- 50 %, Electronic Gain Button Definitions, Regular: 100 mv (offset lin) 100 mV (offset ref) 200mV/full scale. Enh: 51 mV (offset lin), 51 mV (offset ref) 100 mV/full scale. Highest: 25 mV (offsetlin) 25 mV (offset ref) 50 mV/full scale.

Calibration: Calibration was accomplished using angiotensin II as an external standard. Zoom Range +-1.0%, Peak Assignment Tolerance- User Defined-500 ppm

4.3.7 Calculations

Percent ^{15}N labeleing was calculated as described in reference 23.

Acknowledgements

Chapter 4, in full, is currently being prepared for submission in 2011. Eduardo Esquenazi, Tara Byrum, William Gerwick, and Pieter Dorrestein. The dissertation author was the primary investigator on these studies.

4.4 CHAPTER 4 REFERENCES

1. D. J. Newman and G.M. Cragg, "Natural Products as Sources of New Drugs over the Last 25 Years," *Journal of Natural Products* 70 no. 3(2007): 461-477.

2. J. W. Blunt, B. R. Copp, W. P. Hu, M. H. Munro, P. T. Northcote, and M. R. Prinsep, "Marine Natural Products," *Nat. Prod. Rep.* 25 (2008), 25, 35 – 94

3. A. V. Ramaswamy, P. M. Flatt, D. J. Edwards, T. L. Simmons, B. Han, and W. H. Gerwick,in *Frontiers in Marine Biotechnology*, eds. P. Proksch and W. E. G. Müller (Norfolk, England: Horizon Bioscience, 2006), 175-224.

4. J. L. Fortman and D. H. Sherman, "Utilizing the Power of Microbial Genetics to Bridge the Gap Between the Promise and the Application of Marine Natural Products," *ChemBioChem* 6 (2005): 1-19.

5. G. M. Cragg and D. J. Newman, "Plants as a Source of Anti-Cancer Agents," *Journal of Ethnopharmacology* 100 (2005): 72–9.

6. T. L. Simmons, R. C. Coates, B. R. Clark, N. Engene, D. Gonzalez, E. Esquenazi, P. C. Dorrestein, and W. H. Gerwick, "Biosynthetic Origin of Natural Products Isolated from Marine Microorganism-Invertebrate Assemblages," *Proc. Nat. Acad. Sci. USA*. 105 (2008): 4587–94.

7. T. L. Simmons and W. H. Gerwick, Oceans and Human Health, eds. P. Walsh, H. Solo-Gabriele, L. E. Fleming, S. L. Smith, and W. H. Gerwick (New York: Elsevier, 2008).

8. M. T. Hamann and P. J. Scheuer, "Kahalalide F: A Bioactive Depsipeptide from the Sacoglossan Mollusk Elysia Rufescens and the Green Alga Bryopsis sp.," *Journal of the American Chemical Society*, 115 no. 13 (1993): 5825-6.

9. M. Hildebrand, L. E. Waggoner, H. Liu, K. H. Sharp, C. P. Ridley, and M. G. Haygood, "Approaches to Identify, Clone, and Express Symbiont Bioactive Metabolite Genes," *Natural Product Reports* 21 (2004):122-42.

10. L. T. Tan, "Bioactive Natural Products from Marine Cyanobacteria for Drug Discovery," *Phytochemistry* 68 (2007): 954-79.

11. R. T. Williamson, I. P. Singh, and W. H. Gerwick, "Taveuniamides: New Chlorinated Toxins from a Mixed Assemblage of Marine Cyanobacteria," *Tetrahedron* 60 no. 33 (2004): 7025-33.

12. L. M. Nogle and W. H. Gerwick, "Somocystinamide A, a Novel Cytotoxic Disulfide Dimer from a Fijian Marine Cyanobacterial Mixed Assemblage," *Organic Letters* 4 no. 7 (2002): 1095-8.

13. G. G. Harrigan, W. Y. Yoshida, Richard E. Moore, D. G. Nagle, P. U. Park, J. Biggs, V. J. Paul, S. L. Mooberry, T. H. Corbett, and F. A. Valeriote, "Isolation, Structure Determination, and Biological Activity of Dolastatin 12 and Lyngbyastatin 1 from Lyngbya Majuscula/Schizothrix Calcicola Cyanobacterial Assemblages," *Journal of Natural Products* 61 no. 10 (1998): 1221-5.

14. D. G. Nagle, P. U. Park, and V. J. Paul, "Pitiamide A, a New Chlorinated Lipid from a Mixed Marine Cyanobacterial Assemblage," *Tetrahedron Letters* 38 no. 40 (1997): 6969-72.

15. D. G. Nagle, V. J. Paul, and M. A. Roberts, "Ypaoamide, a New Broadly Acting Feeding Deterrent from the Marine Cyanobacterium Lyngbya majuscula," *Tetrahedron Letters* 37 no. 35 (1996): 6263-6.

16. E. Esquenazi, C. Coates, L. Simmons, D. Gonzalez, W. H. Gerwick, and P. C. Dorrestein, "Visualizing the Spatial Distribution of Secondary Metabolites Produced by Marine Cyanobacteria and Sponges Via MALDI-TOF Imaging," *Mol Biosyst* 4 (2008): 562–70.

17. M. Erhard, H. von Döhren, and P. Jungblut, "Rapid Typing and Elucidation of New Secondary Metabolites of Intact Cyanobacteria Using MALDI-TOF Mass Spectrometry," *Nat. Biotechnol.* 15 (1997): 906–9.

18. M. Welker and M. Erhard, "Consistency Between Chemotyping of Single Filaments of Planktothrix Rubescens (Cyanobacteria) by MALDI-TOF and the Peptide Patterns of Strains Determined by HPLC-MS," *Journal of Mass Spectrometry* 42 (2007): 1062–8.

19. A. B. Hummon, J. V. Sweedler, and R. W. Corbin, "Discovering New Neuropeptides Using Single-Cell Mass Spectrometry," *Trends in Analytical Chemistry* 22 no. 9 (2003): 515-21

20. S. S. Rubakhin and J. V. Sweedler, "Characterizing Peptides in Individual Mammalian Cells Using Mass Spectrometry," *Nature Protocols*, 2 no. 8 (2007): 1987-97.

21. A. Amantonico, J. Oh, J. Sobek, M. Heinemann, and R. Zenobi, "Mass Spectrometric Method for Analyzing Metabolites in Yeast with Single Cell Sensitivity," *Angewandte Chemie* 120 (2008): 5462–5.

22. R. W. Castenholz, "Culturing of Cyanobacteria," *Meth. Enzymol.* 167 (1988): 68-93.

23. K. Biemann Mass Spectrometry: Organic Chemical Applications. , McGraw-Hill, New York, 1962, 223-231.

5.0 CHAPTER 5

ION MOBILITY MASS SPECTROMETRY ENABLES THE EFFICIENT DETECTION AND IDENTIFICATION OF HALOGENATED NATURAL PRODUCTS FROM CYANOBACTERIA WITH MINIMAL SAMPLE PREPARATION

5.0.1 Abstract

Direct observation of halogenated natural products produced by different strains of marine cyanobacteria was accomplished by electrospray ionization and matrix assisted laser desorption ionization and gas phase separation via ion mobility mass spectrometry of extracts as well as intact organisms.

5.1 Introduction

Natural product and natural product inspired compounds account for some 70% of all current pharmaceutical products on the market[1]. Although the pharmaceutical industry has wavered in its dependence on natural products as leads during the last 40 years, there has been a resurgence of interest recently. This is likely the result of a failure of combinatorial chemistry to deliver very many clinically useful drugs, the rise of the genomics which is giving a resurgence of interest into natural products, and the development of user-friendly but powerful mass spectrometry (MS) and nuclear magnetic resonance (NMR) techniques to identify and de-replicate novel natural products from a variety of organisms [2,3]. These bioactive compounds, usually characterized as secondary metabolites, vary widely in chemical structure and

physiological targets and span a range of potential clinical uses[1,4].

Bacteria and plants have traditionally accounted for the majority of bioactive metabolites, however, marine organisms, such as sponges, tunicates, cyanobacteria and assorted microorganisms, have emerged as exciting and relatively unexplored sources of novel chemistries, likely a product of evolving within a very different set of environmental conditions [5]. A number of marine derived natural products have entered clinical and preclinical trials and hold promise for a variety of diseases, with a particular emphasis on cancer chemotherapeutics [6,7].

Although the field of marine natural products drug discovery holds significant attractions, it is not without its limitations. The producing organisms are frequently found in close association with one another, forming complex assemblages that result in challenges in the identification and isolation of the producing organism [3]. It is estimated that cyanobacteria and bacteria account for nearly 80% of reported bioactive marine natural products that have advanced past the pre-clinical phase [8]. During the discovery process, these assemblages of poorly understood organisms often result in very complex mixtures of metabolites that represent significant analytical challenges to the natural products chemist [3].

It has recently been suggested that there is an urgent need for the development of new more powerful and high-throughput methods for the structural analysis of natural products [9]. In this regard, ion mobility mass spectrometry has the potential to accelerate the characterization of natural products. Travelling wave Ion Mobility Mass Spectrometry, which is often paired with Matrix Assisted Laser Desorption

Ionization (MALDI) and Electrospray Ionization (ESI) sources, essentially provides an additional separation step in the gas phase without the loss of sensitivity [10]. This enables the separation of ions that have similar mass to charge ratios (*m/z*) but which possess differing collisional cross-sections. The results are displayed as trend-lines defined by both *m/z* value and drift time thru the ion mobility chamber containing an inert gas (nitrogen, argon, etc). Ions with the smallest masses and tightest configurations or most aerodynamic shape emerge first, and are assigned lower drift times. Larger and spatially bulky molecules emerge later, and thus have longer drift times. Overall, this enables the separation of matrix signals (from the MALDI preparation) as well as different classes of molecules from one another [10,11]. This is an especially advantageous addition in the study of small molecules because most natural products, quorum sensors, pheromones, and other bioactive natural products involved in cell-to-cell communication and adaptive metabolism are observed in the region below *m/z* 2000.

This report describes proof-of-principle experiments characterizing halogenated metabolites of three species of *Lyngbya*, a genus of mainly tropical marine cyanobacteria and prolific producer of potently bioactive metabolites [12]. These natural products can be observed not only in crude extracts but also from intact cyanobacterial filaments using Ion Mobility instrumentation (Waters Synapt G1 Mass Spectrometers equipped with ESI or MALDI surces). The ESI-Ion Mobility experiments described herein resulted in clear separation of multiply halogenated metabolites (and possibly the combination of cyclic and halogenated) from other

metabolites and assorted small molecules. This capability was especially useful in allowing overlapping isotopic signals to be more clearly resolved into their true isotopic ratios. The imaging experiments on the MALDI instrument allowed the highest spatial resolution images yet reported for the distribution of specific natural products in a marine organism [13,14]. Ion mobility data were also gathered on the same organisms, giving a powerful insight into the composition and distribution of these interesting metabolites. Indeed, natural product imaging results have been powerful approaches for addressing the origin of biosynthesis of several previously characterized compounds, and provide further evidence of their distribution along cyanobacterial filaments [14]. The addition of ion mobility allowed us to separate matrix interference and *m/z* signals stemming from pigments and assorted small molecules from halogenated and other natural products in the gas phase without the need of chromatography.

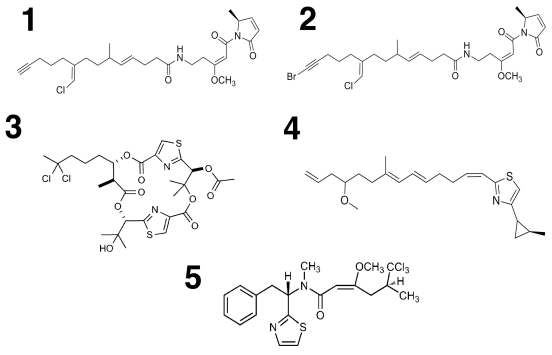

Crude extracts of two strains of the cyanobacterium *Lyngbya majuscula,* JHB and 3L, were run on an ESI ion-mobility instrument (Figure 5.1). In the JHB extract, four trend-lines were resolved (highlighted in Figure 5.1A), indicating separation of

the various classes of metabolites. The spectra for these trend-lines are shown in figure 1B and contain some notable observations; trend-line 1 gives rise to unknown metabolites, possibly nitrogen containing linear molecules that have slower mobility. Trend-line 2 contains peptides and metabolites that have a similar charge to hydrodynamic radii to peptides, moving more quickly relative to their mass than the ions in trend-line 1, and include the halogenated compounds jamaicamide B **(1)** and jamaicamide A **(2**). However, trend-line 3 contained the halogenated and cyclic compound, hectochlorin (**3**), while trend-line 4 contained doubly charged ions. Similar results were obtained from the crude extract of *L.majuscula* 3L, however in this case, the approach yielded three clear trend-lines (Figure 5.1C). Trend-line 1 contains the majority of the metabolites observed, including the linear, non-halogenated compound curacin A (**4**), while trend-line 2 contained barbamide (**5**), a highly halogenated compound containing three chlorine atoms, as well as several putative undescribed analogs of the molecule. Trend-line 3 contained doubly charged ions (Figure 5.1D). Thus, it is possible to separate out compounds with varying levels of halogenations as well as those that are cyclic or linear in overall construction.

Live intact filaments of three different strains of cyanobacteria, *Lyngbya majuscula* JHB, *Lyngbya majuscula* 3L and a recently collected *Lyngbya majuscula* from Papua New Guinea (PNG), were removed from culture, washed in water, airbrushed with universal matrix on the target plate, and then subjected to MALDI imaging with the Synapt system from Waters Co. The resulting data was imported into BioMap (Novartis) software and analyzed. Over a dozen metabolites associated

with these filaments were observed; some of the *m/z* values were present in all three species while others were found only found in specific strains. In Figure 5.2A, the *m/z* 511 ion, which corresponded to the sodium adduct of the neurotoxin jamaicamide B (**1**) (expected 511.242 [M+Na], observed 511.24), was found associated with the JHB strain, while the *m/z* 374 signal corresponded to the anticancer agent curacin A (**4**) previously isolated from the 3L strain (expected 374.2520 [M+H], observed 374.2478). Finally, an unknown ion with a mass at *m/z* 925 corresponded to the less

Figure 5.1. Ion mobility separation of known natural products from crude extracts of *Lyngbya majuscula*.
Panels A and C show the main trend-lines (T#) associated with classes of molecules containing similar ion-mobility behavior in *L. majuscula* JHB and 3L, respectively, T4 and T3 respectively, contain doubly charged ions. B. Spectra associated with the trend-lines in panel A (T1-T3)- T1 likely contains unidentified linear, nitrogen-containing hydrocarbons. T2 contains the linear halogenated natural products, jamaicamide B (**1**) and A (**2**) as well as the majority of small peptides and metabolites associated with this strain. T3 contains the cyclic, halogenated compound hectochlorin (**3**), and possibly related analogs. D. Contains the spectra associated with panel C (T1 and T2), with trend-line 1 containing the linear natural product curacin A (**4**) as well as the majority of small peptides and metabolites associated with this strain. T2 contains the highly halogenated natural product barbamide and related analogs.

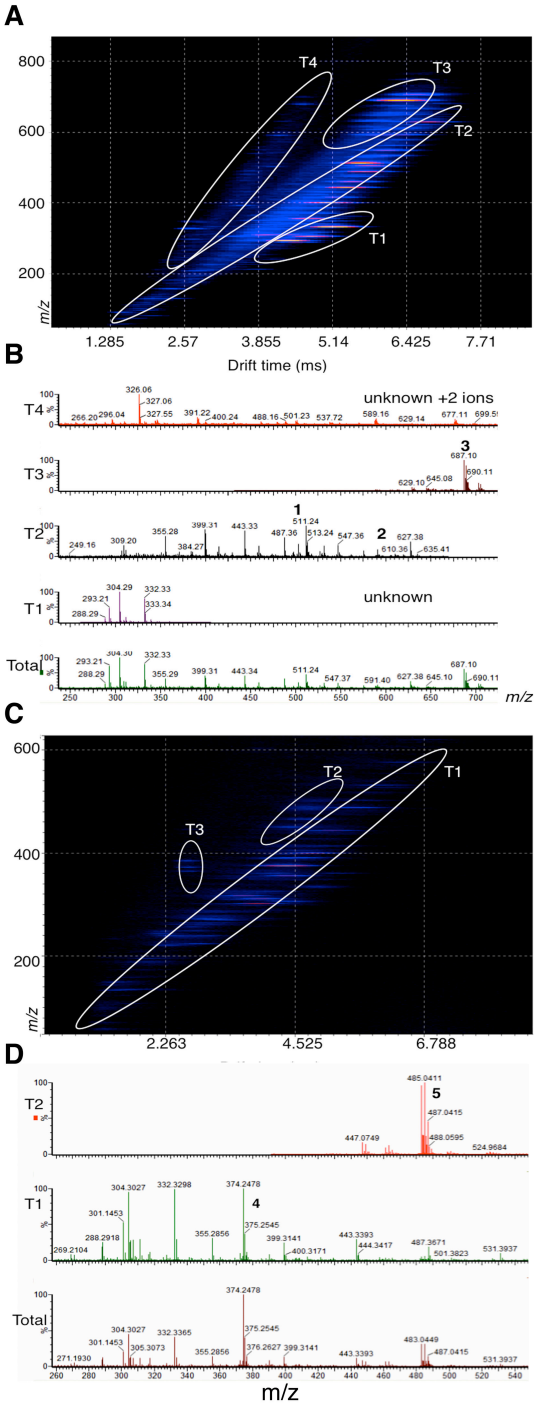
A
T4
T3
T2
T1
800
600
400
200
m/z
1.285
2.57
3.855
5.14
6.425
7.71
Drift time (ms)
B
unknown +2 ions
T4
T3
T2
T1
Total
unknown
m/z
C
T2
T1
T3
600
400
200
m/z
2.263
4.525
6.788
D
T2
T1
Total
m/z

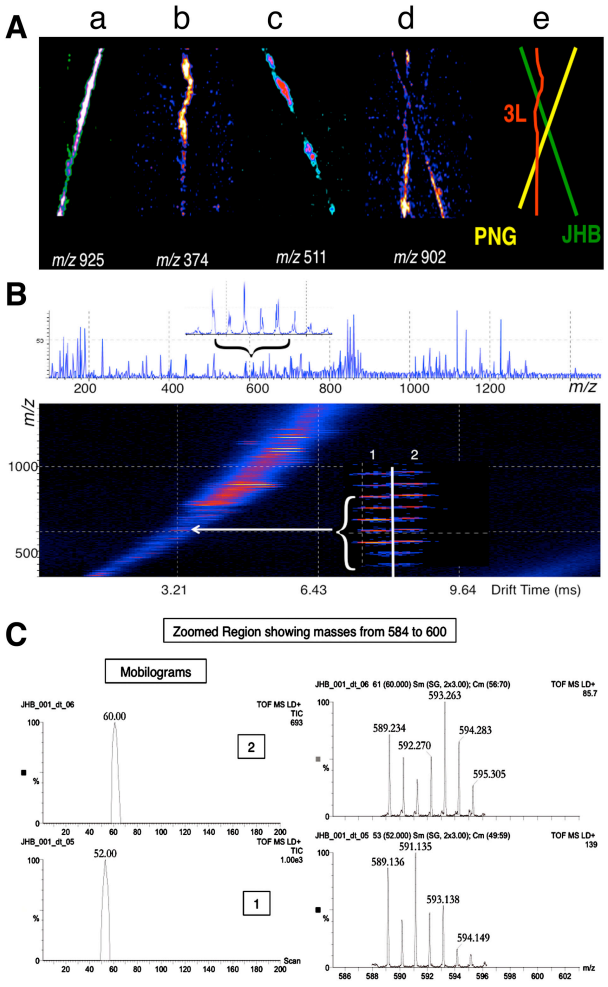

Figure 5.2. MALDI imaging of filaments of *L.majuscula* paired with ion-mobility. A. Three filaments from different strains were overlaid and imaged by MALDI, arrangement is shown in (e). The localization of natural products associated with specific strains is confirmed in a-c, with an unknown metabolite in PNG (a), curacin A (**4**) in 3L (b), and jamaicamide A in (**1**) JHB (c). Part d shows an unknown compound, possibly a chlorophyll-derived metabolite common to all three strains. B. Top, MALDI spectra from the same culture as the imaged filament, inset contains the region containing the isotopic profile for (**2**) overlapping another ion cluster. Bottom, ion mobility drift time analysis for this sample, inset shows the same jamaicamide A region and the two different ion mobility trends associated with the overlapping isotopic clusters. C. Analysis of the same two mobilograms (drift times) associated with trend-line 1 and 2 in the panel above. The peak at 60 (top left) is associated with the spectra on the top right, and is probably derived from matrix and pheobarbide. The peak at 52 (bottom left) is associated with the spectra on the bottom right, and matches the mass and isotopic profile for the halogenated compound jamaicamide A.

well investigated PNG strain. Each of these data was localized to the single producing organism and showed very few background signals. In addition, the spatial resolution of the image was generated by an oversampled rastering of the laser, resulting in 50 μm resolution, the highest spatially resolved MALDI images yet obtained for any cyanobacterium. Therefore, imaging via ion mobility MS provides a very rich data set from both a data quality and resolution perspective. Additionally, the depth of the data set obtained by ion mobility is an extra dimension of these experiments.

The above MALDI imaging experiments were run in conjunction with ion-mobility using whole-cell preparations; thus, it was possible to generate ion mobility trend-lines for the JHB experiment (Figure 5.2B). Because the carrier gas was nitrogen in this experiment, the separation wasn't as robust as in the ESI based experiments that used argon. Nonetheless, this experiment yielded separation of ions with similar masses. In whole cell and MALDI imaging preparations on this instrument, the *m/z* region between 587 and 593 in *L. majuscula* JHB is composed of overlapping isotope clusters from a breakdown product of chlorophyll (pheobarbide *a*, *m/z* 592.1 [M+H]) and other unknown, possibly matrix-associated signals, as well as that of jamaicamide A (**2**) (*m/z* 589.152 [M+Na]), a neurotoxic and ichthyotoxic metabolite containing both a chlorine and a bromine atom. The results in figure 5.2B and 2C, show how the ion mobility component of the analysis was able to separate out jamaicamide A based on its differing mobility from these overlapping signals, in part due to its multiple halogenations.

5.2 Methods

Lyngbya majuscula strain JHB was originally collected in Hector's Bay, Jamaica in 2002. *L. majuscula* 3L was collected in Curacao, Netherlands Antilles in 1996, and *L. majuscula PNG* was collected in Milne Bay Papua New Guinea in 2005. Pan and Erlenmeyer flask cultures of each strain were maintained at Scripps Institution of Oceanography, UCSD in SW BG-11 media [15] at 29°C, under 16h light/8 h dark cycles at approximately 5 μE m^{-2} s^{-1}.

In ESI experiments, approximately 2.5 g (wet weight) of fresh biomass of either *L. majuscula* JHB and 3L were extracted with DCM/MeOH. Both extracts were sent to Pleasanton, CA for ESI ion mobility mass spectrometry on the Waters® ESI SYNAPT ™HDMS™. Mobility data was viewed in Driftscope (Waters Co.) and regions showing differences in drift time vs. *m/z* were selected and analyzed further.

For MALDI imaging, single filaments of each of the three *L. majuscula* strains (JHB, 3L, and PNG) were rinsed in a drop of mqH_20 and placed on a glass microscope slide such that a cross was constructed (Figure1). Using an airbrush, the sample was uniformly coated with a MALDI matrix solution (70 mg/ml HCCA/DHB (Universal MALDI matrix from Sigma) in 80% ACN, 19.8% milliQ H_20, and 0.2% μl TFA) and imaged on a Waters® MALDI SYNAPT ™HDMS™. Data was analyzed with Biomap software (Novartis).

For the MALDI dried spot preparation, approximately 1 μg of biomass from each strain was rinsed in milliQ H_20 and placed in a 1.5 ml eppendorf tube using ethanol-cleansed tweezers. MALDI matrix solution (1.0 μl per 0.1 μg of biomass)

was added to the wells. After 20 seconds, 1 µl of this matrix extract was deposited on a 96 well target plate and allowed to dry prior to running on the MALDI SYNAPT ™HDMS™.

For more information on experiments see supplemental.

5.3 Conclusion

The identification and dereplication of natural products, especially from crude extracts deriving from complex marine assemblages, is a difficult endeavour but one which can be effectively investigated using modern soft-ionization mass spectrometry techniques. However, in most cases, the complexity of these samples remains challenging because spectral signals can overlap, increasing the effort required to identify and dereplicate the underlying compounds. In the proof-of-principle experiments reported here, the addition of ion-mobility to modern ESI and MALDI approaches greatly simplified the parsing of crude extracts into different structural classes of molecules. Halogenated compounds are widely known to have enhanced bioactivity and lipid solubility and are thus attractive as lead compounds [16]. Similarly, complex cyclic compounds are indicative of specialized and highly specific three dimensional topologies that derive from interesting biosynthetic mechanisms. The ion-mobility mass spectrometry experiments reported were consistently able to separate out different structural classes of metabolites, including known halogenated and possibly cyclic ones, as well as identifying unknown analogs or new compounds, from both whole cell and crude extracts of different strains of the natural product rich marine organism *L. majuscula*. Thus, we conclude that this new method in mass

spectrometry could greatly simplify the discovery and de-replication of new bioactive lead compounds in natural product screening and drug discovery programs.

5.4 CHAPTER 5 ACKNOWLEDGMENTS

Chapter 5, in full, has been submitted to Chemical Communications in 2010. Eduardo Esquenazi, Michael Daly, Tasneem Barainwala, William H. Gerwick and Pieter C. Dorrestein. The dissertation author was the primary investigator and author of this paper.

5.5 CHAPTER 5 REFERENCES

1. D. J. Newman and G.M. Cragg, "Natural Products as Sources of New Drugs over the Last 25 Years," *Journal of Natural Products* 70 no. 3(2007): 461-477.

2. B. H. Bode and R. Mueller, "The impact of bacterial genomics on natural product research," *Angewandte Chemie* [International Edition] 44, no. 42 (2005): 6828-46.

3. T.L. Simmons, R.C. Coates, B.R. Clark, N. Engene, D. Gonzalez, E. Esquenazi, P.C. Dorrestein, W.H. Gerwick, *Proc Nat Acad Sci USA.,* 2008*,* 105: 4587-4594.

4. A. Ganesan., *Curr. Opinion in Chemical Biology* 12 no. 3 (2008): 306-17.

5. A. V. Ramaswamy, P. M. Flatt, D. J. Edwards, T. L. Simmons, B. Han, and W. H. Gerwick, in *Frontiers in Marine Biotechnology*, eds. P. Proksch and W. E. G. Müller (Norfolk, England: Horizon Bioscience, 2006), 175-224.

6. R. H. Feling, G. O. Buchanan, T. J. Mincer, C. A. Kauffman, P. R. Jensen, and W. Fenical, *Angewandte Chemie* [International Edition] 42 no. 3 (2003): 355-7.

7. T. L. Simmons, E. Andrianasolo, K. McPhail, P. Flatt, and W. H. Gerwick, *Mol. Cancer Ther,* 4 (2005): 333.

8. T. L. Simmons and W. H. Gerwick, "Oceans and Human Health," eds. P. Walsh, H. Solo-Gabriele, L. E. Fleming, S. L. Smith, and W. H. Gerwick (New York: Elsevier, 2008).

9. J.W.-H. Li and J.C. Vederas., Science., 2009, 325 (5937): 161-165.

10. S. D. Pringle, K. Giles, J. L. Wildgoose, J. P. Williams, S. E. Slade, K. Thalassinos, R. H. Bateman, M. T. Bowers, and J. H. Scrivens, *Int. J. Mass. Spec.* 261 no. 1 (2007): 1-12.

11. S. N. Jackson, M. Ugarov, T. Egan, J. D. Post, D. Langlais, J. A. Schultz, and A. S. Woods, *Journal of Mass Spectrometry* 42 (2007): 1093-8.

12. J. W. Blunt, B. R. Copp, W. P. Hu, M. H. Munro, P. T. Northcote, and M. R. Prinsep, "Marine Natural Products," *Nat. Prod. Rep.* 26 (2009): 170–244.

13. E. Esquenazi, Y. L.Yang, J. Watrous, W. H. Gerwick, and P. C. Dorrestein, *Nat. Prod. Rep.* 26 (2009): 1521-34.

14. E. Esquenazi, C. Coates, T. L. Simmons, D. Gonzalez, W. H. Gerwick, and P.C. Dorrestein. *Mol. Biosyst.* 4 (2008): 562-70.

15. R. W. Castenholz, "Culturing of Cyanobacteria," *Meth. Enzymol.*167 (1988): 68–93.

16. M. Z. Hernandes, S. M. Cavalcanti, D. R. Moreira, W. F. de Azevedo Jr, and A. C. Leite. *Curr. Drug Targets* 11 no. 3 (2010): 303-14.

CHAPTER 5 SUPPORTING INFORMATION

Experimental Procedures

ESI synapt experiments

For ESI SYNAPT ™HDMS™experiments, approximately 2.5 g (wet weight) of fresh biomass, for both L.majuscula JHB and 3L was placed in a 100ul beaker and soaked 20 ml of 2:1 DCM/MeOH for 30 minutes on hot plate (low setting). The biomass and liquid were then filtered with cheesecloth and filter paper. The biomass was returned to the beaker and the process was repeated 5 times, with the resulting liquid extraction combined after each step. The resulting extract was place in a rotavap until dry. A small amount of ACN was used to re-suspend and load the extract into a C-18 Sep-Pak column pretreated with ACN. Using a round bottom flask as a collection vessel, the column was washed through twice with ACN, followed by methanol until clear. The further purified extract was placed in a rotavap until dry. The dried extract was transferred to a small glass vial using ether, dried under nitrogen, and placed in a hi-vacuum overnight. ***Calibration*** Calibration was performed with NaI from m/z 50-2000 ***Instrument Parameters*** Sample were dissolved in 50:50 H2O:MeOH 0.1%Formic Acid and infused using nanospray needles. Data was acquired in Mobility mode. Capillary Voltage = 1.0 V Cone Voltage = 10-25 V IMS Wave Height ramped from 5-10 V

MALDI imaging and dried spot experiments

For the MALDI experiments, ~1 g wet weight cultures of each of the three strains were removed from the parent culture, placed in 50 ml culture flasks and flown

to the Waters facility in Milford Massachusetts for MALDI imaging. For imaging, single filaments of each of three Lyngbya majuscula strains (JHB, 3L, and PNG) were rinsed in a drop of mqH20 and laid down on the glass microscope slide so that a cross was made (Figure1). A MALDI matrix solution (70 mg/ml HCCA/DHB (Universal MALDI matrix from Sigma) in 80 % acetonitrile, 19.8 % milliQ H20, and 0.2 % µl TFA) was prepared and the sample was coated with this matrix using an airbrush. (make/model) 50 passes of 5 cycles were applied such that an uniform coating was deposited on the slide. The sample was allowed to dry between in each pass in order to avoid delocalization of the ions under investigation.

For the MALDI dried spot preparation, for each strain approximately 1 µg of biomass was rinsed in milliQ H20 and placed in an 1.5 ml eppendorf tube using ethanol-cleansed tweezers. MALDI matrix solution (1.0 µl per 0.1 µg of biomass) was added to the wells or tubes. After 20-30 seconds, 1 µl of this matrix extract was deposited on a 96 well target plate and allowed to dry prior to running on the MALDI SYNAPT ™HDMS™.

Parameters:

MS System:	Waters® MALDI SYNAPT ™HDMS™
Ionization Mode:	Positive Ion
Laser Type:	Nd:YAG
Repetition Rate:	200 Hz
Acquisition Range:	Varied depending on sample being analyzed
Collision Energy:	Trap CE=6.0eV

Instrument Calibration

Matrix: Alpha-Cyano-4-Hydroxycinnamic Acid (CHCA) – 10 mg/mL in Acetonitrile: Water at 1:1 with 0.1% TFA. Calibration Mixture:

lPEG oligomers (PEG 200, 400, 600, 800, 1000, 2000 and 3000) were prepared at concentrations of 10 mg/mL in water. Sodium Iodide solution (NaI) was prepared at 2mg/mL in 50:50 Acetonitrile:Water . A mixture was prepared by mixing 10 µL of each PEG oligomer with 10 µL of the NaI solution. A 10-fold dilution was made of this mixture into water and this was then mixed 1:1 with matrix and 1 µL spotted. Calibration data was obtained from 100-2000 Da in IMS mode

6.0 CHAPTER 6

FUTURE DIRECTIONS

Some future directions and conclusions are found in the discussions at the end of each chapter, and at the end of the introduction. What follows are some expansions of those conclusions, suggested experiments or broader, theoretically possible extensions of those approaches and studies.

^{15}N Feeding

The results revealing the timing of bromination of jamaicamide A (Chapter 2) are in strong agreement that the addition of bromine is occurring after biosynthesis of jamaicamide B by an uncharacterized halogenating enzyme. Nothing else is known about this enzyme regarding its specificity for jamaicamide B or its ability to use other halogens. Several experiments come to mind that could further support these findings and provide a greater insight into this enzyme. Firstly, several alkyne terminating compounds could be introduced into a properly buffered preparation of *L.majuscula* JHB in the presence of excess NaBr. It should be possible to monitor the bromination of these substrates by the same dried droplet MALDI technique, although it might require various experimental conditions to be tested (dark, removal of oxygen, etc). A second suggested experiment is exploring the ability of this enzyme to use other halogen atoms. Briefly, the bromide component of the media should be removed entirely if possible, and new halide component introduced in sufficient concentration. A culture of *L.majuscula* JHB is then grown in this media under complete darkness for

several days. If the new halogen is incorporated into the jamaicamide B molecule, the resulting mass shift increase should be detectable by MALDI dried droplet analysis.

On a different vein, another promising idea is the use of the ^{15}N approach to reveal cryptic metabolites. As was the case with cryptomaldamide and *L.majuscula* JHB (Chapter 2 Appendix) the ^{15}N temporal shifts visualized with Bruker's ClinProTools heatmap function can reveal cryptic metabolites undergoing active biosynthesis that might have been overlooked in previous extractions. In the *Lyngbya majuscula* 3L study it is apparent that there are two peptidic compounds with masses at 325 and 400 undergoing active turnover. The presence of these compounds has been confirmed with Robin Kinnel who has done some further extractions but yet remain uncharacterized. Either these compounds or additional studies utilizing this isotopic approach in other strains could lead to more novel chemistry from both new collections or previously studied strains.

More broadly, the ^{15}N feeding studies in combination with small whole cell analysis by MALDI (described in Chapter 2) opens up the ability to study the in-vivo dynamics of individual secondary metabolite biosynthesis as well as glimpse at how the entire nitrogen containing metabolome changes over time. Besides the applications discussed in the chapter, it is my strong belief that further, more refined, experiments could yield some truly important findings in our understanding of marine natural products. In general, the endogenous purpose of secondary metabolites, almost by definition, is very poorly understood. There are several theories (Coley

1985, Herms and Mattson 1992, Cronin and Hay 1996) addressing the allocation of resources to secondary metabolites, most of these without regard to specific classes or compounds. With the described approach, a much more defined, and specific, set of rules regarding the production of a particular metabolite under a set of conditions might be achieved.

One way to facilitate a large scale and high impact study is with a simple program that can do automatic peak detection, intensity measurement, and calculate percent isotope incorporation. In this way, the response in production and turnover of many nitrogen containing metabolites (whether primary, secondary, or cryptic) to changes in the nutrient composition of the media, the introduction of a predators, or microbial pathogens, traditional host organisms, or any other factor (ocean acidification, eutrophication, etc) can be empirically calculated. Besides a greater insight into marine ecology, combining this information with genomic and proteomic analyses and molecular biology approaches could provide means by which to regulate specific genetic elements, and aid in the heterologous expression of natural product gene clusters.

MALDI imaging

The results and methods of the studies utilizing natural product MALDI imaging (chapter 3) only represent the beginning of what is already becoming an important method. The students and post-docs in the Dorrestein Lab at UCSD have expanded this approach to the study of microbial interactions, these efforts have led to

the identification of new metabolites and a greater appreciation of adaptive and dynamic metabolic exchanges between microbes- essentially translating microbial communication. As instrumentation and preparations becoming more refined (better resolution, three-dimensional analysis and matrix-free and other imaging mass spectrometry approaches) the future prospect of this field is very exciting.

In regards to marine natural products, increased resolution in combination with single cell approaches (chapter 4) and labeling studies (chapter 2) could allow the symbionts of complex assemblages responsible for intriguing signals to be easily pinpointed and removed for further analysis. Multiple displacement amplification (MDA) of these organisms or metagenomic studies could lead to the identification of novel gene clusters and a largely untapped source of novel chemistry. Furthermore, increased effort in sample preparation (fresher specimens, embedding and sectioning methods) could provide the first ever glimpses of the metabolic exchange occurring in the complex symbiotic systems found on threatened ecosystems (coral reefs) or unique environments (thermal vents).

Another possible use of isotope feeding studies in conjunction with MALDI imaging is the possibility of tracking nutrient cycling or metabolite incorporation in a complex assemblage. One possible experiment could help further address the origin of the potent anticancer lead kahalalide F (Chapter 3 Appendix). Briefly, a culture of the *Bryopsis sp*. (also produces several kahalides and is the foodsource of the nudibranch *Elysia rufescens*) is grown in 100% ^{15}N media until all nitrogen has been isotopically labeled. This isotopically labeled foodsource is then fed to the nudibranch

and the kahalalide F found in its slime could be analyzed by MALDI dried droplet (preserves sample for future samples) or by thin-section MALDI imaging (terminates nudibranch) revealing the amount of ^{15}N incorporation into kahalalide F and perhaps showing the time course of labeling. This could be insightful on several fronts.

More broadly, the ability to do imaging mass spectrometry (MALDI or otherwise) on sophisticated experimental samples greatly expands the utility of the approach. I can envision the use of a microfluidic target plate that could allow the carefully controlled passage of any entity (microbial strain, nutrient, lead compound, growth factor, etc) across or through a preparation containing possible interacting component (s) (another microbial strain, diseased tissue or healthy tissue, etc). A Real time ambient MS probe would be particularly useful for the detecting analysis of new signals arising from the interaction.

In conclusion, the results and new insights produced during my graduate studies are a result of the application of modern mass spectrometry to the producers of natural products directly. This idea remains largely untapped, especially in the case of marine organisms or the human microbiome, and thus future application remains broad and limited only by creative, well-designed experiments. Mass spectrometry in combination with isotope incorporation, imaging and single cell studies can be expanded and combined, yielding spatial and temporal insights into not only the biosynthesis of natural products, but towards a better understanding of the relationships between organisms and secondary metabolism in general. This type of broader understanding will help guide and fine-tune drug discovery efforts in the

future and provide insight into the interface between the microbial and eukaryotic worlds.